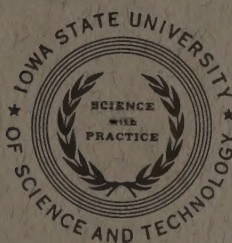


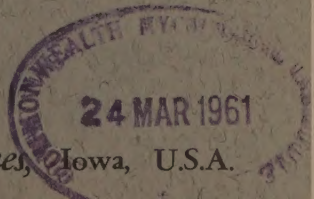
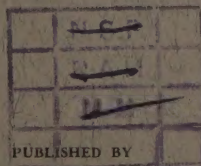
# IOWA STATE JOURNAL OF SCIENCE

*A Quarterly of Research*



## CONTENTS

Seedling emergence and growth responses of dwarf grain sorghum as affected by gibberellic acid.	
F. P. GARDNER and M. J. KASPERBAUER	311
Spherically symmetric charge distributions.	B. C. CARLSON 319
Water yield prediction in southern Iowa based on watershed characteristics.	PAUL R. NIXON and GLENN O. SCHWAB 331
An optical density method of measuring phytoplankton standing crop.	LAWRENCE F. SMALL 343
Solar radiation and sunshine in Iowa.	P. J. WAITE and R. H. SHAW 355
Factors affecting the incidence of reaction tissue in <u>Populus deltoides</u> Bartr.	GRAEME P. BERLYN 367



# IOWA STATE JOURNAL OF SCIENCE

Published August, November, February, and May

-----

EDITOR-IN-CHIEF. . . . . R.E. BUCHANAN  
BUSINESS MANAGER. . . . . MARSHALL TOWNSEND

-----

Published under the joint auspices of the graduate faculty of Iowa State University and the local chapter of Sigma Xi. The administrative board for the academic year 1960-61 includes:

## REPRESENTING THE GRADUATE FACULTY

E.A. BENBROOK, Department of Veterinary Pathology  
HESTER CHADDERDON, Department of Home Economics Education  
HARVEY DIEHL, Department of Chemistry  
E.S. HABER, Department of Horticulture  
H.M. HARRIS, Department of Zoology and Entomology  
C.L. HULSBOS, Department of Civil Engineering  
R.W. ORR, The Library  
J.B. PAGE, Dean of the Graduate College (and Chairman of the  
Administrative Board)

## REPRESENTING SIGMA XI

O.E. TAUBER, Department of Zoology and Entomology  
C.H. WERKMAN, Department of Bacteriology

-----

Manuscripts should be submitted to R. E. Buchanan, 316 Curtiss Hall, Iowa State University, Ames, Iowa.

All matters pertaining to subscriptions, remittances, etc., should be addressed to the Iowa State University Press, Press Building, Ames, Iowa. Subscriptions are as follow: Annual \$6.00 (Canada, \$6.50, other foreign countries \$7.00); single copies \$2.00.

-----

Entered as second-class matter January 16, 1935, at the post office at Ames, Iowa, under the Act of March 3, 1879.



SEEDLING EMERGENCE AND GROWTH RESPONSES  
OF DWARF GRAIN SORGHUM AS AFFECTED BY GIBBERELLIC ACID<sup>1</sup>F.P. Gardner and M.J. Kasperbauer<sup>2</sup>

**SUMMARY.** The effects of gibberellic acid (GA) as a seed treatment and as a foliar spray on dwarf grain sorghum were studied under greenhouse and field conditions. Concentrations of 10 ppm or 100 ppm of GA hastened emergence and increased initial height of the plants, but both of these effects were short-lived. The effect of GA as a seed treatment increased with depth of seeding, resulting in a significant GA x depth interaction. However, after a few days, emergence of the untreated equalled the emergence from treated seeds, and the interaction no longer remained. Responses to GA under field conditions and under greenhouse conditions were similar; both supplied conditions that were nearly optimum for growth. GA applied as a seed treatment had no effect on the mature height, lodging, maturity or yield of seed as measured under field conditions. GA applied as a foliar spray had no effect on growth of the sorghum plants or on mature height, lodging, maturity or seed yield. The narrow range of responsiveness during the growth cycle of the dwarf plant was discussed.

---

The potential use of gibberellins in crop production has aroused much attention. Two comprehensive reviews covering a wide range of responses in numerous plant species with this growth stimulant have been prepared (6, 7). The effect of gibberellic acid (GA) on reversal of natural dwarfism has been demonstrated with peas (3), tomatoes (5), Malus (1) and corn (4). A differential response of dwarf varieties or genotypes within species to GA has been reported (4).

Gibberellic acid applied to seeds has resulted in faster seedling emergence (2, 8); however, with cotton the total number of plants that emerged was greatly reduced (2).

Sorghums used for commercial grain production are distinctly dwarf types. Although considerable work has been done on the response of dwarfs to GA in other species, no experiments of this nature on sorghum dwarfs have been reported. On the basis of previous findings with other dwarfs, it might be hypothesized that they would revert to normal growth

---

<sup>1</sup> Contributed from the Agronomy Department, Iowa State University. Journal Paper No. J-3764 of the Iowa Agricultural and Home Economics Experiment Station, Ames, Iowa. Project No. 1321.

<sup>2</sup> Associate Professor of Agronomy, Iowa State University and Graduate Assistant of Agronomy, Botany and Plant Pathology, respectively.

upon GA treatment of sufficient concentration.

It is characteristic of grain sorghum to grow slowly during the early part of the season. Thus, it offers little competition to weeds during early stages of growth, and weed control by row cultivation is difficult due to its small seedling size. Any thing that would hasten growth of the sorghum seedlings during this critical period might be of considerable value in reducing the competitive effects from weeds.

This investigation was conducted to determine the effect of GA on seedling emergence, growth and other responses of dwarf grain sorghum (Sorghum vulgare) under greenhouse and field conditions.

### EXPERIMENTAL PROCEDURE

The first experiment was conducted in a 75°F greenhouse using two entries, R.S. 610 and Reliance, a hybrid and an open-pollinated variety, respectively. Treatments employed were: (1) Six depths of seeding; 1, 2, 3, 4, 5 and 6 inches; (2) Two GA concentrations - 0 ppm (distilled water) and 500 ppm in distilled water. A split-plot design with four replicates was used in which depths and variety x GA combinations constituted the whole plots and subplots, respectively.

The seeds were soaked for 10 hours and allowed to surface dry just prior to planting in a mixture of equal parts of soil and sand on a greenhouse bench. Each treatment was represented by a row of 50 spaced seeds. Emergence was recorded at 2-day intervals, and height was recorded after emergence was complete.

In the first field experiment, GA was used as a seed treatment on R.S. 610 hybrid. The following treatments in all possible combinations were used:

1. GA concentration: 0 (distilled water), 10, 100 ppm and a dry check;
2. Planting depths, 1, 2, and 3 inches.

The field plantings were made on May 31, 1958, using a randomized block design with four replicates. The area selected was a uniform Webster silt loam of high fertility and organic matter. Moisture was excellent at seeding and continued to be favorable throughout the season.

Each treatment was applied to 80 seeds hand-spaced in a 12-foot row spaced 40 inches from adjacent rows. The proper depths of planting were obtained by a specially designed furrow opener. Seeds were soaked for 10 hours and surface dried just prior to planting. Weeds were controlled with mechanical cultivators and pulled by hand from the rows. Emergence was recorded daily, and plant height was measured on a row segment of 20 plants at 5-day intervals during the first month and less frequently thereafter.

The second field experiment employed GA as a foliar spray on young plants of R.S. 610 variety. Experimental conditions and procedures were similar to those previously described. Spray treatments were initiated when the plants had reached a height of about 12 inches. Treatments were as follows: A single application of 0, 100 and 200 ppm and repeated



application using 100 ppm as an initial spray followed by 5 additional weekly applications with a 20 ppm solution of GA. All solutions contained a liquid detergent, and the entire plant surface was completely covered. Drifting of the spray was prevented by the use of a canvas shield. Height measurements were recorded weekly on a row segment of 20 plants.

## RESULTS

### Greenhouse

The effect of GA, as a seed soak, on emergence of R.S.610 hybrid sorghum from the various depths of seeding can be seen in Figure 1.

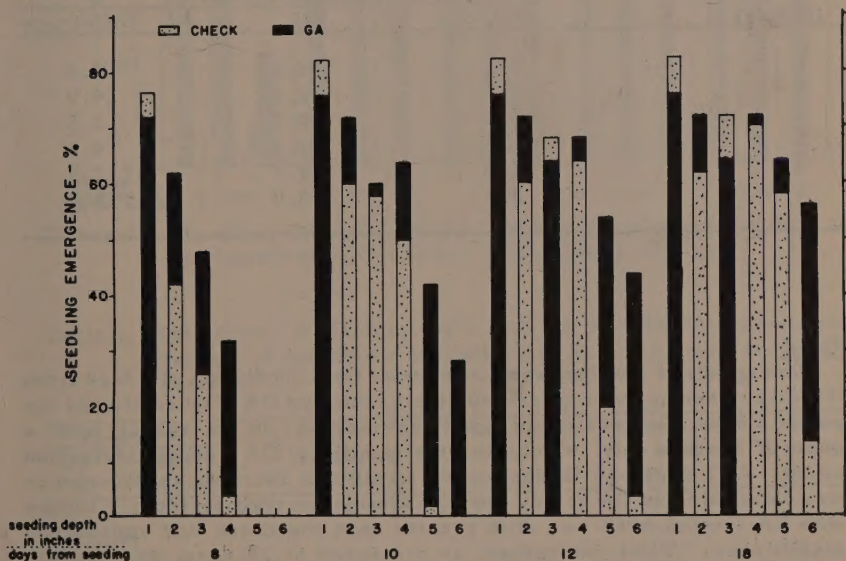


Figure 1. The effect of planting depth and GA as a seed treatment on seedling emergence of R.S.610 grain sorghum in the greenhouse.

Emergence data were not recorded on the Reliance variety due to weak germination with all treatments. The magnitude of response to GA increased with increasing depth of seeding up to 6 inches which resulted in significant GA x depth interaction. At the end of 8 and 10 days, emergence from GA treated seeds of R.S.610 was greater than the checks by a highly significant amount with all seedings deeper than 2 inches. At 10 days, 30% of the GA treated seeds had emerged from 6 inches as contrasted to no emergence from the check seed at this depth. After 18 days no significant difference in emergence existed between the treated and untreated plants at planting depths of 4 inches or less, but emergence of treated seed from 6 inches was almost 5-fold greater than the untreated. The poor emergence of the untreated seed from this depth may

have resulted from seedling diseases and eventual starvation of the seedlings. This condition may have been less pronounced with the rapidly growing sprouts of the GA treated seed.

From Table 1, it can be seen that GA increased plant height by 2.5 to 4.0 inches during the experimental period, irrespective of seedling depth.

Table 1. Comparison of seedling height from GA treated and control seeds of R.S. 610 grain sorghum planted at various depths.

Seeding depth (inches)	Plant Height (inches)		
	Control	GA	Difference
1	9.0	12.5	3.5
2	8.5	12.5	4.0
3	8.0	10.5	2.5
4	8.0	12.0	4.0
5	7.0	9.5	2.5
6	5.0	9.0	4.0

### Field

Emergence of sorghum seedlings under field conditions at 5 days from the date of seeding was increased significantly by GA (Figure 2). At the end of 6 days, GA resulted in significant increase in emergence from a depth of 3 inches only, which caused a significant GA x depth interaction effect. At 7 days and thereafter no significant increase in emergence was obtained from GA at any depth, although emergence from 3 inches with GA treated seed was still greater than the check and approached significance. Total emergence, as measured at 20 days, was significantly less with 100 ppm than from the check and 10 ppm at all depths of planting.

The effect of GA on plant height was likewise short-lived, as can be seen from Figure 3. Gibberellic acid increased height initially, but after 20 days no significant differences were obtained. Increasing seedling depth decreased the height of plants, the effect lasting longer than the GA effect. No significant interactions were obtained.

Table 2 presents the effect of GA and depth of seeding on a number of characters at harvest. Neither GA nor seeding depth had any significant effect on lodgings, number of heads per row, seed yield or maturity.

Since the effect of GA was short-lived where applied as a seed treatment, the second field experiment was designed to apply single and repeated dosages as foliar spray, the results of which are shown in Table 3. No treatment with GA, a single dosage of 100 to 200 ppm or repeated applications to deliver the equivalent of 200 ppm, had any observable effect on plant height, lodging, maturity or seed yields.

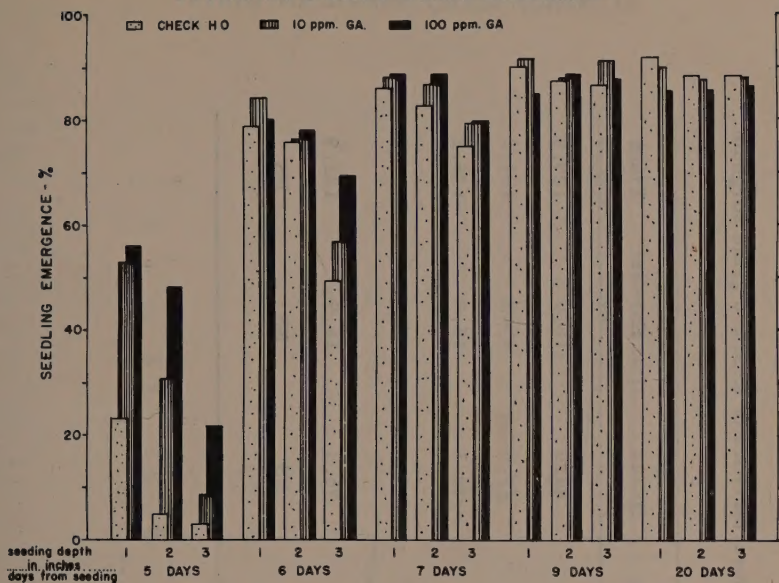


Figure 2. The effect of planting depth and GA as a seed treatment on emergence of R.S. 610 grain sorghum in the field.

Table 3. The effect of planting depth and GA as a seed treatment on a number of agronomic characters in R.S. 610 grain sorghum at harvest.

Treatment		Lodging (%)	Number Heads per row	Moisture in seed (%)	Seed yield (bu/A)
GA	Depth (inches)				
0 ppm	1	19.1	79.5	16.5	137.1
	2	6.9	79.5	13.9	129.1
	3	17.5	78.3	17.1	135.3
	av.	14.5	79.1	15.8	133.8
10 ppm	1	14.3	80.5	16.6	135.3
	2	20.1	82.0	16.6	138.5
	3	11.6	77.8	16.3	126.9
	av.	15.3	80.1	16.5	133.5
100 ppm	1	9.8	76.5	16.2	136.5
	2	14.3	76.7	16.3	128.5
	3	11.5	78.3	16.1	139.6
	av.	11.9	77.2	16.2	134.9
LSD 05		NS	NS	NS	NS



Table 3. The effect of GA as a foliar spray on growth and other characteristics of R. S. 610 grain sorghum.

Treatment	Height (inches)			Lodging (%)	Number Heads per row	Moisture at Harvest (%)	Yield (bu/A)
	Jul. 12*	Jul. 19	Aug. 2				
Check	32.4	43.0	49.7	63.3	80.0	16.0	129.9
100 ppm	32.5	44.7	51.1	63.6	76.0	15.9	134.3
200 ppm	35.6	43.6	50.8	62.8	78.3	15.9	135.2
100 ppm initial + 5 applications							
20 ppm	31.4	43.1	51.1	64.6	76.3	16.9	122.9
LSD 05	NS	NS	NS	NS	NS	NS	NS

\*Date of first spray application.



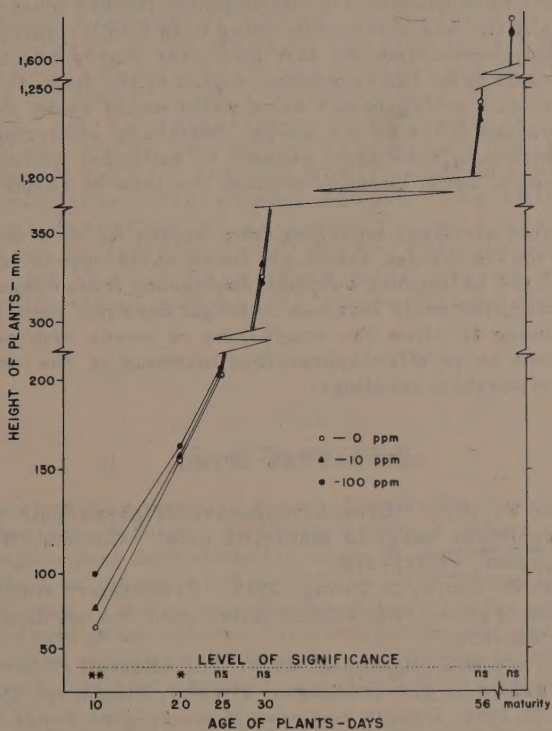


Figure 3. The effect of GA as a seed treatment on seedling height of R.S.610 grain sorghum in the field.

## DISCUSSION

Although the sorghums used in these experiments were dwarf types, they were completely nonresponsive to GA, except in the early seedling stages. Other dwarfs in corn reportedly did not respond to GA (4), and the dwarfing mechanism in sorghum may be similar to the nonresponsive dwarfs in corn. The fact that GA increased the early seedling emergence and height only would suggest that the mesocotyl and perhaps the first and second internodes were affected. Individual internodes were not examined to determine the loci of response, but such an investigation likely would have been enlightening and warrants further investigation.

No response to GA was obtained by using it as a foliar spray on young plants. This may result from the fact that after emergence the mesocotyl, which seems to be the responsive region of the plant, is no longer active. The use of a detergent and warm water would seem to preclude insufficient coverage of GA on the leaves. Naturally occurring GA-like substances, which may have been present in sufficient quantities after the seedling stage, could possibly explain the lack of response to the foliar sprays.

Since untreated seedlings emerging from depths up to 4 inches soon caught up with the GA treated seedlings, there would appear to be little practical use of GA to improve sorghum emergence from deeper planting depths. Likewise, the early increase in height does not appear to offer sufficient advantage to allow the smothering of weeds with soil during early cultivations or to offer appreciable increase in the competitive advantage of the sorghum seedlings.

## LITERATURE CITED

1. Barton, Lela V. 1956. Growth responses of physiologic dwarfs of Malus arnaldiana Sorg. to gibberellic acid. Contrib. Boyce Thompson Inst. 18:311-318.
2. Bradford, W. W. and E. C. Ewing. 1958. Preliminary studies on the application of gibberellic acid to cotton seed and seedlings. Agron. Jour. 50:648-650.
3. Brian, P. W. and H. G. Hamming. 1955. The effect of gibberellic acid on short growth of pea seedlings. Physiol. Plantarum 8:669-681.
4. Phinney, B. O. 1956. Growth response of single-gene dwarf mutants in maize to gibberellic acid. Proc. Natl. Acad. Sci. U.S. 42:185-189.
5. Plummer, T. H. and M. L. Tomes. 1958. Effects of indoleacetic acid and gibberellic acid on normal and dwarf tomatoes. Bot. Gaz. 119:197-200.
6. Stodola, F. H. 1958. Source book on gibberellins 1828-1957. Agr. Res. Service U.S.D.A. Peoria, Illinois.
7. Wittwer, S. H. and M. J. Bukovac. 1957. Gibberellins new chemicals for crop production. Mich. Agric. Exp. Sta. Quart. Bull. 40:203-215-224.



# SPHERICALLY SYMMETRIC CHARGE DISTRIBUTIONS<sup>1</sup>

B.C. Carlson

Institute for Atomic Research and Department of Physics  
 Iowa State University, Ames, Iowa

**SUMMARY.** The classical electrostatic self-energy of a spherically symmetric charge distribution is written as the integral of an energy density that differs from the usual squared electric field strength. This density vanishes in empty space surrounding the charge distribution. It is sometimes a convenient choice for integration, as is shown by two examples of interest in nuclear physics: the harmonic-well distribution and the distribution with Fermi shape. The self-energy of the Fermi distribution is given to good accuracy by a polynomial of fifth degree in the skin thickness. The form of the energy density is generalized to be valid for distributions not having spherical symmetry.

- - - - -

## I. INTRODUCTION

In a spherically symmetric charge distribution the electric field at radius  $r$  is produced only by the charges inside a sphere of that radius, and the magnitude of the field is  $1/r$  times the potential of these charges alone. The total potential is  $\phi(r) = \phi'(r) + \phi''(r)$ , where  $\phi'(r) = rE(r)$  is the potential due to these inner charges and  $\phi''(r)$  is the potential due to the charges outside the sphere. The electrostatic self-energy of the distribution can be written as the integral over all space of a nonnegative energy density, usually taken to be (in rationalized mks units)  $(\epsilon_0/2) E^2 = (\epsilon_0/2)(\phi'/r)^2$ .

This expression for energy density is not unique, for the spatial location of the energy has no physical significance. We shall show in Sec. II that another choice of energy density is  $(\epsilon_0/2)(\phi''/r)^2$ , a function that vanishes outside a sphere enclosing all the charges. This function is sometimes particularly easy to integrate; as a simple example the classical self-energy is calculated in Sec. III for a harmonic-well distribution, which is often used to represent the charge of a very light nucleus. A less trivial integration is carried out in Sec. IV to find the self-energy of a Fermi distribution, frequently used for medium and

<sup>1</sup> Work was performed in the Ames Laboratory of the U. S. Atomic Energy Commission.

heavy nuclei. A more general form of the second choice of energy density, valid for distributions that are not spherically symmetric, is given in Sec. V.

## II. POTENTIAL AND SELF-ENERGY OF A SPHERICALLY SYMMETRIC DISTRIBUTION

In this section we derive expressions for the potential, self-energy, and energy density in terms of  $\phi''(r)$ , henceforth called  $\tau(r)$  and defined mathematically in Eq. (2.2a). The results are given by Eqs. (2.3a), (2.5a) and (2.6a). It is instructive to carry along in parallel the derivation of familiar expressions for the same quantities in terms of the electric field  $E(r)$ . The two sets of equations will be distinguished by letters following the equation numbers.

Two equivalent forms of Poisson's equation for a spherically symmetric distribution are (in rationalized mks units):

$$\frac{1}{r} \frac{d^2}{dr^2} r\phi = -\rho/\epsilon_0, \quad (2.1a)$$

$$\frac{1}{r^2} \frac{d}{dr} r^2 \frac{d\phi}{dr} = -\rho/\epsilon_0. \quad (2.1b)$$

The first integrals of these equations define the quantities  $\tau$  and  $E$ :

$$\tau(r) = \frac{d}{dr} (r\phi) = \frac{1}{\epsilon_0} \int_r^\infty \rho(r') r' dr', \quad (2.2a)$$

$$E(r) = -\frac{d\phi}{dr} = \frac{1}{\epsilon_0 r^2} \int_0^r \rho(r') r'^2 dr'. \quad (2.2b)$$

We have used the boundary conditions that  $\tau$  vanishes at large distances and that  $E$  vanishes at the origin. The quantity  $\tau(r)$ , previously denoted by  $\phi''(r)$ , is the potential at  $r$  due to charges outside a sphere of radius  $r$ : the potential due to these charges has the same value at the surface of the sphere that it has at the origin, where the contribution from a shell of radius  $r' > r$  is clearly

$$\rho(r') \cdot r'^2 \cdot dr' / \epsilon_0 r'.$$

A second integration gives the potential

$$\phi(r) = \frac{1}{r} \int_0^r \tau(r') dr', \quad (2.3a)$$



$$\phi(r) = \int_r^{\infty} E(r') dr' . \quad (2.3b)$$

Alternatively, by combining Eqs. (2.2), we obtain the expected relation

$$\phi = \frac{d}{dr} (r\phi) - r \frac{d\phi}{dr} = \tau + rE = \phi'' + \phi' . \quad (2.3c)$$

In the limit of large  $r$ , Eq. (2.3a) shows that the total charge is related to  $\tau$  by the equation

$$Q = 4\pi\epsilon_0 \int_0^{\infty} \tau(r) dr ;$$

integration by parts converts this to the usual integral for  $Q$ .

The electrostatic self-energy of the distribution is

$$U = \frac{1}{2} \int \rho\phi \, d\underline{r} = 2\pi \int_0^{\infty} \rho\phi \, r^2 dr . \quad (2.4)$$

We replace  $\rho$  by the left sides of Eqs. (2.1) and integrate by parts:

$$U = -2\pi\epsilon_0 \int_0^{\infty} r\phi \, \frac{d^2}{dr^2} (r\phi) \, dr = 2\pi\epsilon_0 \int_0^{\infty} \tau^2 \, dr , \quad (2.5a)$$

$$U = -2\pi\epsilon_0 \int_0^{\infty} \phi \, \frac{d}{dr} \left( r^2 \frac{d\phi}{dr} \right) \, dr = 2\pi\epsilon_0 \int_0^{\infty} (rE)^2 dr . \quad (2.5b)$$

Eq. (2.5b) states the familiar result that  $(\epsilon_0/2)E^2$  may be regarded as a density of electrostatic energy; Eq. (2.5a) shows that a second non-negative quantity,  $(\epsilon_0/2)(\tau/r)^2$ , may also be regarded as an energy density when spherical symmetry is present. (The general case, without spherical symmetry, is discussed in Sec. V.) The contrast between these two energy densities illustrates the point, emphasized by Mason and Weaver (1), that the spatial distribution of electromagnetic energy has no physical significance. As an example we consider a uniform distribution filling the interior of a sphere. According to the conventional choice, the energy density decreases as  $r^{-4}$  outside the sphere, and only one-sixth of the total energy is located inside the sphere. On the other hand, since  $\tau$  vanishes outside the limits of a charge distribution that is confined to a bounded region of space, the density  $(\epsilon_0/2)(\tau/r)^2$  assigns all the energy to the regions occupied by charge.

Two more expressions for the total energy, no longer having integrands with a definite sign, are obtained by integrating Eqs. (2.5) by parts:

$$U = -2\pi\epsilon_0 \int_0^\infty r \frac{d}{dr} (\tau^2) dr = 4\pi \int_0^\infty \tau \rho r^2 dr, \quad (2.6a)$$

$$U = 2\pi\epsilon_0 \int_0^\infty \frac{1}{r} \frac{d}{dr} (r^2 E)^2 dr = 4\pi \int_0^\infty E \rho r^3 dr. \quad (2.6b)$$

The equivalence of expressions (2.6a) and (2.6b) can be seen directly: if they are written as double integrals by using the integral definitions of  $\tau$  and  $E$ , they differ from each other only in the order of integration. A common expression for  $U$ , usually obtained by substituting Eq. (2.3c) in Eq. (2.4), is half the sum of Eqs. (2.6a) and (2.6b).

The integral in Eq. (2.6b) is readily understood as the work done in assembling the charge distribution by adding spherical shells of progressively larger radius:  $4\pi\rho r^2 dr$  is the charge contained in a shell,  $rE$  is the potential at radius  $r$  due to the previously assembled shells of lesser radius, and their product is the increment of work. Equation (2.6a) has an exactly similar interpretation, in which one assembles shells of progressively smaller radius.

### III. THE HARMONIC-WELL DISTRIBUTION

The use of Eq. (2.5a) or (2.6a) instead of Eq. (2.5b) or (2.6b) sometimes shortens the calculation of the self-energy. A Gaussian distribution of charge furnishes an example; so also does a "harmonic-well distribution," which includes a Gaussian distribution as a special case. The charge density is

$$\rho(r) = \rho_0 \left(1 + \beta \frac{r^2}{a^2}\right) e^{-r^2/a^2}, \quad (3.1)$$

and the total charge is

$$Q = \pi^{3/2} \rho_0 a^3 \left(1 + \frac{3}{2} \beta\right), \quad (3.2)$$

Eq. (3.1) is a useful approximation for the charge distribution in very light nuclei ( $A \leq 16$ ) having spherical symmetry, the parameter  $\beta$  being one-third the number of protons in the  $p$ -shell of a harmonic oscillator potential (2).

The electric field is found from Eq. (2.2b) to be

$$E(r) = \frac{\rho_0 a^3}{2\epsilon_0} \frac{1}{r^2} \left[ \gamma \left( \frac{3}{2}, \frac{r^2}{a^2} \right) + \beta \gamma \left( \frac{5}{2}, \frac{r^2}{a^2} \right) \right],$$



where the incomplete gamma function is

$$\gamma(s, x) = \int_0^x t^{s-1} e^{-t} dt.$$

The quantity  $\tau$  happens to be simpler in this case:

$$\tau(r) = \frac{\rho_0 a^2}{2\epsilon_0} \left(1 + \beta + \beta \frac{r^2}{a^2}\right) e^{-r^2/a^2}. \quad (3.3)$$

(On the other hand,  $E$  would be simpler if the charge density were a Gaussian multiplied by a polynomial of odd degree in  $r$ .) By substituting in Eq. (2.5a) or (2.6a) and using the complete gamma function, we quickly obtain

$$U = \frac{\rho_0 a^5}{2\epsilon_0} \left(\frac{\pi}{2}\right)^{3/2} \left(1 + \frac{5}{2}\beta + \frac{27}{16}\beta^2\right). \quad (3.4)$$

The central density,  $\rho_0$ , can be eliminated by using Eq. (3.2) to form the ratio  $U/Q^2$ , which depends only on the shape of the distribution.

#### IV. THE FERMI DISTRIBUTION

Several recent studies of nuclear Coulomb energies (3, 4, 5, 6) have included the effects of a diffuse nuclear surface by assuming a trapezoidal distribution of charge. (The density of a trapezoidal distribution is constant in an interior region and then decreases to zero as a linear function of radius in a surface region; although the density is a continuous function, its slope is discontinuous.) A similar but more realistic charge distribution, having no discontinuities in its derivatives, is the Fermi model, which has been used in analyzing much of the electron scattering data. Although the calculation of self-energy for a Fermi distribution involves some integrals that are not elementary, we shall find in this section that the final result has a simple form. Like the self-energy of a trapezoidal distribution it is given, to high accuracy, by a polynomial of fifth degree in the thickness of the surface region. Only the classical part of the Coulomb energy is being considered here; the Coulomb energy of a physical nucleus includes quantum-mechanical corrections for exchange and other correlation effects.

The density in the Fermi model is represented by a Fermi function:

$$\rho(r) = \rho_0 \left[1 + e^{(r-a)/b}\right]^{-1}. \quad (4.1)$$

As the parameter  $b$  approaches zero, the density approaches a uniform distribution with radius  $a$ . The density is 90% of  $\rho_0$  at a radius of  $a - b \ln 9$ , 50% at  $a$ , and 10% at  $a + b \ln 9$ . The distance between the 90% and 10% points, often called the skin thickness, is  $2b \ln 9 = 4.39 b$ . Hofstadter

and collaborators have determined the skin thickness and the radius  $a$  of nuclear charge distributions by measuring the nuclear scattering of high-energy electrons (2):

$$a = (1.07 \pm 0.02) A^{\frac{1}{3}} \times 10^{-13} \text{ cm},$$

$$4.39 b = (2.4 \pm 0.3) \times 10^{-13} \text{ cm}.$$

We observe that  $a/b$  is approximately  $2A^{\frac{1}{3}}$ ; even for a nucleus as light as  $\text{Ca}^{40}$  its value is 6.8 and the value of  $\exp(-a/b)$  is 0.001. These numbers will guide us in making approximations; also, they show that the central density is nearly  $\rho_0$ .

The total charge is

$$Q = 4\pi\rho_0 \int_0^{\infty} [1 + e^{(r-a)/b}]^{-1} r^2 dr.$$

Taking  $(r-a)/b$  as a new variable, we obtain

$$Q = 4\pi\rho_0 a^2 b [f_1(-\lambda) + 2\lambda^{-1} f_2(-\lambda) + \lambda^{-2} f_3(-\lambda)], \quad (4.2)$$

where

$$\lambda = a/b, \quad (4.3)$$

$$f_s(x) = \int_x^{\infty} \frac{t^{s-1} dt}{e^t + 1}. \quad (4.4)$$

The function  $f_s$ , differing from a Debye function only by the sign in the denominator, is a species of incomplete Riemann zeta function:

$$f_s(0) = (s-1)! (1 - 2^{1-s}) \zeta(s), \quad (4.5)$$

$$\zeta(s) = \sum_{n=1}^{\infty} \frac{1}{n^s}. \quad (4.6)$$

The numbers  $f_s(-x)$  and  $f_s(x)$  are related by

$$f_s(-x) = [1 + (-1)^s] f_s(0) + (-1)^{s+1} [x^s/s + f_s(x)] \quad (4.7)$$

To prove this, one separates that part of the integral for  $f_s(-x)$  that extends from  $-x$  to 0, changes the sign of the integration variable, and uses the identity

$$(e^{-x} + 1)^{-1} = 1 - (e^x + 1)^{-1}.$$



Eq. (4.7) shows that  $Q$  can be written in terms of  $f_s(\lambda)$ , where  $\lambda$  is positive and large compared to unity. For positive  $x$ , the denominator of Eq. (4.4) can be expanded in powers of  $\exp(-t)$ . Integrating term by term, we obtain  $f_s(x)$  as a series of incomplete gamma functions:

$$f_s(x) = x^{s-1} \sum_{n=1}^{\infty} \frac{(-1)^{n+1}}{n} e^{-nx} {}_2F_0(1-s, 1, -1/nx), \quad (4.8)$$

$${}_2F_0(\alpha, \beta, z) = 1 + \alpha\beta z + \alpha(\alpha+1)\beta(\beta+1) z^2/2! + \cdots \quad (4.9)$$

The latter series terminates when  $\alpha$  is a negative integer; because we deal with positive integral  $s$ , the  ${}_2F_0$  series in Eq. (4.8) is a polynomial in  $1/x$ .

Recalling that  $\exp(-\lambda) \lesssim 0.001$ , we shall henceforth drop all terms of order  $\exp(-2\lambda)$ ; for example,

$$\begin{aligned} f_s(\lambda) &\rightarrow e^{-\lambda} \lambda^{s-1} {}_2F_0(1-s, 1, -1/\lambda) \\ &= (s-1)! e^{-\lambda} \sum_{r=0}^{s-1} \frac{\lambda^r}{r!} \end{aligned} \quad (4.10)$$

Even the terms of order  $\exp(-\lambda)$  are unimportant, but will be retained to permit an accurate estimate of the error made by discarding them. With this approximation we find from Eqs. (4.2) and (4.7) that the total charge is

$$\begin{aligned} Q &= 4\pi\rho_0 a^3 \left[ \frac{1}{3} + 2\lambda^{-2} \zeta(2) + 2\lambda^{-3} e^{-\lambda} \right] \\ &= \frac{4\pi\rho_0 a^3}{3} \left[ 1 + \left(\frac{\pi b}{a}\right)^2 + 6\left(\frac{b}{a}\right)^3 e^{-a/b} \right] \end{aligned} \quad (4.11)$$

An entirely similar calculation shows that the mean square radius of the distribution is

$$\begin{aligned} \langle r^2 \rangle &= \frac{4\pi}{Q} \int_0^{\infty} \rho(r) r^4 dr \\ &= \frac{4\pi\rho_0 a^5}{5Q} \left[ 1 + \frac{10}{3} \left(\frac{\pi b}{a}\right)^2 + \frac{7}{3} \left(\frac{\pi b}{a}\right)^4 + 120 \left(\frac{b}{a}\right)^5 e^{-a/b} \right] \\ &= \frac{3a^2}{5} \left[ 1 + \frac{7}{3} \left(\frac{\pi b}{a}\right)^2 - 6 \left(\frac{b}{a}\right)^3 e^{-a/b} \right] \end{aligned} \quad (4.12)$$

In the last line, terms of order  $(b/a)^5 \exp(-a/b)$  have been dropped.

In calculating the self-energy, we find that the quantity

$$\tau(r) = \frac{\rho_0 b}{\epsilon_0} \left[ a f_1 \left( \frac{r-a}{b} \right) + b f_2 \left( \frac{r-a}{b} \right) \right]$$

is simpler than  $E(r)$ , which involves also  $f_3$ . Substitution in Eq. (2.5a) and change of integration variable lead to

$$\begin{aligned} U &= \frac{2\pi\rho_0^2 a^2 b^3}{\epsilon_0} \int_{-\lambda}^{\infty} [f_1(x) + \lambda^{-1} f_2(x)]^2 dx \\ &= \frac{2\pi\rho_0^2 a^2 b^3}{\epsilon_0} (K_{11} + 2\lambda^{-1} K_{12} + \lambda^{-2} K_{22}), \end{aligned} \quad (4.13)$$

where

$$K_{rs} = \int_{-\lambda}^{\infty} f_r(x) f_s(x) dx. \quad (4.14)$$

We shall calculate  $K_{11}$  and give only the results of applying the same method to  $K_{12}$  and  $K_{22}$ . The first step is to write

$$K_{11} = J_{11} + \int_0^{\lambda} [f_1(-x)]^2 dx, \quad (4.15)$$

where the number

$$J_{rs} = \int_0^{\infty} f_r(x) f_s(x) dx \quad (4.16)$$

is independent of  $\lambda$ . Substituting

$$f_1(-x) = x + f_1(x)$$

from Eq. (4.7), we obtain

$$K_{11} = J_{11} + \lambda^3/3 + 2 \int_0^{\lambda} x f_1(x) dx + \int_0^{\lambda} [f_1(x)]^2 dx. \quad (4.17)$$

The last term is equal to

$$J_{11} - \int_{\lambda}^{\infty} [f_1(x)]^2 dx;$$

this reduces to  $J_{11}$  by Eq. (4.10) because we neglect terms of order  $\exp(-2\lambda)$ . (Similarly  $K_{22}$  contains  $J_{22}$  twice, but  $K_{12}$  contains  $J_{12}$  twice with opposite signs.) The remaining integral in Eq. (4.17) is a special case of

$$(m+1) \int_0^\lambda x^m f_s(x) dx = f_{s+m+1}(0) - f_{s+m+1}(\lambda) + \lambda^{m+1} f_s(\lambda). \quad (4.18)$$

To prove this, one integrates by parts and uses the relation

$$x^{m+1} \frac{df_s}{dx} = \frac{df_{s+m+1}}{dx}. \quad (4.19)$$

Again dropping terms of order  $\exp(-2\lambda)$  by use of Eq. (4.10), we have

$$K_{11} = \frac{1}{3} \lambda^3 + 2J_{11} + \frac{3}{2} \zeta(3) - 2e^{-\lambda}(\lambda+1). \quad (4.20)$$

The results for  $K_{12}$  and  $K_{22}$  are

$$K_{12} = -\frac{1}{8} \lambda^4 + \frac{1}{2} \zeta(2) \lambda^2 + \frac{1}{2} [\zeta(2)]^2 - \frac{7}{2} \zeta(4) + e^{-\lambda} \left[ \frac{3}{2} \lambda^2 + 4\lambda + 4 - \zeta(2) \right], \quad (4.21)$$

$$K_{22} = \lambda^5/20 - \frac{1}{3} \zeta(2) \lambda^3 + [\zeta(2)]^2 \lambda + 2J_{22} + \frac{15}{2} \zeta(5) - 3\zeta(2) \zeta(3) - e^{-\lambda} [\lambda^3 + 4\lambda^2 + 8\lambda + 8 - 2\zeta(2)(\lambda+2)]. \quad (4.22)$$

Substitution of these expressions in Eq. (4.13) shows that  $U$  is a polynomial of fifth degree in  $1/\lambda$  plus a remainder consisting of exponential terms:

$$U = \frac{2\pi \rho_0^2 a^5}{\epsilon_0} \left[ \frac{2}{15} + \sum_{n=2}^5 B_n \lambda^{-n} + R(\lambda) \right],$$

$$B_2 = \frac{2}{3} \zeta(2), \quad B_4 = 2[\zeta(2)]^2 - 7\zeta(4),$$

$$B_3 = 2J_{11} + \frac{3}{2} \zeta(3), \quad B_5 = 2J_{22} + \frac{15}{2} \zeta(5) - 3\zeta(2)\zeta(3),$$

$$R(\lambda) = 2\lambda^{-3} e^{-\lambda} - 4[2 - \zeta(2)] \lambda^{-5} e^{-\lambda}. \quad (4.23)$$



The zeta-function is tabulated (7); we have converted  $J_{11}$  to the integral shown below, which can be evaluated analytically although we have not found it in tables of definite integrals; and we have converted  $J_{22}$  to an infinite series and summed it numerically:

$$\zeta(2) = \pi^2/6,$$

$$\zeta(4) = \pi^4/90,$$

$$\zeta(3) = \pi^3/25.794,$$

$$\zeta(5) = \pi^5/295.12,$$

$$J_{11} = \int_0^1 [\ln(1+t)]^2 t^{-1} dt = \frac{1}{4} \zeta(3),$$

$$J_{22} = 12 \sum_{n=1}^{\infty} \frac{(-1)^{n+1}}{(n+1)^4} \sum_{m=1}^n \frac{1}{m} + 4 \sum_{n=1}^{\infty} \frac{(-1)^{n+1}}{(n+1)^3} \sum_{m=1}^n \frac{1}{m^2}$$

$$= 0.587 + 0.371 = 0.958.$$

The self-energy of a Fermi distribution is therefore

(4.24)

$$U = \frac{4\pi\rho_0^2 a^5}{15\epsilon_0} \left[ 1 + \sum_{n=2}^5 A_n \left(\frac{\pi b}{a}\right)^n + 15\left(\frac{b}{a}\right)^3 e^{-a/b} P\left(\frac{b}{a}\right) + \dots \right],$$

$$A_2 = 5/6$$

$$A_3 = 0.5815$$

$$A_4 = -1/6$$

$$A_5 = 0.0922$$

$$P(b/a) = 1 - 0.71 (b/a)^2.$$

The terms omitted from Eq. (4.24) are of order  $\exp(-2a/b)$ .

For  $a/b = 6.8$  the term in  $b^5$  is 0.002 times the leading term, whereas the exponential term is  $5 \times 10^{-5}$  times the leading term. Hence the polynomial by itself is an excellent approximation in the interesting range of parameters. The same remark applies to the total charge in Eq. (4.11) and to the mean square radius in Eq. (4.12). The ratio  $Q^2/U$  obtained from Eqs. (4.11) and (4.24) agrees with the value given to terms of order  $b^2$  by Moszkowski (8).

Equation (4.24) bears a close resemblance to the self-energy of a trapezoidal distribution, which is also a polynomial of fifth degree (4).

## V. ENERGY DENSITY OF A GENERAL DISTRIBUTION

It is natural to ask whether the energy density  $(\epsilon_0/2)(\tau/r)^2$  can be generalized to distributions not having spherical symmetry. A simple extension of

$$\tau = \frac{d}{dr} (r\phi) = \phi - rE$$

is the vector

$$\underline{\tau} = \nabla (r\phi) = \frac{\underline{r}}{r} \phi - r\underline{E}. \quad (5.1)$$

When spherical symmetry is present,  $\underline{\tau}$  is in the radial direction and has magnitude  $\tau$ .

With no assumption of symmetry we have

$$\begin{aligned} (\underline{\tau}/r)^2 &= \left( \frac{\underline{r}}{r^2} \phi - \underline{E} \right)^2 \\ &= E^2 + \frac{\phi^2}{r^2} - 2 \frac{\underline{r}}{r^2} \cdot \underline{E} \phi \\ &= E^2 + \phi^2 \nabla \cdot \left( \frac{\underline{r}}{r^2} \right) + \frac{\underline{r}}{r^2} \cdot \nabla (\phi^2) \\ &= E^2 + \nabla \cdot \left( \frac{\underline{r}}{r^2} \phi^2 \right). \end{aligned}$$

By use of the divergence theorem it follows that  $(\epsilon_0/2)(\underline{\tau}/r)^2$  is an energy density in the general case:

$$U = \frac{\epsilon_0}{2} \int d\underline{r} E^2 = \frac{\epsilon_0}{2} \int d\underline{r} (\underline{\tau}/r)^2. \quad (5.2)$$

Unlike  $\underline{E}$ , the vector  $\underline{\tau}$  depends on the choice of origin and is somewhat artificial unless a natural origin is present because of symmetry.

## ACKNOWLEDGMENTS

I should like to thank several colleagues for helpful criticisms and comments, especially Professor L. J. Laslett for suggesting the physical interpretation of Eq. (2.6a) and for checking the value of a numerical series.

## REFERENCES

1. Mason, M. and W. Weaver. 1929. The Electromagnetic Field. pp.162, 267. Dover Publications, New York.
2. Ravenhall, D.G. 1958. Revs. Modern Phys. 30:430.
3. Cameron, A.G.W. 1957. Can. Jour. Phys. 35:1021.
4. Gunter, W.D. Jr., and R.A. Hubbs. 1959. Phys. Rev. 113:252.
5. Cherry, R.D. 1959. Phys. Rev. 115:1243.
6. Mozer, F.S. 1959. Phys. Rev. 116:970.
7. Adams, E.P. 1922. Smithsonian Mathematical Formulae and Tables of Elliptic Functions, p.140. Smithsonian Institution, Washington, D.C.
8. Moszkowski, S.A. 1957. Models of Nuclear Structure. Handbuch der Physik. 39:417. Springer, Berlin.



WATER YIELD PREDICTION IN SOUTHERN IOWA  
BASED ON WATERSHED CHARACTERISTICS<sup>1</sup>

Paul R. Nixon<sup>2</sup> and Glenn O. Schwab<sup>3</sup>

**SUMMARY.** A simple, rational approach for estimating the water yield of a watershed was developed. The watershed rating obtained by this method is dependent upon measurement and observation of five physical characteristics (climate, soil, land slope, land use, and management and conservation practices). Factors used in determining watershed rating were assigned to these physical characteristics (for southern Iowa conditions) on the basis of experimental data and general observations. The necessity of restricting a given set of factors to a single physiographic region is recognized. A comparison was made, for each of five Iowa watersheds, of water yield estimated from physical characteristics with the measured yield. The estimated median yield from watersheds 525-9,850 acres was within about 12 per cent of the measured median yield. This close agreement is an indication of the usefulness of the method as a means of predicting yield from small ungauged watersheds.

Introduction

Impounded surface runoff for city water supplies and for livestock, domestic, and irrigation needs on farms is becoming increasingly important in southern Iowa. The inability to develop suitable wells in much of the upland area points to the need for water yield (volume of runoff) estimates for the design of storage reservoirs. A generalized picture of water yield from large watersheds is available in the form of published stream flow records. The apparent large yield differences from watersheds in the same locality created the stimulus for this study of the factors that govern water yield.

Investigation

Procedure

The first phase of the investigation included the examination of avail-

<sup>1</sup> Journal Paper No. J-3966 of the Iowa Agricultural and Home Economics Experiment Station, Ames, Iowa. Project No. 1247.

<sup>2</sup> Project leader, ARS-USDA, Lompoc, California, formerly Research Associate.

<sup>3</sup> Professor, Agricultural Engineering, Ohio State University, Columbus, Ohio, formerly Professor of Agricultural Engineering.

able data from Iowa and adjoining states, pertaining to the effect of physical watershed characteristics on water yield. (The term yield, as used in this paper, denotes long term total volume of runoff per unit area.) On the basis of these records, factors were developed for climate, land use, slope, soil, and management and conservation practices. These were considered the most important physical characteristics affecting water yield from small watersheds in southern Iowa. A method was developed for combining these factors to form a watershed rating from which the relative yield of the watershed can be computed.

The second phase involved the investigation of five Iowa watersheds, varying from 525 to 9,850 acres in size, for which reliable estimates of yield could be made from existing stream flow or other records. Land use, slope, soil, and management and conservation practices on these watersheds were determined in considerable detail in the field. Each of these characteristics were divided into several subclasses and the percentage of the watershed area in each subclass was determined. A factor (weighted average of the subclasses) was computed for each physical characteristic of the watershed. The yield rating of each watershed was determined by the product of the weighted averages times the climatic factor (as determined by geographic location).

As a third phase, stream flow data or runoff volume estimated from reservoir records was analyzed for the five watersheds mentioned above. Finally, the yields as estimated by the watershed rating method were compared with measured yield.

#### Physical watershed characteristics

The physical characteristics that control yield were presumed to be: climate (geographical location), land use, land slope, soil, and management and conservation practices. The effect on yield of each physical characteristic was assumed to be independent of the others. Watersheds were rated according to their ability to produce water yield by determining the product of the factors assigned to each watershed characteristic. The following rational equation expresses this relationship:

$$Y = C L S K M$$

where Y = rating of watershed according to its relative ability to produce water yield,  
C = climatic factor,  
L = land use factor,  
S = steepness of slope factor,  
K = soil factor, and  
M = land management and conservation practices factor.

In the application of the above equation to southern Iowa watersheds, factors for each physical characteristic were chosen with respect to an index watershed whose factor for each characteristic is 1.0. Thus, the watershed rating of the index watershed is 1.0 (product of the factors assigned to the characteristics). Physical characteristics which tended to produce yields less than that of the index watershed were assigned to factors less than 1.0, similarly high yielding conditions were assigned

factors greater than 1.0. The median annual yield of the index watershed is 5.80 inches. The median annual yield of any other watershed may be determined by multiplying its rating by 5.80 inches.

An attempt was made to assign to each characteristic, a numerical factor which directly reflected the effect of that condition on the water yield. Inasmuch as some characteristics appear to have a greater effect on water yield than others, the range of values reflect the importance of the factor.

**Climate.** The effect of climate on water yield in the Midwest was determined from published precipitation, evaporation, and water yield maps (U.S. Department of Agriculture, 1941; Horton, 1943; Brune, 1948; Langbein et al., 1949). A comparison of the data suggested that the mean water yield at a given location in the Midwest can be predicted from the mean annual precipitation and mean annual evaporation. However, for a particular watershed unusual features of topography, geology, soil, and land use may result in large deviations from the expected yield.

The precipitation-evaporation-yield pattern of southern Iowa fits into the general pattern of the Midwest. Figure 1 shows the general pattern of distribution of mean annual precipitation and mean annual pan evaporation in southern Iowa. Within each segment formed by "equal depth lines," the estimated mean annual yield was noted. The estimated yield was based upon stream flow records (Iowa Geological Survey, 1953).



Figure 1. Generalized pattern of mean annual precipitation and mean annual pan evaporation in southern Iowa.

A climatic factor map (Figure 2) was prepared from the information shown in Figure 1. This was done by arbitrarily assuming the index watershed, where climatic factor is 1.0, is located in south-central Iowa. As illustrated by Figure 2, the climatic factor decreases to the west and increases to the east from this central location.

Rather than showing the climatic factors of Figure 2 in direct relation to the mean annual yields of Figure 1, the climatic factors were reduced by 10% toward the east and increased by 10% toward the west. This was done in an attempt to more closely represent the influence of climate alone by discounting the effect of soil changes on water yield. Riecken



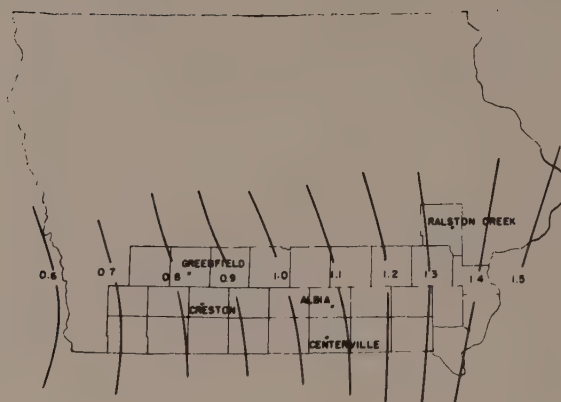


Figure 2. Climatic factor map for southern Iowa.

and Smith (1949) show a tendency for decreased infiltration and permeability from west to east in southern Iowa. The 10% correction was selected on the basis of soil factors to be discussed later. Neither topography nor land use show much change across southern Iowa (Riecken and Smith, 1949; Iowa State Department of Agriculture, 1952).

**Land use.** Land use factors were based on data collected by Browning *et al.* (1948) and Smith *et al.* (1945). Because the data were collected from small erosion and runoff plots and from very small watersheds, the quantitative results serve only as an indication of the effect of land use on water yield from larger areas. Figure 3 shows the effect of land use on total runoff for a period of ten years at the Clarinda, Iowa, and at the Bethany, Missouri, conservation experiment stations. The land use classifications, shown in bold print with corresponding factors will be referred to later in computing the weighted land use factor.

**Slope.** In this study the effect of land slope upon water yield is based largely on experimental plot data reported by Hays, McCall, and Bell (1949) and Hays (1955). Because information on the effect of land slope is very limited, the data provides only a rough approximation. The site conditions at La Crosse, Wisconsin, where the data were collected, are unlike southern Iowa with respect to climate and geology.

A slope factor curve used for predicting water yield in southern Iowa is shown in Figure 4. This curve is a logarithmic function of slope. A plot of the La Crosse data is shown for comparison. The factors for slopes below about 8% were reduced because of the increasing importance of surface storage on flat slopes and the probability of higher infiltration rates on slopes below 2% (Duley and Kelley, 1939). This gain in soil moisture on flat slopes may result in increased evapo-transpiration rather than increase in ground water flow.

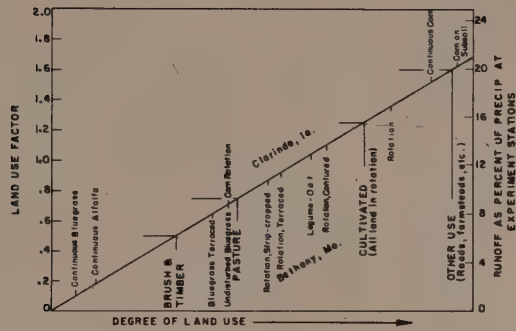


Figure 3. Estimated effect of land use on water yield.

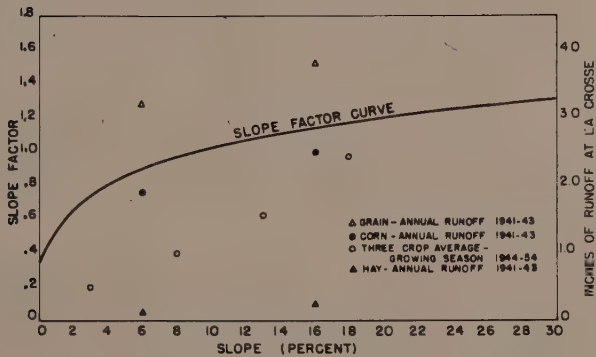


Figure 4. Estimated effect of land slope on water yield.

Table 1. Estimated effect of soil on water yield.

Soil	Estimated infiltration rate (in./hr.)	Relative permeability of subsoil	Typical depth topsoil (ft.)	Internal aeration	Soil factor
Judson-Wabash	0.8-1.3	(variable - colluvial and alluvial soil)			0.6
Fayette	0.5-1.0	moderate	0.7	good	0.7
Sharpsburg	0.4-0.6	slow-moderate	1.1	fair	0.8
Winterset	0.3-0.5	slow-moderate	1.3	poor	0.8
Haig	0.3-0.5	very slow-slow	1.3	poor-fair	1.0
Grundy	0.2-0.4	very slow-slow	1.0	poor-fair	1.1
Shelby	0.2-0.4	very slow-slow	0.7	fair-good	1.1
Lindley	0.2-0.4	very slow	0.7	poor-good	1.2
Weller	0.2-0.4	very slow	0.8	poor-fair	1.3
Seymour	0.2-0.4	very slow	1.2	poor-fair	1.3
Edina	0.2-0.3	very slow	1.2	poor	1.4

Soil. The effect of different soil conditions upon water yield must, in the absence of controlled field observations be approximated from physical measurements of the soil. The factors selected for some southern Iowa soils, as shown in Table 1, were based on infiltration rate, subsoil permeability, depth of topsoil, and internal aeration. Textural classification of these soils falls into one or more of the following classifications: loam, silt loam and silty clay loam. No correlation is apparent between the factor assigned and either soil texture or the soil parent material.

Management and conservation practices. Conservation practices, such as contouring, strip cropping, and terracing have an appreciable effect on total runoff from small plots (Browning et al., 1948; Hays, McCall, and Bell, 1949; and Smith et al., 1945). However, little experimental data are available regarding the effect on water yield from watersheds of such complex and interdependent land conditions as erosion history, cropping history, erosion control, cultural operations, and level of soil fertility. Management-conservation factors were picked for the five watersheds studied, by judgment based upon a knowledge of the watersheds. Table 2 shows the values chosen and the conditions influencing selection.

#### Watershed rating

Five watersheds under 9,850 acres were selected for making a comparison of measured water yield with yield estimated by watershed characteristics. These were Ralston Creek and the watersheds which serve the Albia, Centerville, Creston, and Greenfield municipal reservoirs (see Fig. 2). The first step in developing the watershed yield rating was to determine, by field investigation, the proportion of the watershed occurring in the various subclasses of land use, slope, soil, and management and conservation. A weighted average was then determined for each characteristic. Table 3 illustrates the method by the use of the data for the Centerville watershed. The same procedure was followed for each of the other watersheds.



Table 2. Land management and conservation effect on water yield.

Watershed	Conservation practices	Soil productiveness	Pasture management	Weighted factor
Albia	average	average	moderately grazed	1.00
Centerville	average	high	lightly grazed	.80
Creston	average	high	lightly grazed	.80
Greenfield	below average	low	heavily grazed	1.20
Ralston Creek	below average	average	heavily grazed	1.10

Table 3. Factors assigned to Centerville watershed.

	Proportion of watershed	Factor	Product
<b>LAND USE</b>			
Cultivated	0.56	1.25	0.70
Pasture	.28	.75	.21
Brush and timber	.04	.50	.02
Other	.12	1.60	.19
Weighted average			1.12
<b>SLOPE (%)</b>			
0 - 1.9	0.17	.49	0.08
2 - 4.9	.26	.75	.20
5 - 9.9	.44	.93	.41
10 - 19.9	.13	1.11	.14
Weighted average			.83
<b>SOIL TYPE</b>			
Shelby	0.13	1.10	0.14
Seymour	.70	1.30	.91
Edina	.17	1.40	.24
Weighted average			1.29

The management and conservation factor for each watershed was assigned primarily on the basis of information reported in Table 2. The climate factors were obtained from Figure 2. As shown in Table 4, the watershed rating is the product of the factors (weighted averages) assigned to the characteristics.

Table 4. Relative watershed ratings.

Watershed	Characteristic					Rating
	Climate	Land use	Slope	Soil	Management conservation	
Albia	1.08	1.13	0.89	1.10	1.00	1.19
Centerville	1.05	1.12	0.83	1.29	0.80	1.01
Creston	0.84	1.15	0.81	0.85	0.80	0.53
Greenfield	0.83	0.88	1.02	0.96	1.20	0.86
Ralston Creek	1.35	1.02	0.97	0.70	1.10	1.03

#### Gauge-reservoir records

An estimate of the median annual yield from Ralston Creek (the only gauged Iowa watershed under 15,000 acres in size having more than 5 years of record) was made by an examination of 28 years of stream gauge record (State University of Iowa, 1924-1952). The four reservoir watersheds studied were the only known ones in Iowa available with adequate records maintained for more than 5 years. For these, a monthly water balance was made using water consumption from the reservoir, precipitation, and storage records. Monthly evaporation from the reservoir was estimated from stage information and records of the three closest Weather Bureau Class A evaporation stations. Allowance was made for estimated seepage and accelerated fringe transpiration around the water surface. Yield estimates were limited to months in which no spillway discharge occurred as accurate spillway discharge records were not available. All told, about 70% of the records from the selected watersheds were usable. An estimate of median annual yield for each reservoir watershed was made after a study of monthly precipitation-yield relationships and the effect of prior month's precipitation on current month's yield.

#### Comparison of Estimated with Measured Water Yield

The median annual yields for a hypothetical common period, based upon measured runoff, are shown by line (A) of Table 5. The second line (B) shows the median annual yields estimated from watershed ratings assigned on the basis of watershed characteristics. These median yields were estimated by multiplying the watershed rating by the index median yield of 5.80 inches per year.

Application. An impounding reservoir should be designed to meet a specified water demand for a given recurrence interval. Figure 5 shows the estimated water yield from the index watershed for various recurrence intervals. The yield from any other watershed may be assumed

Table 5. Comparison of median annual yield (inches per year).

Method	Watershed				
	Albia (686 acres)	Center- ville (2,550 acres)	Creston (9,850 acres)	Green- field (525 acres)	Ralston Creek (1,930 acres)
Gauge-Reservoir (A)	7.84	5.34	3.08	4.51	6.72
Rating (B)	6.90	5.86	3.08	4.99	5.98
Ratio B/A	.88	1.10	1.00	1.10	.89

to be equal to the index watershed yield times the watershed rating. In addition to the single year yield, cumulative minimum yields for periods of two, three, and four consecutive years are shown. This figure is based upon published stream gauge records (especially those for Ralston Creek and the Chariton River).

Figure 5 shows that for large recurrence intervals, the two-year yield is always more than double the single year yield. Advantage can be taken of this fact by designing reservoirs with capacity to carry over stored water into a dry year. Although this method of water yield prediction gave favorable results in comparison to the median yield, it may not be reliable at higher recurrence intervals. Additional runoff data are needed to make reliable comparisons at the high recurrence intervals.

Allowance for sedimentation must be made in the design of impounding reservoirs. Sediment production from southern Iowa watersheds (100 to 10,000 acres in size) can roughly be expressed by the equation:

$$S = 1.4 A^{-.21}$$

where  $S$  = sediment production (ac-ft/100 ac/yr)  
 $A$  = watershed area (acres).

Sediment production at individual sites is commonly within the range -50% to +80% of the predicted amount. Differences of land use, topography, soil, and management-conservation practices account for the great differences in sediment production rates from site to site.

### Discussion

An examination of Table 5 shows that the estimated yield is not far different from the measured yield (compensating errors may partly account for this). Lack of agreement may be attributed to erroneous theory regarding the behavior of the phenomena that govern yield, incorrect assignment of values to rating factors, insufficient data and errors in measured yield.

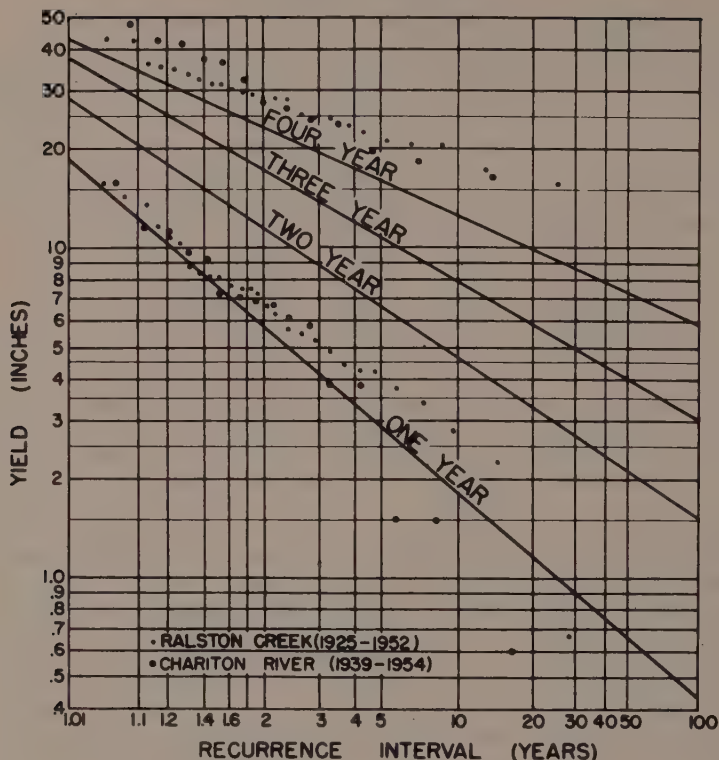


Figure 5. Water yield from the index watershed.

The assumption made in this paper that the influence of one characteristic on water yield is independent of other characteristics is not necessarily valid. While the method may provide a useful tool, it must be recognized as an approximation. Only five characteristics were considered in estimating the yield; geology and watershed size are outstanding examples of other characteristics that are important, especially under certain conditions. Geology was included only indirectly (soils and slope) because it is fairly uniform in southern Iowa. The area is underlain by relatively impermeable glacial till covered by loess soil to a depth of 0 to 10 feet. The effect of watershed size on water yield per yield per unit area is obscured by more pronounced influences, such as the five physical characteristics considered in this paper. The limited ground water contribution, during dry periods from watersheds of all sizes in this area suggests that the yield per unit area is little affected by watershed size (in the range 525-9,850 acres).

The factors assigned to the various classifications of watershed characteristics are only estimates based upon limited observations; continued research is needed to provide more precise values. A shortage of



runoff data makes the factors assigned to land management and conservation open to question. Errors and assumptions in computing the measured yield also provide a source of error. The median annual water yield estimated from stream gauge and reservoir records is believed to be accurate within  $\pm 15\%$ .

Water yield estimates, based upon watershed rating, as determined by the physical characteristics of a watershed, appear to provide reliable estimates of water yield. Despite the limiting and approximate assumptions used in the development of the prediction method, it may have practical applications if confined to small watersheds (300 to 10,000 acres in size) in regions of uniform physiography.

#### Acknowledgments

The authors are indebted to the following municipal water department superintendents for the records and information which they provided; Guy A. Perry, Lawrence R. Creagan, Sr., George Seibert, and Burton Sherman. Thanks is extended to the following Soil Conservation Service technicians and their staffs for the aid they extended in providing information about the physical characteristics of the watersheds of this study: William E. Stark, Herbert M. Kayser, Robert R. Winders and Dale C. Baker. The kindnesses of J.W. Howe and V.R. Bennion, in providing general background material and in making available the records of the Ralston Creek watershed, are appreciated. Grateful acknowledgment is made to D.D. Smith and E. Robert Baumann for valuable contributions during the course of this investigation. Thanks is given to Glen R. Peterson for many hours of diligent computing work.

This study was conducted as one phase of irrigation investigations sponsored by the Aluminum Company of America at the Iowa Agricultural and Home Economics Experiment Station.

#### REFERENCES

- Browning, G.M., et al. 1948. Investigation in erosion control and the reclamation of eroded land at the Missouri Valley Loess Conservation Experiment Station, Clarinda, Iowa, 1931-42. U.S.D.A. Tech. Bull. 959.
- Brune, G.M. 1948. Rates of sediment production in midwestern United States. U.S. Soil Conservation Service SCS-TP-65, illustration facing p.12.
- Duley, F. L. and L. L. Kelly. 1939. Effect of soil type, slope, and surface conditions on intake of water. Nebraska Agric. Exp. Sta. Res. Bull. 112.
- Hays, O.E. 1955. Annual report of the La Crosse Experiment Station (Proj. SWC-66-2) for 1954, La Crosse, Wisconsin. U.S. Dept. Agr. Res. Serv. (mimeo.).
- \_\_\_\_\_, A.C. McCall, and F.G. Bell. 1949. Investigations in erosion control and the reclamation of eroded land at the upper Mississippi Valley Conservation Experiment Station, near La Crosse, Wisconsin, 1933-43. U.S. Dept. Agr. Techn. Bull. 973.

- Horton, R. E. 1943. Evaporation maps of the United States. Trans. Amer. Geophys. Union 24:743-753.
- Iowa Geological Survey. 1953. Surface water resources of Iowa October 1, 1942 to September 30, 1950. Water-supply Bull. No. 3, Iowa City Iowa, The Survey.
- Iowa State Department of Agriculture. 1952. 1951 Iowa Yearbook of Agriculture, Des Moines, Iowa. pp. 522-539.
- Langbein, W.B., et al. 1949. Annual Runoff in the United States. U.S. Geological Survey, Cir. 52, Plate 1.
- Riecken, F. F. and G. D. Smith. 1949. Principal upland soils of Iowa (their occurrence and important properties). (Revised), Iowa Agric. Exp. Sta. Bull. Agron. 49, (mimeo.).
- Smith, D.D., et al. 1945. Investigations in erosion control and the reclamation of Shelby and related soils at the conservation experiment station, Bethany, Mo., 1930-42. U.S.D.A. Agr. Tech. Bull. 883.
- State University of Iowa. 1924-1952. Annual reports of hydrologic studies of Ralston Creek watershed. Iowa City, Iowa. (mimeo.).
- U.S. Department of Agriculture. 1941. Yearbook of Agriculture, 1941. Washington, D.C., U.S. Govt. Print. Off. p. 871.

AN OPTICAL DENSITY METHOD OF MEASURING  
PHYTOPLANKTON STANDING CROP<sup>1</sup>

Lawrence F. Small

Department of Zoology and Entomology  
Iowa State University  
of Science and Technology  
Ames, Iowa

**SUMMARY.** Estimation of phytoplankton standing crop involves collection of adequately representative samples and determination of the phytoplankton per sample. For each estimate, one liter of lake water was centrifuged in a continuous-flow centrifuge at the rate of one liter per eight minutes, the concentrate was made up to 30 milliliters with 90% reagent-grade acetone, and the extraction was allowed to take place for one-half hour at a constant temperature of 120°F. Longer extraction is more complete, but deterioration of chlorophyll may be greater than the increased extraction. Use of two liters per sample did not give better results than one liter samples. When the extraction phase was completed, the green supernate was read in a Bausch & Lomb "Spectronic 20" spectrophotometer at a 665 mμ wave length to obtain the optical density of chlorophyll "a". The optical densities can then be converted to "units of count" providing the species composition remains fairly constant.

- - - - -  
Introduction

Phytoplankton serves as the "pasture" of lakes and of the ocean, producing the basic food upon which the aquatic animals live. Measurement of its abundance is, however, a slow tedious process. Moyle (1949) mentions that quantitative plankton sampling was discontinued in general

<sup>1</sup> Journal Paper No. J-3969 of the Iowa Agricultural and Home Economics Experiment Station, Ames, Iowa. Project No. 1374, Iowa Cooperative Fisheries Research Unit, sponsored by the Iowa State Conservation Commission and Iowa State University of Science and Technology, with the cooperation of the Fish and Wildlife Service, United States Department of the Interior. This paper is part of a thesis submitted to partially fulfill the requirements of a Master Of Science degree. The Atomic Energy Commission supported part of this project under Grant AT (11-1) 59.

lake productivity studies in Minnesota because the labor required to collect and examine an adequate series of samples, considering seasonal variation and sampling errors, made the value of such work questionable.

The present study was undertaken to develop techniques for quickly measuring the standing crop of phytoplankton in Clear Lake in north-central Iowa. Clear Lake is eutrophic and unstratified (Pearcy, 1953) with an area of 3,642 acres (at outlet level) and a maximum depth, in August, 1958, of 15 feet. The phytoplankton is composed predominantly of blue-green algae and diatoms.

A satisfactory technique for estimating the standing crop involves two steps: determination of the amount of phytoplankton in a sample of water, and collection of samples of water adequately representative of the lake.

#### Determining the Amount of Phytoplankton per Sample

A critical appraisal of the available techniques for determining the amount of phytoplankton in a sample concentrate, in light of the objective of this study, automatically eliminated several techniques. Direct counts through a microscope (Allen, 1919, 1922; American Public Health Association, 1946; Clark, 1956; Fleming, 1940; Gilbert, 1942; Gran, 1932; Hentschel, 1938; Kutkuhn, 1958; Littleford, *et al.*, 1940; Rawson, 1953, 1956; Sheard, 1947; Tucker, 1948; and many others) were discarded because of the time involved. There was no foreseen solution for cutting down the time and still retaining accuracy. The sedimentation technique, with subsequent counting over an inverted microscope (Utermöhl, 1931), was discarded for the same reason, though this is probably one of the most accurate methods known (Braarud, 1958). Pigment extraction techniques (Creitz and Richards, 1955; Freed, 1957; Gardiner, 1943; Gessner, 1944; Harvey, 1934; Krey, 1958; Lund and Talling, 1957; Manning and Juday, 1941; Marshal, 1956; Richards with Thompson, 1952; Riley, 1938; Rodhe, 1948; Ryther and Yentsch, 1957; Tucker, 1949; Wohlschlag and Hasler, 1951; Wright, 1958; Yentsch and Ryther, 1957; and others) were also quite time-consuming, but several steps in the general process seemed worthy of investigation with respect to cutting down the time involved without losing accuracy. Basically the technique is to extract the pigment from a known volume of sample or sample concentrate in a suitable solvent and obtain the extinction coefficient of light, or the optical density, in the extract, either through the use of a colorimeter, or, in more specific work with separate pigments, a spectrophotometer using a narrow waveband critical for the pigment in question. Optical density can then be converted by means of a standard curve to number of organisms per unit volume, to "units of count" (Tucker, 1948), or to milligrams of carbon per unit volume, or per unit surface area, for ready comparison with primary production data (Cushing, 1958). Several pitfalls in interpreting pigment extraction results were noted:

1. Different species of algae possess different pigments.
2. Amount of pigment per cell or algal unit is different in different species of algae, if for no other reason than that species vary greatly in size.



3. Chlorophyllous debris, such as plant fragments other than algae, may add to the extract.
4. Chlorophyll in dead algal organisms may add to the extract. This factor becomes particularly important if chlorophyll is used as an index of "photosynthetic potential" rather than an index of standing crop (Currie, 1958; Ketchum, *et al.*, 1958; Krey, 1958; Ryther, 1956), where standing crop is defined as the number of organisms present at a given instant per unit volume of water, regardless of physiological state of the organisms.
5. Age of the population might possibly affect the quantity of chlorophyll per individual cell, or the absorption spectrum of the extracted chlorophyll.
6. Incomplete extractions underestimate the standing crop.
7. Differential extractions, with regard to species, confound extraction results and thus confound conversion to enumeration data.
8. Undue delay between extraction and reading in the spectrophotometer might cause breakdown of the chlorophyll in the presence of light, and change the absorption spectrum.

At first glance, the pigment extraction technique, with these limitations imposed upon it, might seem to be a poor choice for a basic technique on which to begin experimentation. Most of the pitfalls in the technique can be avoided or corrected for, however.

The particular extraction method used as a basis for experimentation was that of Richards with Thompson (1952). It was found after experimentation (Table 1) that results from the method (which required an 18-hour extraction time at 105°F) could be closely approximated by the following technique: 1 liter of lake water was centrifuged in a continuous-flow centrifuge at the rate of 1 liter per 8 minutes, this concentrate was transferred to a colorimeter tube and made up to 30 ml with 90% reagent-grade acetone, and extraction was allowed to take place for  $\frac{1}{2}$  hour at a constant temperature of 120°F. The green supernate was then read in a Bausch & Lomb "Spectronic 20" spectrophotometer at a 665 m $\mu$  wavelength to obtain the optical density of chlorophyll "a". Three of the four samples with lowest optical density (least amount of chlorophyll "a") showed a better extraction at 120°F for  $\frac{1}{2}$  hour than at 105°F for 18 hours. Normally, the reverse would be expected (as shown by the other seven samples) because the longer time should insure more complete extraction. Possibly in these three situations complete extraction had been realized long before the 18-hour time limit, and a deterioration of the extract took place prior to reading. If this were true, the  $\frac{1}{2}$  hour extraction at 120°F is better for estimating samples of low chlorophyll content. In the "richer" extracts deterioration may have occurred also, but this was masked by the fact that pigment was still being extracted. Since readings on the  $\frac{1}{2}$  hour extracts differed by less than 14% from the cor-

Table 1. Comparison of short-term extractions with long-term extractions.

Date	Optical density readings X100		Difference	Percentage of difference
	1/2 hour at 120°F	18 hours at 105°F		
August 8	1.25	1.00	+ .25	20.0
July 26	2.25	2.00	+ .25	11.1
July 8	2.25	2.50	+ .25	11.1
July 21	2.50	2.25	- .25	10.0
August 15	3.00	3.25	- .25	8.3
August 1	3.75	4.25	+ .50	13.3
July 15	4.25	4.75	- .50	11.8
July 2	4.75	5.00	+ .25	5.3
August 20	4.75	5.25	+ .50	10.5
August 27	7.50	8.00	+ .50	6.7

responding readings on the 18-hour extracts, when these were higher, the quicker method was thought to be an adequate estimate of the "true" optical density of the extract.

By selecting a pigment common to all species in the lake (chlorophyll "a"), and obtaining the optical density of this pigment as closely as possible (by using the 665 mμ wavelength, which is selective for chlorophyll "a" extracted in 90% acetone), the effect of any other pigment in the extract is almost completely stripped out. The concentration of chlorophyll "a" is not the same in different species, but assuming that amount of chlorophyll "a" is a linear function of cell size (which is probably not entirely true), cells can be expressed as "units of count" (Tucker, 1948) to empirically standardize cell size and hence chlorophyll content (Table 2). By extracting and counting different concentrations of paired samples, a standard curve (Figure 1) was constructed which will allow the comparable number of units of count to be read off for each optical density reading. There is an obvious weak point in this particular conversion method, however. The assignments of quantity of cells to equal one unit of count are at best educated guesses; thus the number of units of count equalling one optical density reading will probably change slightly with each gross change in species composition, due to the inability of the units of count to completely standardize the different amounts of chlorophyll "a" in different phytoplankton species. Different standard curves might be needed during different seasons of the year if the species composition changed radically.

The use of optical density readings does not evaluate species composition changes. Different optical density readings (and units of count) only reflect changes in total volume, or total standing crop. Generally this is all that is wanted, but it may on occasion be of interest to know what percentage of the total volume is represented by certain species, or certain groups, or certain sizes of algae. Rapid examination of a sample can provide estimates of percentage composition, using units of count for each species.

Table 2. Important phytoplankton of Clear Lake and the quantitative value equalling one unit for enumeration.

Plankter	Quantity to equal 1 unit	Plankter	Quantity to equal 1 unit
Diatoms		Green algae	
<u>Asterionella</u>	8 cells	<u>Actinastrum</u>	1 colony
<u>Fragilaria</u>	100 micra	<u>Coelastrum</u>	1 colony
<u>Melosira</u>	100 micra	<u>Gleocystis</u>	1 colony
<u>Navicula</u>	1 cell	<u>Pediastrum</u>	1 colony
<u>Stephanodiscus</u>	1 cell	<u>Scenedesmus</u>	4 cells
<u>Synedra</u>	1 cell	<u>Staurostrum</u>	1 cell
<u>Tabellaria</u>	8 cells		
Blue-green algae			
<u>Anabaena</u>	100 micra	<u>Microcystis</u>	10,000 sq. micra
<u>Aphanizomenon</u>	100 micra		
<u>Gomphosphaeria</u>	1 colony	<u>Oscillatoria</u>	100 micra
<u>Lyngbya</u>	100 micra	<u>Gleotrichia</u>	1 colony
<u>Merismopedia</u>	1 colony	<u>Coelosphaerium</u>	1 colony

Chlorophyllous debris may also affect optical density readings, if present in large amounts. Brief microscope checks should reveal any extensive amounts of debris in the sample. If large amounts are present, chlorophyll extractions should not be attempted. In this study, mean units of count were closely correlated with optical density readings (Figure 1), which, along with microscope checks, would indicate little effect on the extractions from chlorophyllous debris.

Chlorophyll from dead algal organisms was extracted along with the chlorophyll from living cells; hence, the chlorophyll extractions in this study represented estimates of standing crop as previously defined, regardless of physiological state of the individual cells. The estimation of "photosynthetic potential" from chlorophyll extractions becomes rather meaningless unless the total population being estimated is known to be actively growing (in which case the assumption that no "dead" chlorophyll is present is probably valid). Krey (1958) suggests that a component specific for living photoplankton, such as an amino acid or an enzyme, might be the key for separation of photosynthetically active cells from dead cells, but no means of separation is now known. Further complicating the problem of using chlorophyll as a measure of photosynthetic potential is the fact that one unit of "living" chlorophyll under different circumstances is able to assimilate different quantities of carbon dioxide.

The effect of changing quantity or optical quality of chlorophyll "a" per cell with age, if it exists, was not corrected for, and thus this study necessarily operated under the broad assumption that it did not exist, or, if it did, that the ratio of "old" to "new" cells was constant in the population. If in truth there is a change in chlorophyll per cell with age,

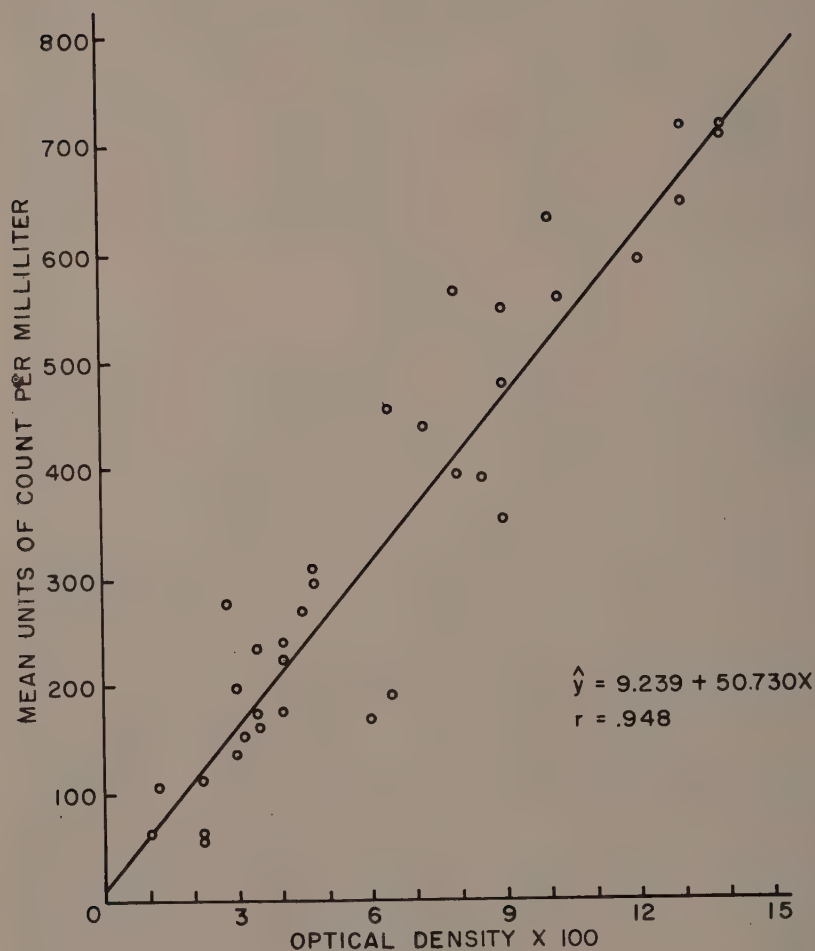


Figure 1. Relationship between average number of counted phytoplankton units per milliliter of water and optical density readings on extracted surface samples in Clear Lake, Iowa, during the summer of 1958.

the chances of obtaining noncomparable standing crop estimates over a year's time, for example, are great. The assumption of constant ratio of old to new cells probably would become entirely invalid during and following phytoplankton pulses, or blooms.

The close agreement of the quick extractions with the Richards with Thompson extractions (Table 1) would indicate that the former went to completion, or nearly so. Thus by increasing the temperature of extraction on small sample concentrates, the time of extraction was effectively reduced without appreciably altering the accuracy of the results. If complete extraction is attained, the problem of differential extraction, with regard to species, does not exist. Should this not be the case, however, and should a particular species or group of algae in the sample not release its chlorophyll as readily as others in the sample, the unextracted fraction will be tied up largely by that species or group in which extraction is slow. If that particular species or group is a major part of the total population, standing crop estimates of the total population will be underestimated. Also, if this large segment of the population is one subject to great numerical fluctuation, one standing crop estimate will not be comparable with the next, regardless of the precision with which the rest of the over-all technique is performed.

Extraction of representative pure cultures of algae indicated that blue-green algae and diatoms were extracted quite satisfactorily by the quick extraction method, but green algae (Pediastrum boryanum, Staurastrum gracile) were not completely extracted. Since Clear Lake is a predominantly blue-green algae-diatom lake, the technique was probably satisfactory using samples from such an environment, but the seemingly incomplete extraction of the green algae would bear further investigation before using the quick extraction technique on samples from waters with green algae.

If delay between extraction and reading of the extract in the spectrophotometer is necessary, the samples must be placed in total darkness immediately after extraction until their optical densities can be determined. Creitz and Richards (1955) mentioned that chlorophyll extracts could be kept for several days in absolute darkness without any appreciable effects on their optical densities, and an experiment in the Clear Lake Laboratory verified this. In three extractions held in total darkness, deterioration of the chlorophyll was not spectrophotometrically evident for at least eight days.

#### Collecting and Concentrating the Sample

It was felt that time spent in collecting and concentrating samples from the lake could be cut down without affecting the accuracy of the determinations appreciably. Collection of samples with plankton nets was avoided since nets do not effectively filter nanoplankton which may contribute significantly to the standing crop (Kutkuhn, 1958). A method whereby known volumes of lake water were suction-filtered through type AA millipore filters and the pigment extracted directly from the filters (Creitz and Richards, 1955) met with little success at Clear Lake, for several reasons. The small size of the filterable sample (30 ml), made necessary by the "richness" of the lake, was probably the foremost of



these reasons. Also, nonchlorophyllous detritus (silt, root fibers, etc.) affected filtration, recovery of the pigment from the filters was not adequate, and filtration and extraction from the filters was slow.

Ballantine (1953) stated that centrifugation appeared to be the most satisfactory method of concentrating nanoplankton, from the standpoints of simplicity, time involved, and accuracy. Hartman (1958), however, found that this method was inaccurate if the results were based on only one centrifugation, and suggested that three centrifugations of the same sample were needed to duplicate colorimetric readings on the centrifuge runoff. It was found in this study that no more than 3.3% of the total phytoplankton was lost in one centrifugation at the rate of 1 liter per 8 minutes. The average loss approximated 2.0% (assuming that total phytoplankton was recovered with three centrifugations). Thus it was felt that one centrifugation offered a satisfactory balance of accuracy and speed, and was superior to other methods of concentration tried. The lake samples themselves were easily and rapidly taken with a 3-liter Kemmerer water sampler. The big objection to the centrifugation method, that of breaking up the delicate cells, was nullified by the fact that this study dealt with the chlorophyll "a" content of the concentrate, not the cells as visually recognizable entities.

The original sample volume of water used for each extraction was 1 liter. It was thought that readings on extractions from 1-liter samples might be subject to a great deal of error because of the relatively small amount of pigment extracted from the concentrate. Thus, on each of several sampling runs, a 2-liter sample was collected simultaneously with the 1-liter sample and optical densities of the chlorophyll extracts were compared. Since good correlation was obtained between the two sets of readings (Figure 2) it appeared that 1-liter samples, which required less time to centrifuge, were consistent enough to give good estimations within the general density range of phytoplankton in Clear Lake.

Naturally, statistical sampling schemes must be followed in collecting samples from the lake, to insure adequate representation of the phytoplankton throughout the lake volume. Without collections that take into account horizontal and vertical distribution of the organisms, and possible changes in the population with time of day, the most exacting of techniques used to concentrate and extract the samples will not give accurate standing crop estimates for the lake as a whole. Sampling schemes will not be discussed in this paper, however.

It is hoped that in this study a technique for concentrating and analyzing phytoplankton for standing crop estimates in a lake has been developed whereby state conservation departments, federal agencies, and other organizations not directly concerned with basic research on phytoplankton can get quick, accurate information on productivity and lake type. The technique presented is not the most accurate and precise method known, but is one which should offer a good balance between accuracy needed in most general lake survey work and the time to be used in such survey work.

#### Acknowledgments

The author appreciates the guidance given by Drs. John D. Dodd and

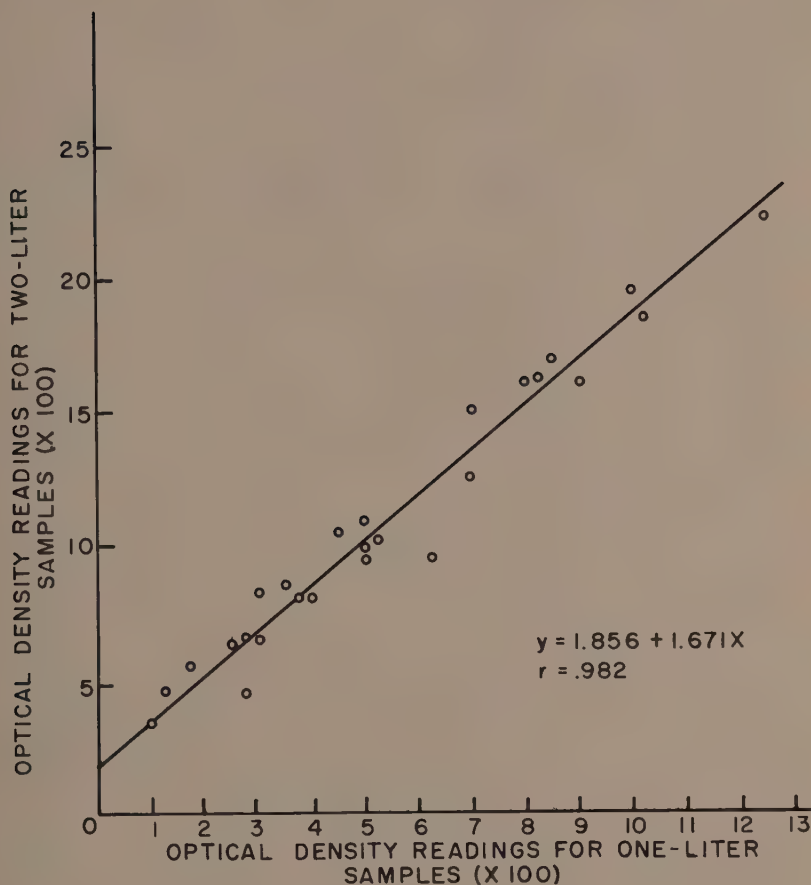


Figure 2. Relationship between extracted 2-liter surface samples and extracted 1-liter surface samples at Clear Lake, Iowa, during the summer of 1958.

Kenneth D. Carlander, the suggestions on colorimetric methodology from Dr. F.E. Lind and the assistance in the field given by Cornelius I. Weber, Robert Cooper, and others of the Iowa Cooperative Fishery Research Unit.

Literature Cited

- Allen, E.J. 1919. A contribution to the quantitative study of plankton. Jour. Marine Biol. Assn. 12:1-8.
- Allen, W.E. 1922. Quantitative studies on marine phytoplankton at La Jolla in 1919. Univ. Calif. Publ. Zool. 22:329-347.
- American Public Health Association. 1946. Standard methods for the examination of water and sewage. 1936. 8th ed. 2nd ptg. Amer. Pub. Health Assn. New York. xiv + 309 pp.
- Ballantine, D. 1953. Comparison of the different methods of estimating nannoplankton. Jour. Marine Biol. Assn. U.K. 32:129-148.
- Braarud, T. 1958. Counting methods for determination of the standing crop of phytoplankton. Internatl. Council Explor. Seas, Reunions et Proc.-Verb. 144:17-19.
- Clark, William J. 1956. An evaluation of methods of concentrating and counting the phytoplankton of Bear Lake, Utah-Idaho. M.S. Thesis, Utah State Agric. Coll., Logan, Utah.
- Creitz, G.I. and F.A. Richards. 1955. The estimation and characterization of plankton populations by pigment analyses. III. A note on the use of "millipore" membrane filters in the estimation of plankton pigments. Jour. Marine Res. 14:211-216.
- Currie, R.I. 1958. Some observations on organic production in the north-east Atlantic. Internatl. Council Explor. Seas, Reunions et Proc.-Verb. 144:96-102.
- Cushing, D.H. 1958. The estimation of carbon in phytoplankton. Internatl. Council Explor. Seas, Reunions et Proc.-Verb. 144:32-33.
- Fleming, R.H. 1940. The composition of plankton and units for reporting populations and production. Proc. 6th Pacific Sci. Congress, Calif. 1939. 3:535-540.
- Freed, S. 1957. Equilibria as origin of differences in spectra of chlorophyll in different solvents. Science 125:1248-1249.
- Gardiner, A.C. 1943. Measurement of phytoplankton population by the pigment extraction method. Jour. Marine Biol. Assn. 25(4):739-744.
- Gessner, F. 1944. Der Chlorophyllgehalt der Seen als Ausdruck ihrer Produktivitat. Arch. Hydrobiol. 40:687-732.
- Gilbert, J.Y. 1942. The errors of the Sedgewick-Rafter counting chamber in the enumeration of phytoplankton. Trans. Amer. Micros. Soc. 61:217-226.
- Gran, H.H. 1932. Phytoplankton, methods and problems. Jour. du Conseil 7(3):343-358.
- Hartman, Richard T. 1958. Studies of plankton centrifuge efficiency. Ecology 39(2):374-376.
- Harvey, H.W. 1934. Measurement of phytoplankton population. Jour. Marine Biol. Assn. 19:761-774.
- Hentschel, Ernst. 1938. Über quantitative Seihmethoden in der Planktonforschung. Jour. du Conseil 13:304-308.
- Ketchum, B.H., et al. 1958. Productivity in relation to nutrients. Internatl. Council Explor. Seas, Reunions et Proc.-Verb. 144:132-140.
- Krey, J. 1958. Chemical methods of estimating standing crop of phytoplankton. Internatl. Council Explor. Seas, Reunions et Proc.-Verb. 144:20-27.

- Kutkuhn, Joseph H. 1958. Notes on the precision of numerical and volumetric plankton estimates from small-sample concentrates. *Limnol. and Oceanogr.* 3(1):69-83.
- Littleford, R.A., C.L. Newcombe, and B.B. Shepherd. 1940. An experimental study of certain quantitative plankton methods. *Ecology* 21(3):309-322.
- Lund, J.W.G. and J.F. Talling. 1957. Botanical limnological methods with special reference to the algae. *Bot. Rev.* 23:489-583.
- Manning, W.M. and R.E. Juday. 1941. The chlorophyll content and productivity of some lakes in northeastern Wisconsin. *Trans. Wis. Acad. Sci. Art, Lett.* 33:363-393.
- Marshall, N. 1956. Chlorophyll "A" in the phytoplankton in coastal waters of the eastern Gulf of Mexico. *Jour. Marine Res.* 15(1):14-32.
- Moyle, John B. 1949. Some indices of lake productivity. *Trans. Amer. Fish. Soc.* 76(1946):322-334.
- Pearcy, William G. 1953. Some limnological features of Clear Lake, Iowa. *Iowa State Coll. Jour. Sci.* 28(2):189-207.
- Rawson, D.S. 1953. The standing crop of net plankton in lakes. *Jour. Fish. Res. Bd. Canada* 10(5):224-237.
- \_\_\_\_\_. 1956. The net plankton of Great Slave Lake. *Jour. Fish. Res. Bd. Canada* 13(1):53-127.
- Richards, F.A. with T.G. Thompson. 1952. The estimation and characterization of plankton populations by pigment analyses. II. A spectrophotometric method for the estimation of plankton pigment. *Jour. Marine Res.* 11:156-172.
- Riley, G.A. 1938. The measurement of phytoplankton. *Int. Rev. d. Ges. Hydrobiol. u. Hydrog.* 36:371-373.
- Rodhe, Wilhelm. 1948. Environmental requirements of fresh-water plankton algae. *Symbolae Botanicae Upsalienses* X:1. 149. pp.
- Ryther, John H. 1956. The measurement of primary production. *Limnol. and Oceanogr.* 1(2):72-84.
- \_\_\_\_\_. and C.S. Yentsch. 1957. The estimation of phytoplankton production in the ocean from chlorophyll and light data. *Limnol. and Oceanogr.* 2(3):281-286.
- Sheard, K. 1947. Net plankton volume determinations. *Rpts. B.A.N.Z. Antarctic Res. Exped. Ser. B.* 6(1):1-19.
- Tucker, A. 1948. The phytoplankton of the Bay of Quinte. *Trans. Amer. Micros. Soc.* 67(4):365-383.
- \_\_\_\_\_. 1949. Pigment extraction as a method of quantitative analysis of phytoplankton. *Trans. Amer. Micros. Soc.* 68(1):21-33.
- Utermöhl, H. 1931. Neue Wege in der quantitativen Erfassung des Planktons. *Verh. Int. Ver. Limnol.* 5.
- Wohlschlag, D.E. and A.D. Hasler. 1951. Some quantitative aspects of algal growth in Lake Mendota. *Ecology* 32(4):581-593.
- Wright, John C. 1958. The limnology of Canyon Ferry Reservoir. I. The phytoplankton-zooplankton relationships in the euphotic zone during September and October, 1956. *Limnol. and Oceanogr.* 3(2):150-159.
- Yentsch, C.S. and J.H. Ryther. 1957. Short term variations in phytoplankton chlorophyll and their significance. *Limnol. and Oceanogr.* 2(2):140-142.





## SOLAR RADIATION AND SUNSHINE IN IOWA<sup>1</sup>

P.J. Waite and R.H. Shaw<sup>2</sup>

**SUMMARY.** Solar radiation data for Ames 1954-1960 were summarized, and the results compared with those of Lincoln, Nebraska, and Madison, Wisconsin. These stations provide data which give the range of values to be expected across Iowa.

Sunshine observations for the first order Weather Bureau stations were summarized as to monthly means, distribution of monthly means and distribution of daily values for the 1930-1959 period.

The charts show that percent of possible sunshine generally decreases from west to east. In December the average difference in radiation across Iowa is about 25 langley's per day while in June it is only about 10 langley's per day. During the summer the average difference in radiation is small across Iowa, although, of course, on individual days, local cloudiness may result in large differences across the state.

- - - - -

The sun is the basic source of supply for all nonnuclear energy which drives the physical and biological processes of the earth. It emits tremendous amounts of energy with fluctuations of only 1 or 2% (5). However, the amount received at the surface of the earth varies greatly with season and location due to the angle of the sun which changes with time of day, time of year and latitude. The length of day also varies with season and latitude. The angle (intensity) and length of day (duration) combined with the effects of clouds, smoke, fog, and dust determine the amount received on a horizontal surface at the surface of the earth. The amount received on a horizontal surface is quite different from that received on walls or sloping surfaces (9) but these differences will not be discussed here.

Solar radiation is used in a multitude of ways. It causes evaporation from ponds, lakes and wet ground surfaces; it causes plant transpiration; it is used in heating the soil and air; it is used in photosynthesis of plants and its duration or photoperiodism has important effects on many plants. It is essential to agriculture, industry, and recreation, and affects our lives in many ways.

<sup>1</sup>Journal Paper No. J-3987 of the Iowa Agricultural and Home Economics Experiment Station, Ames, Iowa. Project No. 1280.

<sup>2</sup>State Climatologist, U.S. Weather Bureau, Des Moines, Iowa and Professor of Agronomy (Agricultural Climatology), Iowa State University, Ames, Iowa.

In Iowa, radiation has been recorded both as intensity and duration of sunshine. This paper summarizes what these observations have shown.

## DATA USED AND DISCUSSION

### Solar Radiation

The instrument used to measure the intensity of solar radiation is the Eppley pyrliometer. This instrument (4) is a specialized thermopile. The receiving element is hermetically sealed in a lamp bulb of soda lime glass which transmits only about 10% of the incident radiation at  $.29 \mu$  and  $5 \mu$  but near 90% from  $.34$  to  $2.6 \mu$ . At the time of sealing, the bulb is carefully heated and exhausted to expel adsorbed moisture and is then filled with dry air to prevent any condensation of moisture on its inner surface due to exposure to low temperatures. The bulb, which is 3" in diameter, is mounted on a metal base with leveling screws. The inner or hot ring is painted with lampblack and the outer or cold ring is smoked with magnesium oxide. These blackened and whitened surfaces absorb longwave radiation equally well, but the magnesium oxide has a high coefficient of reflection for radiation having the wave length of solar radiation. Therefore when exposed to solar radiation the two rings of this pyrliometer develop a marked temperature difference, and the resulting e.m.f. from the associated thermopile is very nearly proportional to the intensity of the solar radiation.

The basic unit for measuring solar radiation energy per unit area is gram-calories/centimeter<sup>2</sup>, called langleys in the published Weather Bureau Climatological Data National Summary (14). Engineers often use the units BTU/ft<sup>2</sup> where  $1 \text{ BTU/ft}^2 = .27 \text{ cal/cm}^2$ .

Continuous observations of solar radiation on a horizontal surface were started in 1953 at Ames, using a pyrliometer located on top of the Agronomy Building. Some experimental data were recorded prior to that by the Agricultural Engineering Department. Radiation data are also available for stations in states surrounding Iowa (8, 14).

An examination of the radiation which would be received with no atmospheric depletion (13) shows little difference across Iowa from north to south during any day of the summer period, but an average difference of near 50 langleys per day in the winter. Local differences in cloud cover across the state will result in a wider range of the radiation actually received. Lincoln, Nebraska, and Madison, Wisconsin, provide data on the range which would be expected across Iowa from southwest to northeast. The average annual curves (8) are shown for these stations in Figure 1. In addition, Ames data are shown in dots, each dot representing a 6-year weekly mean. During June and July the Ames radiation has been lower than expected although the percent of possible sunshine during these months was near normal. For a longer period the solar radiation would be expected to fall between that of Lincoln and Madison. The highest 10% of the days for each month were selected and a smoothed curve drawn through these data points which were plotted on their respective calendar dates. This is labelled "clear days" in Figure 1. The lowest 10% of the days for each month were also selected, and the

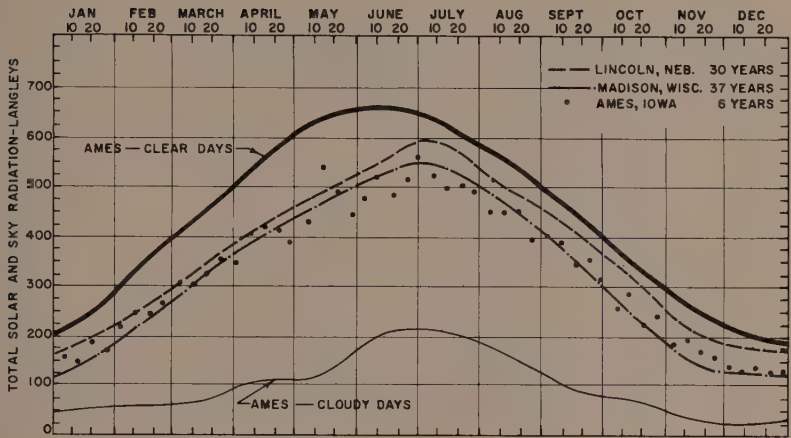


Figure 1. Annual radiation curves for Ames, Iowa, Lincoln, Nebraska, and Madison, Wisconsin.

smoothed curve, labelled "cloudy days," was drawn through these data points. This provides the range of high and low values which might be expected at any time of the year. Any Iowa station would show a wide seasonal difference due to changes in the height of the sun above the horizon. At Ames, the sun has a maximum altitude of  $71^\circ$  in late June, but in late December the maximum altitude is only  $24^\circ$ . Consequently, radiation is high during the summer months and low during the winter months.

Another factor which affects total daily radiation received is the day length. In late June the day length at Ames is about  $15\frac{1}{4}$  hours, in late December it is a few minutes over 9 hours. In the southern part of the state, summer days are a few minutes shorter and winter days a few minutes longer. In the northern part of the state winter days are a few minutes shorter, and summer days a few minutes longer. At the time of the equinox, about March 21 and September 22, days are just over 12 hours duration in all parts of Iowa. On any particular day, the total radiation across Iowa would vary only a relatively small amount, except for the effects of varying local cloud cover.

Radiation totals for each hour of the day show a typical daily pattern. In Figure 2, daily curves for typical clear and heavy overcast days in summer, fall or spring, and winter are shown. These curves show the amount of radiation which would be received at any time of the day under these conditions. Radiation at noon in the summer is twice what it is in the winter.

Reduction in solar radiation is not proportional to cloud cover. McQuigg and Decker (10) stated:

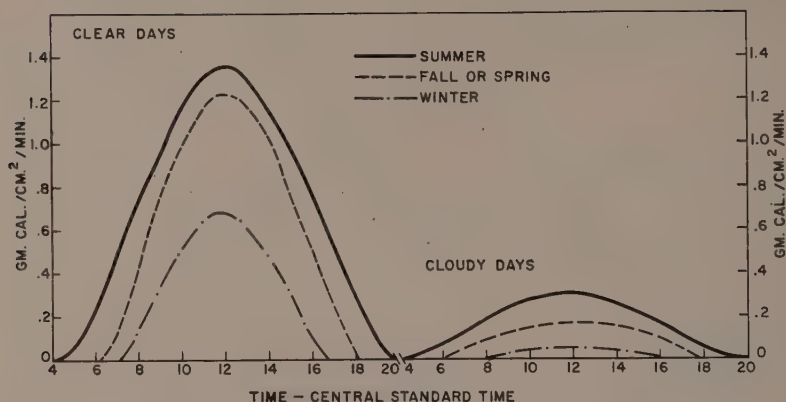


Figure 2. Typical radiation curves for clear and cloudy days for summer, fall or spring, and winter days at Ames.

"Note that scattered clouds (10 to 50 percent cloud cover) do not reduce the amount of energy received very much; even a sky condition with broken clouds (50 to 90 percent cloud cover) does not cause a great reduction in the amount of incoming energy. At mid-day, scattered clouds reduce the amount of energy received by about 5 percent while broken clouds cause a reduction of nearly 20 percent from the energy received with a clear sky. Scattered and broken clouds reduce the amount of energy received by only a small amount because much of the solar energy intercepted by the clouds is reflected to the earth's surface through the clear spaces between the clouds."

The cloudy days represented in Figure 2 are for a very heavy overcast.

In Figure 3, the data for July 20, 1959 are shown to compare solar with net radiation. The solar radiation reached a peak of over 1.3 langley/min near noon. The net radiation over a corn field for July 20 is also shown in Figure 3. The net radiation is equal to the incoming short wave radiation plus longwave sky radiation less the reflected solar radiation and the outgoing longwave radiation from the ground and crop cover. The net radiation is used in evapotranspiration, heating the air, heating the soil, and in photosynthesis. When the moisture supply is adequate, the larger part of this is used in evapotranspiration. It is a very important factor in determining the water use by plants. It takes approximately 58.5 langleys to evaporate 1 mm of water. The net radiation on July 20 would indicate a possible maximum evaporation of about 1 mm per hour at midday and about 7 mm for the day. However, not all of this energy is normally used in evaporation. Denmead (3) measured a transpiration of 6.04 mm for this day. Using Penman's equation (11) he calculated evaporation from an open water surface at 6.59 mm. On some days energy is also advected into an area, and a greater water loss might occur.

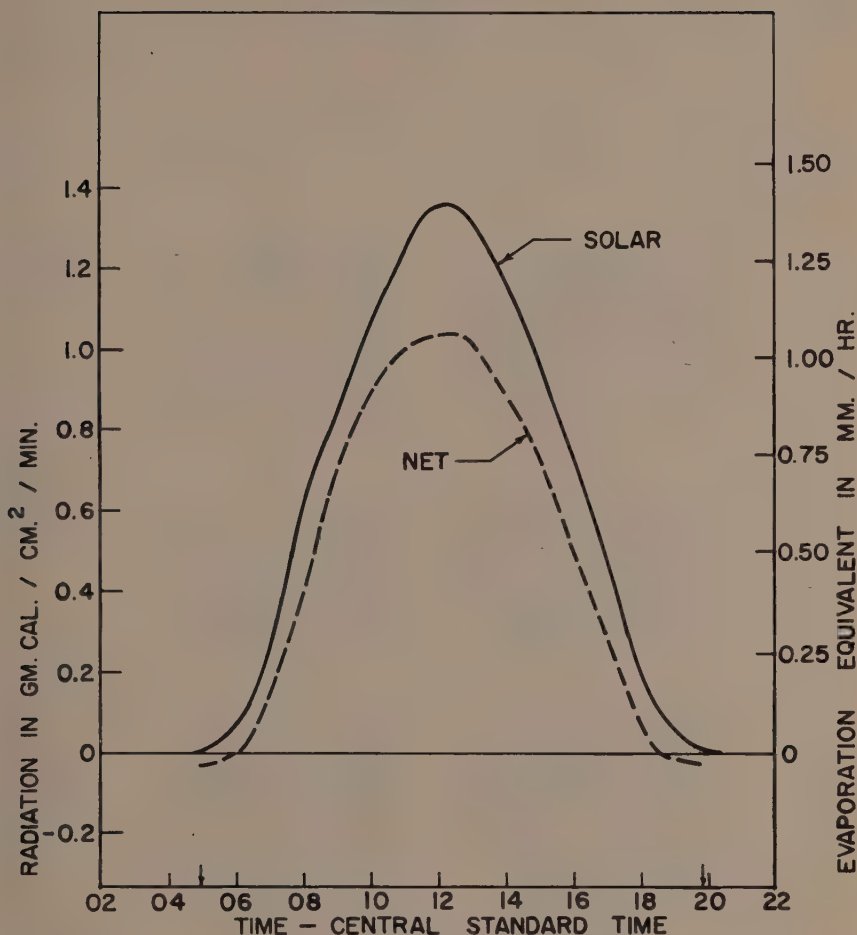


Figure 3. Solar and net radiation for Ames, July 20, 1960.

#### Sunshine Data

Much longer periods of record are available in Iowa for "percent possible sunshine" than for intensity of solar radiation. Fortunately there is a good correlation between them. Stations available (15) for this study were Des Moines, Burlington, Davenport, Dubuque, Charles City and Sioux City, Iowa; Omaha and Lincoln, Nebraska; Madison and La Crosse, Wisconsin; Peoria, Illinois; Columbia and St. Joseph, Missouri; Minneapolis, Minnesota; and Huron, South Dakota. Data have been recorded using a Marvin sunshine recorder (a differential air thermometer with a clear bulb and a black bulb) and/or the differential between two photocells, one shielded from the sun. Both these instruments are set so that sunshine is recorded when the disk of the sun can be seen just



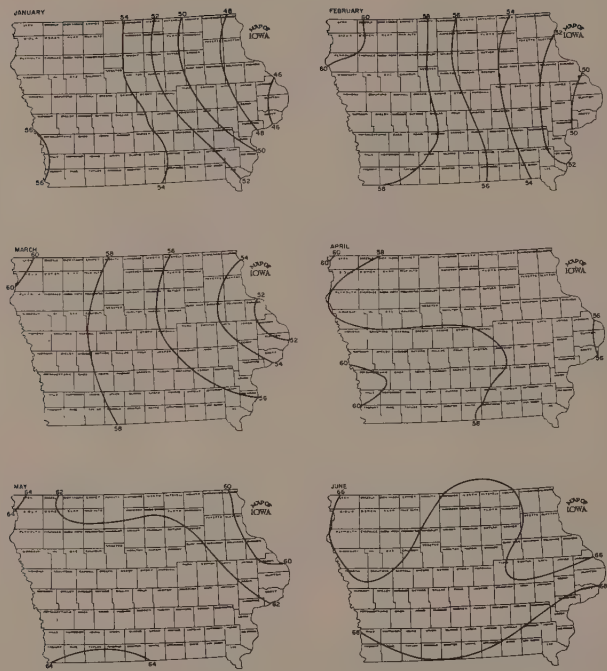


Figure 4. Monthly average percent possible sunshine (January - June)

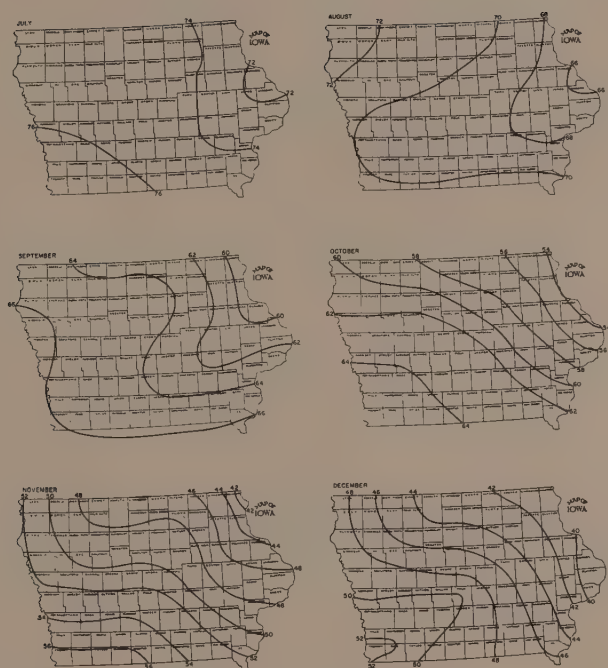


Figure 5. Monthly average percent possible sunshine (July - December)

faintly through the clouds. Although this network of stations is rather sparse, isolines of percent possible sunshine were drawn and except for Burlington, which had a short period of record, showed a consistent pattern.

The percent of possible sunshine generally decreases from west to east. The lowest percentage occurs during the November-January period (Figs. 4, 5), with December having the lowest percent of possible sunshine ranging from 40% in the northeast to 52% in the southwest. By February and March this has increased to 52-60%. There is a continued gradual increase through the spring until the sunshine is 72-76% in July. The percent of possible sunshine then gradually decreases to the winter minimum.

In addition to the mean monthly sunshine, the distribution of the percent possible sunshine for different months is of interest. These data can be seen in Table 1 for Des Moines. From these it can be seen that few months have a percent of possible sunshine less than 30% and few months have more than 90% of possible sunshine. In the last column the average cloudiness during the daylight hours for each month is shown. A high percent possible sunshine occurs with the lowest percent of cloud cover.

Table 1. Distribution, by percent, of average monthly values of percent possible sunshine, and average percent monthly cloudiness during daylight hours at Des Moines, Iowa. (1930-1959)

Month	Percent Possible Sunshine								Ave. cloud- iness
	20-29	30-39	40-49	50-59	60-69	70-79	80-89	90-99	
	%	%	%	%	%	%	%	%	%
Jan.	--	10	27	<u>40</u>	13	10	--	--	58
Feb.	--	10	20	<u>27</u>	<u>30</u>	10	3	--	59
Mar.	--	13	17	<u>40</u>	<u>13</u>	17	--	--	62
Apr.	--	3	20	17	<u>43</u>	17	--	--	60
May	--	--	13	24	<u>40</u>	20	3	--	59
June	--	--	3	13	<u>37</u>	<u>37</u>	10	--	56
July	--	--	--	3	14	<u>53</u>	27	3	45
Aug.	--	--	--	20	27	<u>33</u>	20	--	47
Sept.	--	--	--	17	<u>33</u>	<u>23</u>	27	--	47
Oct.	--	--	13	17	27	<u>40</u>	3	--	48
Nov.	3	13	20	<u>30</u>	27	<u>7</u>	--	--	58
Dec.	3	24	<u>33</u>	<u>30</u>	7	3	--	--	62

Table 2. Distribution of percent possible sunshine for Des Moines, Iowa. Values in table are percent of days with specified amount of sunshine.

Month	Percent Possible Sunshine									
	0-9	10-19	20-29	30-39	40-49	50-59	60-69	70-79	80-89	90-100
Jan.	26.1	3.1	4.4	5.0	5.6	6.1	5.6	10.0	8.4	25.6
Feb.	23.8	4.1	4.4	5.0	5.5	5.5	5.7	9.4	10.0	27.0
Mar.	23.2	5.2	3.5	5.8	5.3	7.3	6.5	8.7	9.4	25.2
Apr.	17.8	5.3	4.5	4.2	5.2	6.7	5.7	10.5	11.3	28.8
May	13.9	4.0	4.0	6.3	6.6	8.9	8.2	10.2	11.6	26.3
June	9.5	3.9	4.9	5.0	6.4	8.4	8.9	10.2	13.2	29.6
July	4.0	2.3	3.5	4.0	6.8	7.6	9.2	10.6	12.3	39.7
Aug.	7.6	3.9	3.4	4.8	5.3	7.3	6.9	13.1	11.1	36.6
Sept.	10.7	3.8	4.7	2.3	4.0	5.2	6.0	11.2	9.5	42.7
Oct.	13.7	5.6	3.7	4.5	3.2	5.2	4.5	7.1	9.5	42.9
Nov.	28.2	5.3	4.0	3.2	5.7	4.8	5.3	7.5	7.7	28.2
Dec.	32.0	4.5	3.5	6.6	5.7	7.2	5.8	7.7	5.7	21.3

Individual days may have from 0 to 100% of possible sunshine. A summary of the daily distribution of percent possible sunshine is given in Table 2. During each month there is a relatively large percent of the days with 90-100% of possible sunshine. The highest percent occurs in the July-October period. In the cool season months, there is also a relatively large amount of days with very low sunshine, but in midsummer few days of this type occur. A distribution peaked at high and low amounts is characteristic of sunshine and cloud cover data.

#### Relation of Sunshine and Solar Radiation

Various workers have studied the relation between hours of sunshine and solar radiation. Sandoval and Shaw (12) have presented graphs which show the relationship for Des Moines sunshine and Ames solar radiation. Fritz and MacDonald (6) developed the equation

$$Q/Q_0 = .35 + .61 S$$

where  $S$  is the percent of possible sunshine,  $Q$  is the amount of solar radiation actually received and  $Q_0$  the radiation during cloudless days. Monthly means were used to compute this. Using this equation, the ratio,  $Q/Q_0$ , can be easily computed for any month for different locations in Iowa. Hamon et al. (7) provided a diagram to compute the radiation for any latitude with different percents of possible sunshine. These two methods give comparable, but not identical, results. The results are summarized in Table 3. Under average cloudiness conditions the average

Table 3. Effect of change in percent possible sunshine, and latitude of solar radiation.

	Langleys per Day	
	December	June
Change of sunshine of 2%		
at 10% sunshine	8-10	20
at 50% sunshine	3- 5	7-10
at 90% sunshine	2	5- 8
Change of latitude of 1°	8	0

effect across Iowa would be 20-25 langleys per day in December, and only about 10 langleys per day in June due to the small range in average percent sunshine. With a range in latitude across Iowa of about 3°, the increase in December from north to south is about 24 langleys per day; in June there is practically no difference. Due to local differences in cloud cover, individual days may show very large differences.

#### LITERATURE CITED

1. Angstrom, A. 1924. Solar and terrestrial radiation. Roy. Meteor. Soc. Quart. Jour. 50:121-125.
2. Black, J.N., C.W. Boynton, and J.A. Prescott. 1954. Solar radiation and the duration of sunshine. Roy. Meteor. Soc. Quart. Jour. 80:231-233.
3. Denmead, O.T. 1960. Private communication.
4. Eppley Pyrheliometer Manual. Bull. 2, Eppley Laboratory, Inc. Newport, R.I.
5. Fritz, Sigmund. 1951. Solar radiant energy and its modification by the earth and its atmosphere. Compendium of meteorology, 13-33. Amer. Meteor. Soc., Boston.
6. \_\_\_\_\_ and T.H. MacDonald. 1949. Average solar radiation in the United States. Heating and Ventilating 46:61-64.
7. Hamon, R.W., L.L. Weiss, and W.T. Wilson. 1954. Insolation as an empirical function of daily sunshine duration. Monthly Weath. Rev. 82:141-146.
8. Hand, I.F. 1949. Weekly mean values of daily total solar and sky radiation. Tech. Paper No.11. U.S. Weather Bureau.
9. \_\_\_\_\_. 1950. Insolation on clear days at the time of solstices and equinoxes for latitude 42°N. Heating and Ventilating 47:92-94.
10. McQuigg, J. and W.L. Decker. 1958. Solar Energy. Res. Bull. 671. University of Missouri, Columbia, Mo.
11. Penman, H.L. 1956. Evaporation: An introductory survey. Netherlands Jour. Agr. Sci. 4:9-27.



12. Sandoval, A. and R.H. Shaw. 1958. Relation of solar radiation measurements at Ames to sunshine observations at Des Moines. Iowa State Coll. Jour. Sci. 33:173-184.
13. Smithsonian Meteorological Tables. 1951. Smithsonian Misc. Collections Vol. 114. Smithsonian Institution.
14. U.S. Weather Bureau. National Climatological Data, Published monthly.
15. \_\_\_\_\_. Local Climatological Data. Published monthly.
16. deVries, D.A. 1955. Solar radiation at Wageningen. Mededelingen van de Landbouwhogeschool. 55:277-304.



FACTORS AFFECTING THE INCIDENCE OF REACTION  
TISSUE IN *POPULUS DELTOIDES* BARTR.<sup>1</sup>

Graeme P. Berlyn<sup>2</sup>

**ABSTRACT.** The present investigation was undertaken to provide information on the effect of various intrinsic and environmental factors on the incidence of tension wood in *Populus deltoides* Bartr. Tension wood is a form of reaction tissue which occurs on the upper side of leaning angiosperm stems. It is characterized by fiber tracheids which possess an unligified, gelatinous appearing, cellulosic layer in their cell walls. Fourteen bottomland cottonwood stands growing on previously studied soils were used in this study. The average age of the timber was 46 years. Three large cores of tissue were extracted from the upper side of each of 84 trees at breast height. The external morphological features of each of the trees were measured and described.

A quantitative histological analysis was developed. Images of cross sections including the cambium and 3 annual increments were projected on paper grid systems. Counts of stimulated and nonstimulated cells in randomly selected grid squares were recorded.

The induction of the gelatinous layer occurs early in cellular ontogeny, i.e. the layer may be observed immediately subjacent to the cambium. The cambium produces gelatinous fibers in small groups (unless 100% reaction occurs), but abrupt variations occur. The proportion of gelatinous fibers is positively correlated with radial growth and the number of cells per unit area. There is a depression of vessel size in reaction tissue. Strong fluctuation in the factors which determine radial growth are associated with equally strong fluctuation in the factors that induce reaction tissue.

<sup>1</sup> Journal Paper No. J-4010 of the Iowa Agricultural and Home Economics Experiment Station, Ames, Iowa. Project No. 1330. The research was conducted in cooperation with the Ames Branch of the Central States Forest Experiment Station, Ames, Iowa. The author is very happy to acknowledge the collaboration of Dr. H. T. David of the Iowa State University Statistical Laboratory in the statistical studies. The author is also indebted to his major professors, Drs. D. W. Bensend and J. E. Sass, and to the Forest Products Laboratory for advice and encouragement.

<sup>2</sup> Instructor in Wood Anatomy, Yale University School of Forestry, New Haven, Connecticut.

This association is limited to certain metabolic intervals as expressed by radial growth. The absolute nature of the cytological response and the distributional form of the histological response suggest a chemical feedback mechanism, possibly mediated by hormonal levels.

A study of the form and distribution of the data was made. Weighted means of samples of 8 grid squares were 129% more efficient than unweighted means. The variance associated with reaction tissue was significantly greater than binomial variance. Untransformed data were shown to provide more information than either the arcsine or square root transformed data. Significant but small positive correlation exists between adjacent squares and significant but small negative correlation exists between distant squares. This suggests that random sampling may be improved upon by utilizing the low variance associated with negative correlation. Selection of grid squares at the vertices of suitable, randomly placed geometrical figures is suggested.

In multiple regression analyses, lean, crown volume, and available phosphorus were found to be highly significantly related to the proportion of gelatinous fibers. Crown volume was also an excellent correlate with many other growth variables. The phosphorus relationship may stem from its role in cellulose synthesis. In tension wood cellulose biosynthesis is stimulated and lignin biosynthesis is depressed. This needs to be checked at more critical levels of phosphorus. Lean was clearly the strongest correlate. For the age and ecological situations of the trees examined in this study there appeared to be one over-all regression coefficient for the proportion of gelatinous fibers regressed on lean. The rate and capacity for reaction tissue production in woody plants are depressed with the onset of senescence, the duration of stimulus, and the cyclic leveling off of diameter growth.

- - - - -

## INTRODUCTION

Although extensive technological research has been done on the reaction tissues of angiosperms and gymnosperms, no comprehensive analysis of the functional relationships between reaction tissue and environmental and hereditary factors is to be found in the literature. Since the presence of tension wood in lumber is associated with extremely high longitudinal shrinkage, twisting and warping, a thorough knowledge of the botanical nature of tension wood is, then, of more than academic interest. For the present study Populus deltoides Bartr., eastern cottonwood, was used as experimental material. This tree is currently of high technological

interest in many areas. It can be grown on submarginal agricultural lands, produces a large volume of merchantable timber in a short period of time, and has a wide ecological and geographical range. Serious limitations to the commercial importance of cottonwood arise from the presence of reaction tissue (tension wood) in this species.

## REVIEW OF PERTINENT LITERATURE

### Incidence and distribution of tension wood

The term reaction tissue is a general term used to refer to tissues found in leaning or otherwise stimulated plant organs. In angiosperms the reaction tissue forms on the upper side of leaning stems and is termed tension wood whereas in gymnosperms the reaction tissue forms on the lower side of the leaning stem and is called compression wood. The tissues in these regions are physically, chemically, and anatomically different from the surrounding tissues. The phenomenon is often associated with eccentric growth. The disposition of reaction tissue in branches is more complex than in stems because the phenomenon is actually morphogenetic in nature, i.e. the physical location of the reaction tissue is more directly related to morphogenetic pattern than to adaxial or abaxial position.

Because of its fundamental relationship to growth and morphogenesis, reaction tissue has been the subject of much basic biological inquiry. A number of recent reviews of the literature are available (Marra, 1942; Onaka, 1949; Dadswell and Wardrop, 1949; Spurr and Hyvarinen, 1954a; Wahlgren, 1956; Westing, 1959; Berlyn, 1960). Reaction tissue is of wide occurrence in woody plants. However, Onaka (1949) states that tension wood seems to be characteristic of broad-leaved trees in the early stages of evolutionary development and is absent in groups such as Ilex, Euonymus, and Rhododendron.

Anatomically the stimulated fiber tracheids (and libriform fibers) of tension wood are characterized by the presence of a layer of gelatinous appearing material in the secondary cell wall. These cells are commonly called gelatinous fibers or tension wood fibers. At present there are at least three known different cell wall organizations of tension wood fibers. The three layers of the secondary cell wall of a normal unstimulated tracheid, fiber tracheid, or libriform fiber may be designated centripetally as  $S_1$ ,  $S_2$  and  $S_3$  (Bailey and Kerr, 1935). The gelatinous layer, when present, can be designated as G. Using this notation, the three main types of cell wall organization are:

a.  $S_1$ ,  $S_2$ ,  $S_3$ , G

b.  $S_1$ ,  $S_2$ , G

c.  $S_1$ , G

(after Wardrop and Dadswell, 1948, 1955;  
Onaka, 1949; Dadswell and Wardrop, 1955).

In addition to this, Wahlgren (1957) describes a central gelatinous layer in the tension wood of overcup oak (Quercus lyrata Walt.), however, the exact wall layers involved were not identified. Actually a distribution of secondary cell wall organizations may exist in tension wood. Apparently



the entire cambial mechanism is altered during induction and initiation. In some observations the vessels appeared to be reduced both in size and number in wood containing tension wood (Chow, 1946; Dadswell, 1945; Dadswell and Wardrop, 1949). Marra (1942) reported that the vessels in the tension wood of silver maple (Acer saccharinum L.) were reduced in size, but were more numerous. Several workers have found that in Populus deltoides, Bartr. the gelatinous fibers are heavily concentrated on the upper side of the leaning stem at breast height, but that in the higher parts of the stem the distribution spreads around the entire bole (Kaeiser, 1955; Kaeiser and Pillow, 1955; Wahlgren, 1956). Gelatinous fibers may occur in both xylem and phloem and they may occur in stems, branches, vines and petioles.

#### Role of tension wood in morphogenesis

The nature of the morphological response has been studied intensively (Hartmann, 1932, 1942; Jaccard, 1938, 1940; Onaka, 1949; Wardrop, 1949, 1945). One of the earliest theories stated that tension wood is a morphological response to tensile stress. This view appeared to be consistent with information on vines, tendrils and petioles (Haberlandt, 1914; Busgen and Munch, 1929; Wardlaw, 1952). However, the inadequacies of this concept became apparent when stems were bent into vertical hoops, in which case the tension wood developed on the upper side with respect to gravity regardless of whether the tissue was under tension or compression (Ewart and Mason-Jones, 1906; Jaccard, 1938, 1940). When the same experiment was applied to coniferous species the compression wood always formed on the lower side regardless of stress (Hartig, 1901; White, 1908; Burns, 1920; Hartmann, 1932, 1942; Sinnott, 1951, 1952). These series of experiments led to the conclusion that reaction tissue was primarily geomorphic in nature. This theory was also supported by a series of centrifugation experiments (Hartmann, 1942; Scott and Preston, 1955; White, 1908; Jaccard, 1940). Jaccard (1940) also noted that irrespective of the initial stress condition tension wood was intimately associated with forces leading to contraction of the stem. He concluded that tension wood is regulatory in nature (cf. Newcomb, 1895) and tends to maintain stems and branches in an equilibrium position with respect to gravity.

Hartmann (1932, 1942) reported the results of over 20 years of research on reaction tissue on a wide variety of woody plants. He postulated that a shoot has an "Innerewachsrichtung," an intrinsic growth direction. When an organ deviates from its "Innerewachsrichtung," reaction tissue forms in such a way that it restores or tends to restore the intrinsic growth direction. The reaction tissue of angiosperms, he said, forms in such a way that it tends to pull (contractive force) the organ back into its foreordained position, whereas in gymnosperms the reaction tends to push the organ back into its intrinsic growth direction (expansive force). Regardless of the teleological and vitalistic implications, Hartmann's concept does identify the locus of reaction tissue under all conditions. For example, Wardrop (1956) bent a branch upward from its original position. Tension wood formed on the lower side where it exerted a measurable "pulling" force in the downward direction. When the branch was bent downward tension wood formed on the upper side.

Sinnott (1951, 1952), using *Pinus strobus* L., duplicated many of Hartmann's experiments and reached similar conclusions. Other studies have shown that the formation of tension wood produces strong contractive forces which seem to arise during differentiation of the fiber cell wall (Jacobs, 1945; Wardrop, 1956).

Surgical experiments performed by H. J. Lutz<sup>3</sup> on artificially bent white pines dramatically illustrate the genesis of an expansive force during compression wood formation. When the lower portions of the upper side of stems were removed or penetrated by saw cuts, recovery to the vertical position was violent, sometimes resulting in such "over-correction" that the crown weight broke the stem in two.

Additional complexity arises because growth movements are also associated with other phenomena such as phototropism, geotropism, plagiotropism, epinasty, etc.

#### Eccentric growth and tension wood formation

The development of tension wood is often associated with eccentric growth. However, this is not always the case, at least in some species (Jaccard, 1938; Wahlgren, 1956; Wardrop, 1956; Lassen, 1958).

Since fiber length is inversely related to radial growth rate (cf. Spurr and Hyvarinen, 1954b) tension wood should theoretically have a similar relationship. However, there is controversy in the literature on this point (Chow, 1946; Dadswell and Wardrop, 1949; Jayme, 1951; Messeri, 1954; Kaeiser and Stewart, 1955; Kaeiser, 1955; Wardrop, 1956; Berlyn, 1960). Wardrop (1956) concluded that the controversy arises because the eccentricity associated with tension wood may result from either a differential time of cambial growth or a differential rate of cambial activity. He also cautions that it is almost impossible to obtain paired samples from which critical comparisons can be made.

#### Mechanism of tension wood formation

Defining tension wood as a morphogenetic phenomenon leaves the mechanism still to be explained. Spurr and Hyvarinen (1954a) state that anyone familiar with the behavior of plant hormones cannot fail to see a close similarity between reaction wood formation and auxin activity. Several workers have successfully induced compression wood with application of 3-indoleacetic acid (Wershing and Bailey, 1942; Onaka, 1949; Fraser, 1952; Sinnott, 1952). It is well known that gravity influences the auxin distribution in plant organs, but bioassays have led to conflicting evidence in regard to leaning trees (see Onaka, 1949; Sinnott, 1952). One of the primary effects of gravity may be its influence on auxin source. In angiosperms, the development of buds, the main sites of auxin synthesis, is primarily on the upper side of leaning stems, while in gymnosperms bud development is greatest on the lower side (cf. Priestly and Tong, 1927; Dadswell and Wardrop, 1949). Decapitation experiments have also been conflicting. Wardrop (1956) found that decapitation prevented reaction tissue formation on bent shoots while Westing (1959) did not observe this cessation of compression wood formation even after prolonged mutilation.

<sup>3</sup> Courtesy Dr. H. J. Lutz, New Haven, Connecticut. Yale University School of Forestry. Private communication, 1960.

The actual mechanisms by which auxins influence plant metabolism are imperfectly known, but it is known that one result of increased auxin activity is an increase in the plasticity of the cell wall (Bonner and Galston, 1952, p. 362). Westing (1959) concludes that since the locus of reaction tissue in the inclined portion of a stem is independent of tip orientation, and since girdling experiments eliminate bound auxin as a factor, increased auxin levels are not involved. He suggests that differential sensitivity to auxin as a result of orientation change is the chief factor involved.

One of the main differences between tension wood and compression wood is that tension wood tissue is poorly lignified while there is increased lignin synthesis associated with compression wood. Peroxidase is assumed to be a necessary component for lignin synthesis. Wardrop and Scaife (1956) found increased peroxidase activity associated with mature tension wood in *Eucalyptus*. They concluded that this indicated a lack of substrate for lignin biosynthesis. Westing (1959) found shifts in peroxidase levels in leaning conifers. He also isolated a tip-dependent Salkowski-positive substance which was not IAA.

It must be admitted that after nearly 100 years of research, the problem of reaction wood remains an enigma. For the present it can only be said that reaction tissue is apparently an auxin mediated anatomical manifestation of various metabolic activities associated with morphogenesis.

## MATERIALS AND METHODS

Fourteen pure stands of even-aged cottonwood growing on previously studied bottomland soils were selected for this project. These experimental areas are located along the Missouri River in western Iowa (Harrison and Monona counties).<sup>4</sup> The average age of the timber was 46 years which approximates early maturity for cottonwood. Each plot occurs on a single soil type. These soils are all alluvial and range in texture from coarse sands to clay. Table 1 is composed of extracts from Brendemuehl's thesis and contains the soil-site information used in the regression analysis section of this study. Preliminary investigations by Brendemuehl showed that the pH of these soils varies from 6.6 to 8.2 with over 90% of the values in the range of 7.0 to 8.0. Phosphorus is readily available to plants in this pH range and was not considered to be severely limiting. Exchangeable potassium on 10 different areas was found to be greater than 400 pounds per acre, an amount which may or may not be excessive under field conditions (cf. Thomson, 1956; Brendemuehl, 1957).

Brendemuehl calculated site indices for these plots by standard methods (cf. Chapman and Meyer, 1949). This site index is defined as the average height attained by the dominant trees of the stand at 50 years. Height growth is presumably the measure least contaminated by density and other extrinsic factors (cf. Hartig, 1901). The utility of site index is that it defines yield without harvesting at any time and is not confounded with age (cf. Thomson, 1956).

<sup>4</sup> Soils information and site indices were recorded in a previous study by R. H. Brendemuehl (1957).

Table 1. Soil-site information on some Missouri bottomlands.

Plot No.	Site Index	Available moisture (%)	Average silt plus clay (%)	Foliar nitrogen (%)	NO <sub>3</sub> -N after 2-weeks incubation (lbs/acre) 0" to 48"	Available phosphorus (lbs/acre) 0" to 48"
9	87	10.1	74.5	2.051	31.1	2.0
12	88	6.8	44.4	1.466	6.8	1.5
10	89	4.6	39.1	1.492	35.0	2.0
2	89	13.6	96.5	1.739	20.6	14.0
20	93	9.9	67.5	1.936	49.0	1.5
1	95	15.4	96.2	2.020	3.8	48.0
5	97	11.2	90.7	1.472	4.1	1.5
22	100	12.0	67.1	1.860	78.8	4.5
18	101	9.8	57.0	1.515	23.3	3.5
13	103	16.3	97.8	1.986	83.9	6.5
14	112	13.6	90.1	2.330	100.6	13.5
3	113	18.0	95.5	2.148	40.9	34.5
16	120	12.1	87.6	2.170	83.8	10.5
23	120	15.5	93.3	2.360	44.9	9.0

In the field studies, eighty-four trees were individually measured, sampled, and described. Leaning trees were limited in number and on the average six suitable trees were available on each of the 14 plots. Data taken in the field included:

1. Plot and tree number.
2. Date of sampling and age of timber.
3. Diameter of breast height in inches (d.b.h.).
4. Two orthogonal crown diameters in feet.
5. Crown length, symmetry, and position in canopy.
6. Total stem height in feet.
7. Lean at breast height (b.h.) in degrees and direction of lean.

Sampling for the histological studies consisted of extracting three large cores of tissue containing xylem, cambium, and phloem. These cores were taken from the upper side of the leaning trees at 4.5 ft (b.h.). One core was taken at the center of the upper side and the other two were extracted one-sixth of the circumference to the left and right. The cores were of sufficient length to include three annual increments of xylem.

A quantitative histological method was developed for the laboratory studies (see Berlyn, 1959). Transections of unembedded wood were cut at approximately 13  $\mu$ . The specimens were oriented so that the cambium



and three annual increments (rings) of xylem appeared in the cross section. Chloriodide of zinc, a temporary stain (diagnostic of cellulose) was used for the main analysis (see Figure 1). Additional permanent slides were made using a safranin-fast green staining combination. The center cores on 13 plots were analyzed, and on plot 2 all three cores were analyzed.

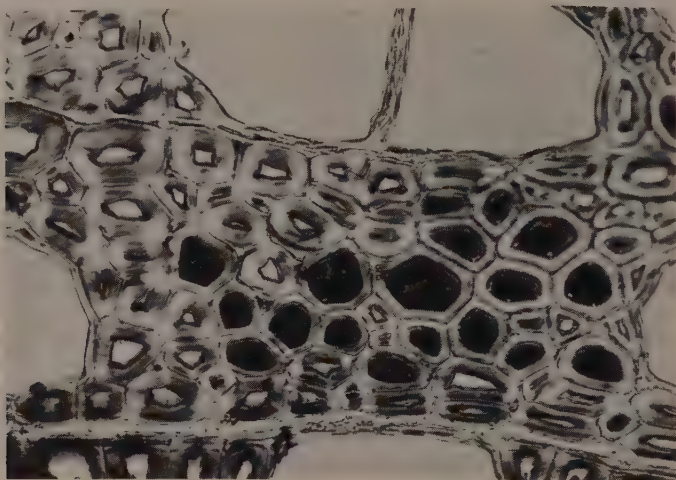


Figure 1. Transverse section showing gelatinous fibers stained with chloriodide of zinc. 400X.

The temporary slides were projected vertically onto a paper grid system (cf. Figure 2) at 139X. The 10 x 10 grid measures 12.5 cm square. At 139X each grid square encloses 0.09 mm x 0.09 mm of tissue or 8100 square microns. Three grid systems were analyzed for each of three annual increments making a total of 9 grid systems per slide. The grid systems within each annual ring were located systematically for maximum coverage. Within a grid system 8 grid squares were selected at random for observation. Each grid square can be identified by its randomly drawn coordinates. For example, the coordinates 3, 6 identify the grid square at the juncture of column 3 and row 6. In each of the squares selected actual counts were made of stimulated and non-stimulated cells. The data were recorded directly in the individual grid squares. A proportion of gelatinous fibers was computed on a per ring and a per tree basis. This index is the number of gelatinous-walled cells divided by the total number of cells in the sample unit ( $G/N = P_i$ ).

Variations of this analytical method were used for special purposes and will be described subsequently. For the correlogram analysis (which will be further described later), sections from five trees of varying lean were prepared in the usual way. On each of the five slides one annual ring was selected for detailed analysis. The objectives were to obtain information on the variance of data taken by this technique and to examine



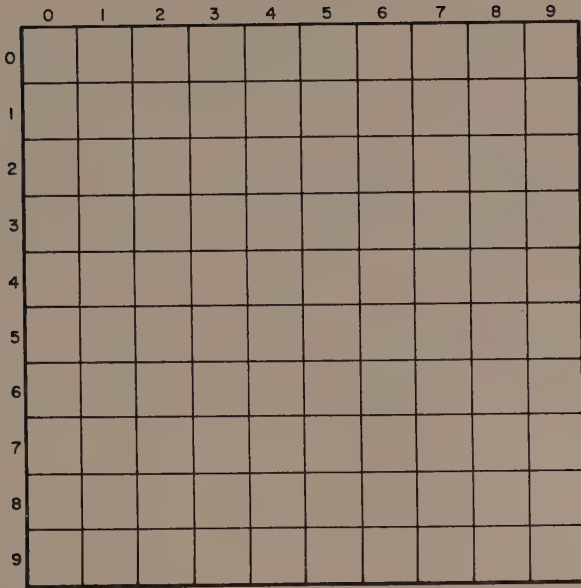


Figure 2 The grid system used in the histological analysis.

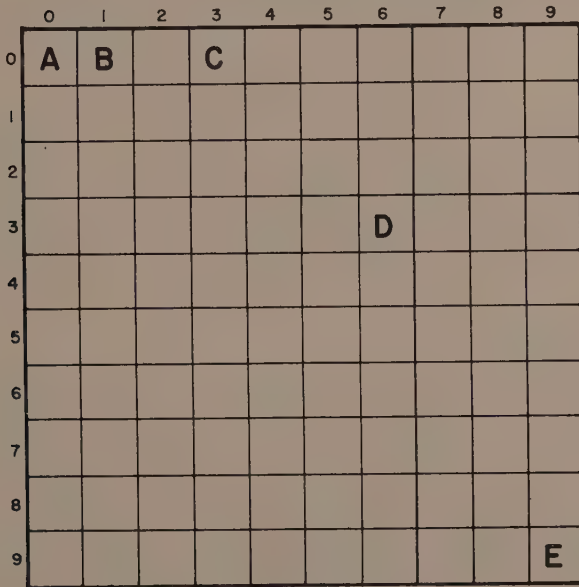


Figure 3. Grid system showing fixed sample.

the mathematical structure of the sampling system. To develop replications a fixed sample of five squares was imposed on each grid system used (Figure 3). Distances between squares are recorded in Table 2. On each annual ring 24 grid systems were analyzed, three at a time. The positioning of each set of three grid systems was identical to the positioning of the three grid systems per ring in the main study. This involved two grid systems near the edges of the section and one in the center. The grid systems were randomly twirled after positioning so that a random placement was effected. Since the grid squares were the same fixed distances from each other it was possible to calculate correlation coefficients between the squares. Also variances of the percent gelatinous fibers (G/N) figures were computed.

Table 2. Distances between squares in millimeters.

Squares	A	B	C	D	E
A	0	0.90	2.70	6.04	11.46
B			1.80	5.25	10.84
C				3.82	9.74
D					6.04

Another variation of the main analysis was developed in order to study the relative efficiency of weighted as compared to unweighted means. This procedure consisted of running a 100% sample on the grid system.

## EXPERIMENTAL OBSERVATIONS

### Field observations

The phototropic response of Populus deltoides was observed in the field studies. Openings in the canopy and the stand margins are a source of lean and therefore reaction tissue. Furthermore, leaning trees exhibited the well-known crown asymmetry, i.e. the concentration of foliage was skewed to the upper side of the leaning stem (cf. Berlyn, 1960).

### Correlogram studies

The specific histological technique for this study has been previously described. This approach was designed to elucidate the geometrical configuration of gelatinous fiber initiation. The squares were at fixed distances and by computing correlation coefficients between the proportion of gelatinous fibers,  $P_i$ , of the five squares it was possible to determine whether certain squares tended to be more like each other than like other squares. For example, squares that were close together could have very similar  $P_i$ , particularly if the gelatinous fibers were laid down by the cambium in relatively large groups. Table 3 contains the grand average correlation coefficients from all five annual rings examined. Each correlation coefficient in the table is an average of 15

Table 3. Grand average of correlation coefficients between grid squares.

Squares	B	C	D	E
A	0.224769	0.062068	0.069882	-0.156675
B		0.033516	-0.061215	-0.137500
C			-0.007167	-0.0204024
D				-0.005091

correlation coefficients because separate correlations were calculated for the eight left, center, and right grid systems on each annual ring. Figure 4 is the grand average correlogram.

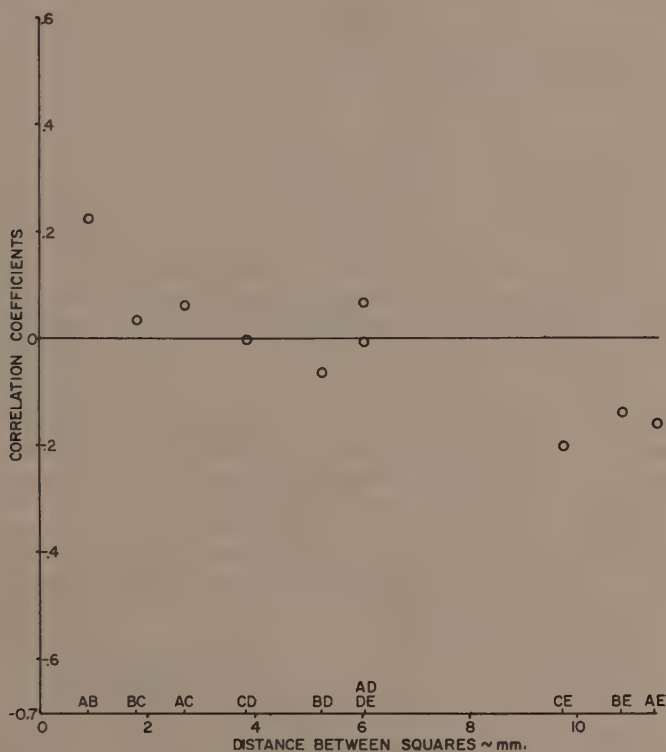


Figure 4. Grand average correlogram.

The question of interest was whether grid squares situated in close proximity on the grid system tend to have more similar  $P_i$  than distantly situated squares. Since the correlation coefficients, which are a measure of linear association, hover around zero, it appears that most of the grid squares are independent. Evidence and potential application, however, involve only the concept of pairwise correlation. As rough illustration the following definition of the stronger but similar property of pairwise independence is given:

$$\begin{aligned} \Pr(P_a < P_i, A < P_b) &= \Pr(P_a < P_i, A < P_b \mid P_e < P_i, D < P_f) \\ &= \Pr(P_a < P_i, A < P_b \mid P_c < P_i, C < P_d) \end{aligned}$$

i. e. the probability that the proportion  $P_i$ , A in square A lies between  $P_a$  and  $P_b$  when the proportion  $P_i$ , D in square D lies between  $P_e$  and  $P_f$  is equal to the probability that the proportion  $P_i$ , A lies between  $P_a$  and  $P_b$  when the proportion  $P_i$ , C in square C lies between  $P_c$  and  $P_d$ .

The question of correlation of  $P_i$  is of course based upon only a finite number of sampling repetitions, hence is subject to the usual sampling variation. It should be further noted that each annual increment selected for this study constitutes a separate population, each with its particular "true" population correlation coefficient. Hence, any empirical correlation coefficient obtained by averaging over empirical ring correlations is in effect an estimate of the average of the true population correlation coefficients.

The correlogram analysis reveals some aspects of the cambial response. For example, if the stimulated cells were laid down in sufficiently large clumps, correlation between proximate squares would be expected to be higher than correlation between more distant squares. If the reaction was more diffuse, the previously described independence would obtain. The data (Figure 4) suggest that there is positive correlation between adjacent squares and negative correlation between distant squares. It may be noted that negative correlation between distant squares might indeed be expected to occur under "clumping," since, if a certain clump of stimulated cells occurs, say in grid square A, it is automatically excluded from grid square E.

It must also be recognized that marked histological population differences can occur, for example when there are abrupt variations in the reaction response of a given increment. The stimulated cells may start or stop abruptly. This, however, is presumably due to discontinuity in the stimulus rather than particulate distribution. This may be a factor in the void of stimulated cells which often appears at the annual terminus.

It may be of interest to close this section with two technical comments alluded to in the above discussions.

#### 1. Significance of the correlation coefficients in Figure 4:

$$\begin{aligned} z &= 1/2 [\ln(1 + r) - \ln(1 - r)] \\ dz/dr &= 1/2 \left[ \frac{1}{1+r} + \frac{1}{1-r} \right] = \frac{1}{1-r^2} , \end{aligned}$$

where  $Z$  = the normal transformation of  $r$   
 $r$  = sample correlation coefficient  
 $\rho$  = population correlation coefficient

$$\text{Var}(r) = (\text{Var } z) \left( \frac{\partial r}{\partial z} \right)^2 \quad (\text{Volk, 1958, p.141})$$

$$\text{Var}(r) = (1/(n-3)) (1-r^2)^2, \text{ where we estimate } \rho \text{ by } r.$$

$$\text{SD} = \frac{1-r^2}{\sqrt{n-3}}, \text{ where } \text{SD}(r) = \text{standard deviation of } r$$

$n$  = number of units in a sample (i.e., 8)

$$\text{SD}(\bar{r}_{15}) = \frac{1-r^2}{\sqrt{15(n-3)}}, \text{ where } (\bar{r}_{15}) \text{ is an average of 15 numbers.}$$

$2 \text{SD}(\bar{r}_{15})$  defines an approximate 95% confidence interval around the zero line. In the case of Figure 4 the half length is 0.2188. The magnitude of the adjacent and most distance correlation coefficients is about 0.23. They are significantly different from zero.

2. Potential usefulness of the negative correlation between distant grid squares:

$$\text{Var}(X+Y) = \text{Var}(X) + \text{Var}(Y) + 2 \text{Cov.}(X, Y) \quad (\text{Snedecor, 1956, p.168})$$

$$\text{Where } \text{Cov.}(X, Y) = \rho_{xy} \sqrt{\text{Var}(X) \text{Var}(Y)}$$

In this case  $\rho_{xy}$  is negative, and hence  $\text{Var}(X+Y)$  is reduced.

These comments indicate that, in this case, random sampling might be improved upon, since the addition of negatively correlated quantities actually leads to lower variance. This could be accomplished by developing a sampling system which utilizes the negative correlation between distant squares.

#### Efficiency of weighted means

In this phase of the study a single grid system was analyzed in its entirety, i.e. data were recorded in each of the 100 grid squares. Tree 33 from plot 5 was used in this study, and the data are recorded in Table 4.

Table 4. Complete grid system analysis of tree 33.

Lean	12
Weighted population mean	0.8820
Weighted sample mean	0.8533
Unweighted population mean	0.8306
Unweighted population variance	0.0493
Sample estimate of population variance	0.02152
Variance of sample means	0.002475
Population binomial variance	0.00763



An unweighted population variance was obtained in the following way:

1. A proportion  $P_i = g_i/n_i$  was computed for each individual grid square where  $g_i$  = number of gelatinous-walled cells and  $n_i$  = total number of cells in the square.
2. A variance of these 100  $P_i$ 's was computed as follows:

$$\sigma^2 = \frac{\sum (P_i - \bar{P})^2}{N - 1} \quad \text{where } N = 100$$

$$\bar{P} = \frac{\sum P_i}{100}$$

A weighted sample was obtained in the following way:

1. Twenty samples of eight grid squares each were randomly drawn off the grid system.
2. A sample mean for each sample was computed as follows:

$$P_i = \frac{\sum_{j=1}^8 g_{ij}}{\sum_{j=1}^8 n_{ij}}$$

This is the total number of gelatinous-walled cells in all eight squares divided by the total number of cells in all eight squares.

3. A sample variance of these weighted means was computed as follows:

$$S^2 = \frac{\sum_{i=1}^k (\bar{P}_i - \bar{P})^2}{k - 1}$$

where  $k$  = number of samples of eight squares = 20

$\bar{P}_i$  = proportion of stimulated cells in the  $i^{\text{th}}$  sample

$\bar{P}$  = mean proportion of stimulated cells of all  $k$  samples

$$= \frac{\sum \bar{P}_i}{20}$$

4. From the above sample mean variance it is possible to obtain an estimate of the population variance:

$$\sigma_w^2 = S^2 \frac{Nn}{N-n}$$

(Snedecor, 1956, p.497)

where  $\sigma_w^2$  is the estimate of the population variance

$S^2$  is the variance of the sample means

$N = 100 =$  total number of squares in the population

$n = 8 =$  number of grid squares per sample.

A binomial variance may also be computed:

$$V = \frac{PQ}{n}$$

where  $V =$  binomial variance

$P =$  population proportion of gelatinous fibers

$Q = (1-P)$

$n =$  average number of cells per grid square

This binomial variance is actually of pseudobinomial character because of the random character.

For tree 33;  $s^2 = 0.002475$ ,  $\sigma_w^2 = 0.02152$ ,  $\sigma^2 = 0.0493$ , and  $V = 0.00763$ . A 95% confidence interval can be computed around the estimated population variance calculated from the weighted sample means.

$$\frac{\frac{Nn}{S^2(N-n)} 19}{\chi^2_{0.025}} \leq \sigma_w^2 \leq \frac{\frac{Nn}{S^2(N-n)} 19}{\chi^2_{0.975}}$$

This yields:

$$0.01245 \leq \sigma_w^2 \leq 0.04589.$$

Note that this interval does not include the unweighted population variance ( $\sigma^2 = 0.0493$ ). Efficiency is gained by using weighted sample means.

$$R.E. = \frac{\sigma_w^2}{\sigma^2} = \frac{0.0493}{0.02152} = 2.291$$

This represents a gain in efficiency of 129%. An approximated 95% CI around the efficiency is:

$$\frac{0.0493}{0.01245} \geq E_f \geq \frac{0.0493}{0.04589}, \text{ hence}$$

$$1.074 \leq E_f \leq 3.960$$

Weighted sample means were used in this study. This section also reveals that sampling variance was not binomial. This latter point will be further clarified in the following section.

### Investigating the advisability of a transformation

When dealing with proportions, especially with proportions subject to substantial variation, it is often advantageous to transform the data to some more stable scale of measurement. However, a transformation offers certain dangers to the exactitude of inferences. This is especially relevant when the denominator of the proportion varies. The data in this study are of the form  $g_i/n_i = P_i$ , where  $g_i$  is the number of anomalous cells and  $n_i$  is the total number of cells for that unit. The  $n_i$ 's vary slightly and the  $P_i$ 's vary from zero to one. In this situation a useful transformation should meet the following stipulations:

1. The situation should be such that the variance is a function of  $P$  ( $V(P)$ ) where  $P$  is the population mean.
2. The variance should be stabilized, i.e.  $V_T(P) \sim V_T$ , where  $V_T$  is the variance of the transformation.
3. Inference on  $\Delta P_T$  should be "similar" to inference on  $\Delta P$ , i.e. the differences in the population means should be similar for the transformation and untransformed case. This stipulation suggests the employment of a single monotone transformation applied to all  $P_i$ 's.
4. In view of Stipulation No. 2,  $\frac{\sqrt{V_T(P)}}{\Delta P_T} \sim \frac{\sqrt{V_T}}{\Delta P_T}$  and not much greater than  $\frac{\sqrt{V(P)}}{\Delta P}$ .

This stipulation requires that the transformation be such that it does not inflate the variance at the expense of sharpness of inference on  $P$ .

Weighting transformed values by  $\sqrt{n_i}$ , the square root of the total number of cells in a sample, poses a danger to the validity of inference as outlined in Stipulation No. 3.

A study of the nature of the variances was designed in order to determine the advisability of a transformation. The question to be resolved was whether to use the untransformed  $P_i$ ,  $\sqrt{P_i}$ , or  $\sin^{-1} \sqrt{P_i}$ .

The arcsine is a commonly used transformation for proportions. This transformation weights more heavily the small percentages which have small variance if the distribution is of the binomial form.

Figure 5 was derived from the five rings used in the correlogram study. The data are presented in Table 5. The variances of  $P_i$ ,  $\sqrt{P_i}$ , and  $\sin^{-1} \sqrt{P_i}$  were computed for each of the five rings. In addition a pseudobinomial variance was computed for each ring from the well known formula  $V = pq/n$ ,

where  $p$  = proportion gelatinous fibers,  
 $q = (1-p)$ ,  
 $n$  = average number of cells per replication (15 squares).

The pseudobinomial again refers to the random denominator.

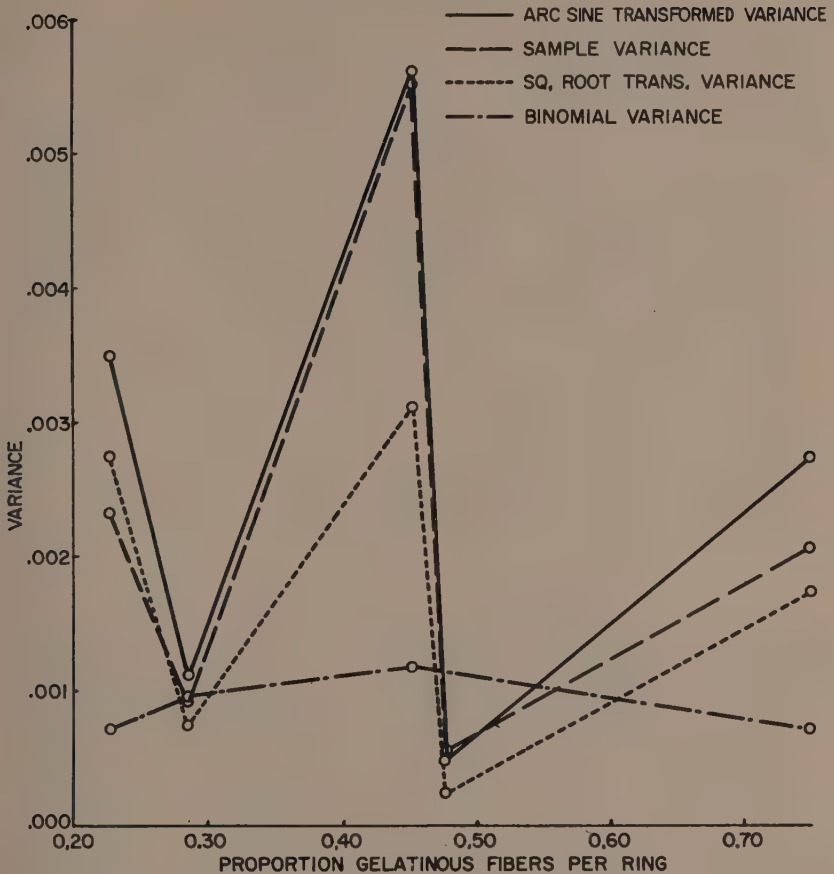


Figure 5. Relationships between the variances of transformed and untransformed data from the correlogram study.

Table 6 consists of combined data from field plots 1 and 5. On each tree an average proportion of gelatinous fibers was computed. This included nine grid systems, three from each of the three annual increments. Proportions were also computed for each of the 9 grid systems and variances of these proportions and the transformations thereof were recorded in the table. Figure 6 is the graphic representation of this data.

Table 7 and Figure 7 illustrate the mathematical relationships between the three forms of the data. These data were also taken from field plots 1 and 5. Essentially, this involves plotting  $P_i$ ,  $\sqrt{P_i}$ ,  $\sin^{-1} \sqrt{P_i}$  against  $P_i$ .

The plots of the variances, Figures 5 and 6, show that Stipulation 1 does not hold. The variance doesn't depend on  $P$  (the mean). On a ratio

Table 5. Variance in relation to proportion gelatinous fibers from correlogram study.

Proportion gelatinous fibers	Variance of proportions	Variance of square roots of proportions	Variance of arc sines of proportions	Binomial variance of proportions
0.22642	0.02490	0.00275	0.00350	0.00080
0.28426	0.00092	0.00075	0.00112	0.00097
0.45099	0.00553	0.00312	0.00562	0.00119
0.47681	0.00056	0.00025	0.00050	0.00113
0.74928	0.00208	0.00175	0.00275	0.00073

Table 6. Variance computations on individual tree basis for plots 1 and 5.

Plot, tree, lean	Average proportion gelatinous fibers	$V(P_i)$	$V(\sqrt{P_i})$	$V(\sin^{-1} \sqrt{P_i})$
1 - 6 - 2	0.02987	0.000501	0.00803	0.00817
5 - 31 - 3	0.0000	0.0000	0.0000	0.0000
1 - 3 - 4	0.4221	0.0331	0.0170	0.0397
5 - 30 - 5	0.0000	0.0000	0.0000	0.0000
1 - 13 - 6	0.5803	0.0975	0.0580	0.1231
5 - 34 - 6	0.09478	0.00710	0.01882	0.02105
1 - 12 - 8	0.7890	0.0176	0.0058	0.032
5 - 29 - 0	0.3283	0.0254	0.0215	0.0316
1 - 5 - 10	0.9188	0.0050	0.0014	0.0144
1 - 4 - 12	0.8121	0.0128	0.0043	0.0272
5 - 33 - 12	0.7960	0.0244	0.0082	0.0459
1 - 8 - 14	0.9364	0.0176	0.0056	0.0424
5 - 32 - 15	0.8230	0.0310	0.0107	0.0715
1 - 11 - 16	0.9281	0.0033	0.0009	0.0111
1 - 7 - 17	0.9107	0.0061	0.0017	0.0256



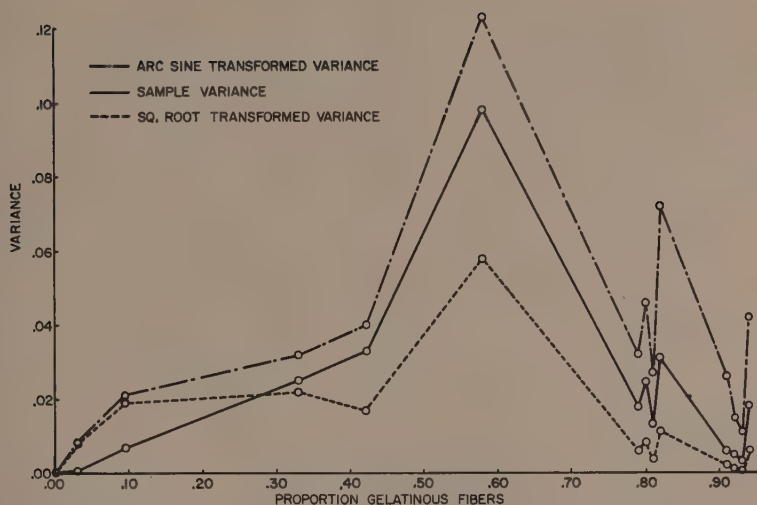


Figure 6. Relationship between the variance of transformed and untransformed data from plots 1 and 5.

basis the arc sine transformation does impart some variance stabilization as shown in Figure 5. That is, the ratio of the highest graph point to the lowest graph point is smaller for the arc sine than for the  $\Pi$  or  $\sqrt{\Pi}$ . The square root is the poorest in this respect. In Figure 6 the untransformed variance is about as stable as the arc sine while the square root is again considerably less stable. The square root transformation deflates the standard deviation  $\sqrt{V_T(\bar{P})}$ .

However, it also deflates  $\Delta P_T$ , the differences in means. This is shown in Figure 7. The differences are deflated for three-fourths of the abscissa values. This can be shown as follows:

$$y = x^{\frac{1}{2}} \\ dy/dx = \frac{1}{2}x^{-\frac{1}{2}}$$

$$\text{when } \frac{1}{2}x^{-\frac{1}{2}} = 1, x = \frac{1}{4}$$

This shows that the maximum point of the square root curve above the straight line  $\Pi$  curve occurs at one-fourth of the  $x$  range. Hence, for three-fourths of the  $x$  range the differences of the means are deflated. The arc sine does accentuate the  $\Delta P_T$ .

Variances are notoriously variable. This of course is evident in Figures 5 and 6. For Figure 5 an approximate 95% confidence interval has half length approximately equal to:

$$\pm 2 \sqrt{\frac{2\sigma^4}{n}} = \sigma^2 \sqrt{8/n} = \sigma^2$$

(Snedecor, 1956, p.73)

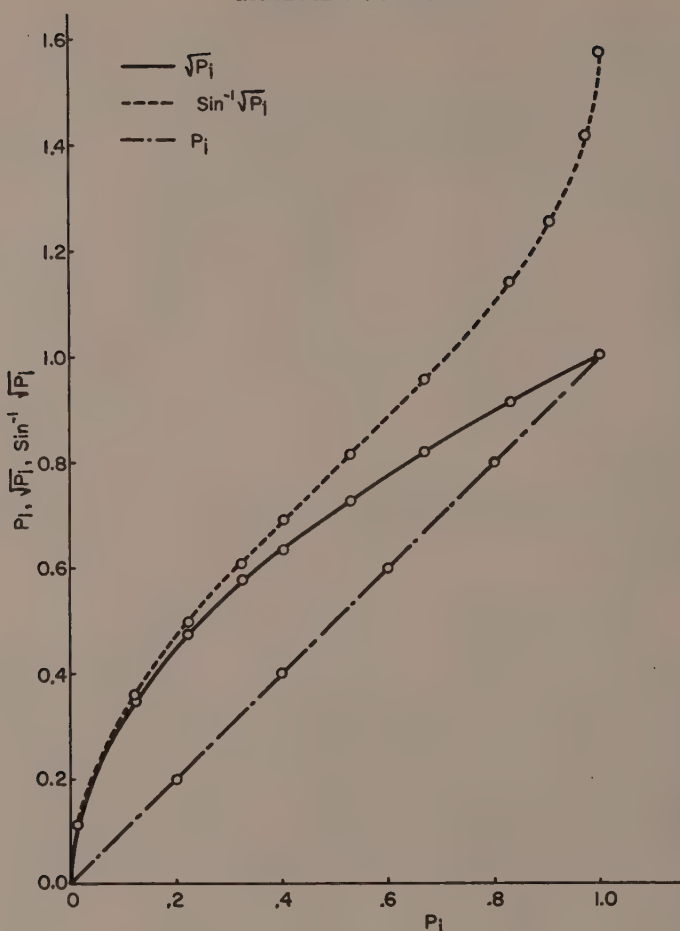


Figure 7. Mathematical relationships between transformed and untransformed data from plots 1 and 5.

This should be considered when studying this graph. The half length of the confidence interval is approximately equal to the ordinate magnitude.

It is apparent that transformations are not desirable in this case. Transformations may validate the use of a specific statistical technique, but may do so at the expense of a considerable amount of information. Conclusions drawn from such transformed data may have little biological validity.

#### Cytohistological observations

During the histological analysis, the width of each annual increment and the number of cells observed in each experimental unit were recorded for 294 annual increments from 84 different trees. After the analytical

Table 7. Mean values with transformations taken from plots 1 and 5.

Pi	$\sqrt{Pi}$	$\sin^{-1} \sqrt{Pi}$
0.0128	0.1132	0.113
0.1222	0.3496	0.357
0.2237	0.4730	0.493
0.2459	0.4959	0.519
0.3267	0.5716	0.608
0.4054	0.6367	0.690
0.5289	0.7273	0.814
0.6667	0.8165	0.955
0.8298	0.9109	1.146
0.9009	0.9492	1.251
0.9767	0.9883	1.418
1.0000	1.0000	1.571

study of the data form, statistical examination of the microscopic data was conducted for cell number, ring-width, and proportion of gelatinous fibers. Ring-width refers to the radial tissue growth of the xylem in millimeters, which occurred during a specific year of interest. The "cell number" designation refers to the number of xylem fiber tracheids (in transection) contained in the 24 grid squares analyzed per tree (eight grids per annual increment). With this measurement it is not possible to ascribe variations to fibers or vessels exclusively; nevertheless, it is a general measure of transverse cellular dimensions.

Microscopic observations indicate that, in general, with a given stimulus, smaller annual increments contain fewer stimulated cells, and below some threshold no gelatinous material is synthesized, regardless of the magnitude of stimulation. This trend is illustrated by Figures 8-12. Figure 8 shows the cambium and the last deposited annual increment of xylem. Note that the population of gelatinous fibers in the most recent increment is sparse. Figure 9 is a picture of the same slide as shown in Figure 8. The photomicrograph shows the radial extent of ring 2 and parts of rings 1 and 3. The population of stimulated cells increases in ring 2 (which is somewhat larger than ring 1) and becomes greater in the much larger ring 3 (lowest increment). A sequence of 2 or more borderline years often occurs before depression of reaction takes place. Time can thus substitute for ring width in the depression of reaction. Figure 10 also depicts the cessation of gelatinous fiber initiation in a small growth increment. Figures 11 and 12 illustrate a sequence from the same slide. In Figure 12 the effects of both time and growth factors on the anatomical expression of the reaction phenomenon are evident. Proceeding toward the cambium there is progressive depression in rings of equal size and extreme depression in the very small (and more recent) annual increment.

Figures 13, 14 and 15 are from three different leaning trees. These slides and other observations indicate that the initiation of the gelatinous layer occurs immediately subjacent to the cambial zone. Presumably

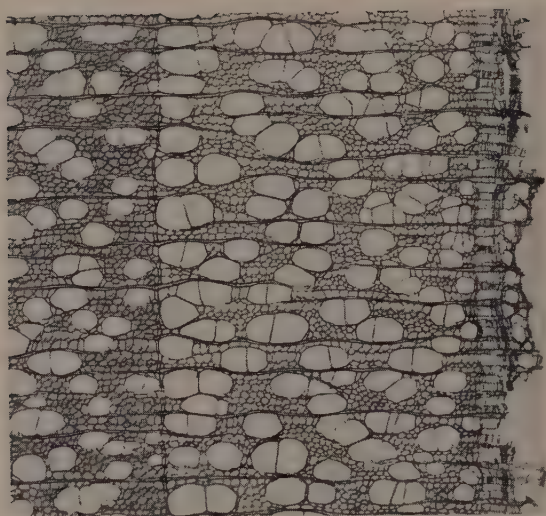


Figure 8. Transverse section showing the cambium and most recent annual increment of xylem. 46x.

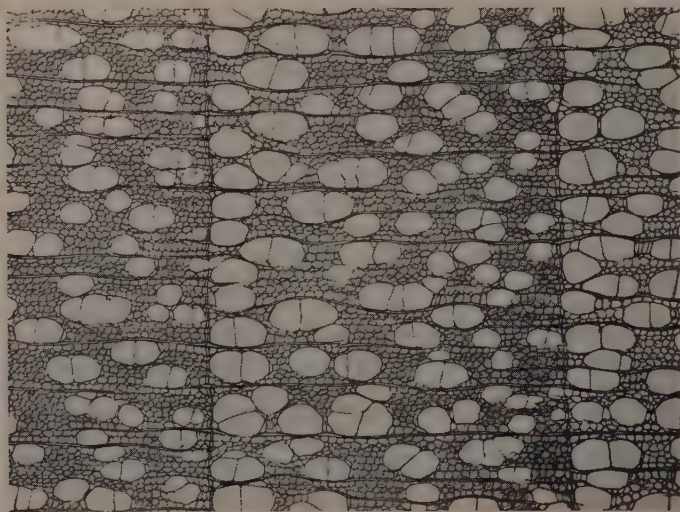


Figure 9. Transverse section from same preparation shown in Fig. 8 illustrating portions of the first, second and third xylem increments (from the cambium). 46x.

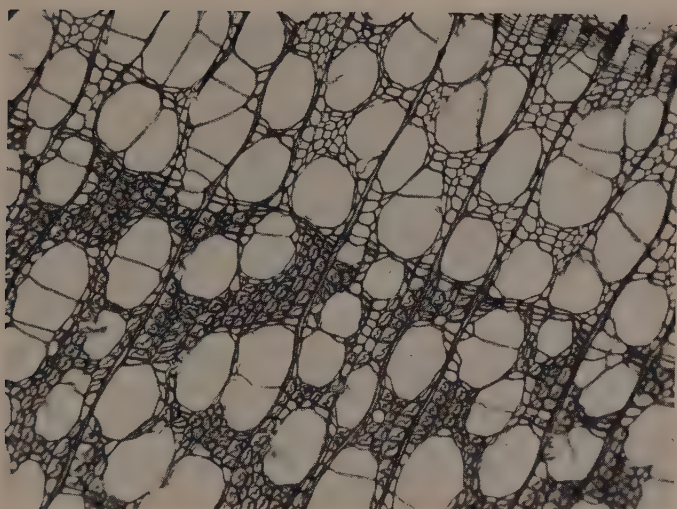


Figure 10. Transverse section showing cambium and subjacent xylem.  
75x.

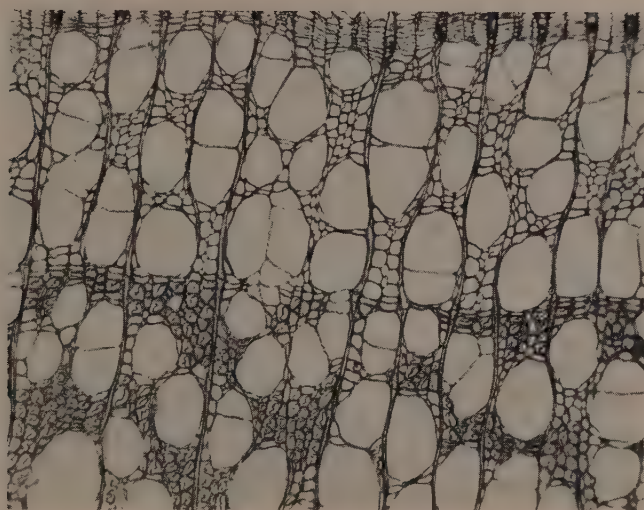


Figure 11. Transverse section showing cambium and subjacent xylem.  
75x.



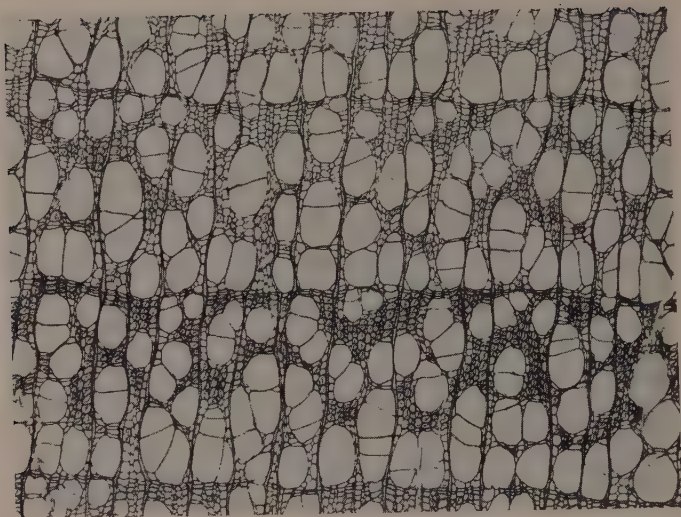


Figure 12. Transverse section showing response variation. 46x.

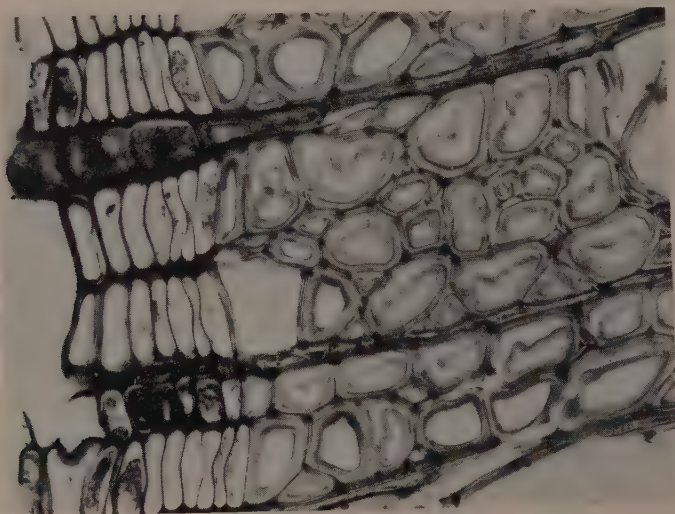


Figure 13. Transverse section illustrating the proximate differentiation of the gelatinous layer with respect to the cambium. 400x.

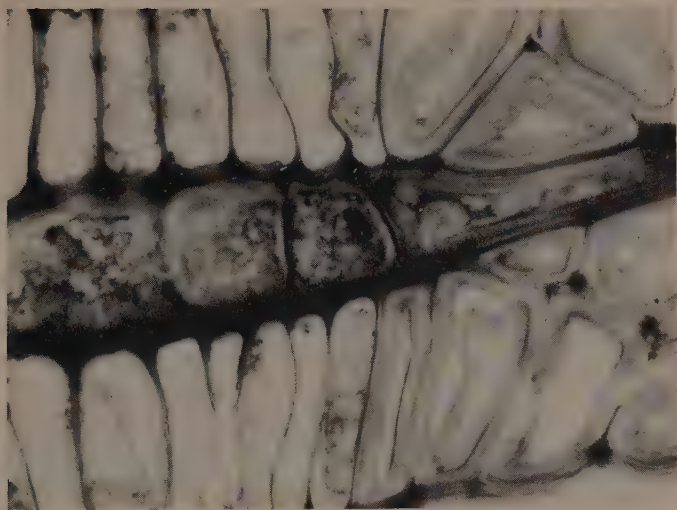


Figure 14. Transverse section of the cambium and subjacent gelatinous fibers. 920x.

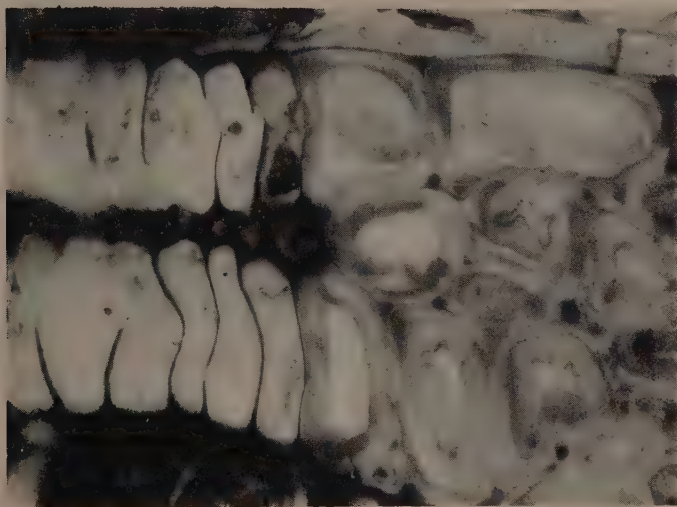


Figure 15. Transverse section again depicting the early appearance of the gelatinous layer. 920x.

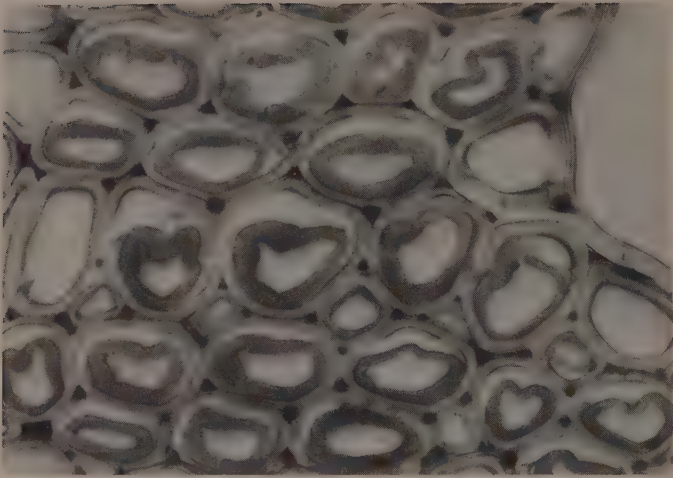


Figure 16. Transverse section showing cytological features of the stimulated cell. 600x.

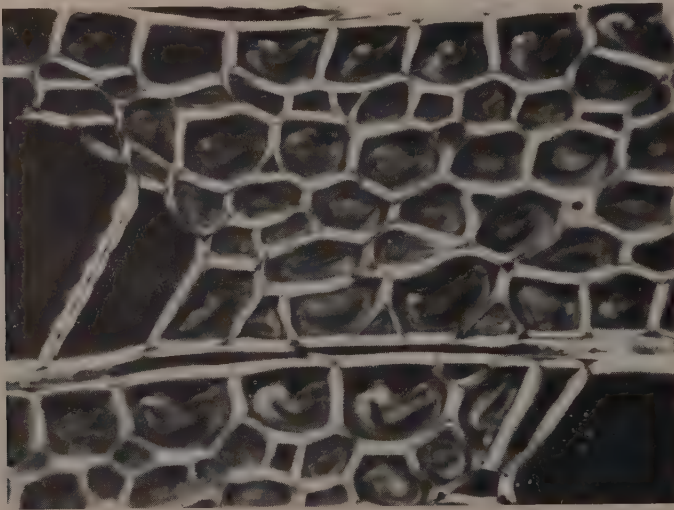


Figure 17. Transverse section of reaction tissue taken with polarized light. 600x.

induction occurs even earlier. The cytological features of the stimulated cell wall are further depicted in Figures 16 and 17. Figure 17 was taken with the polarized light and the opaque appearance of the gelatinous material is due to the axial orientation of the cellulose micelles. Note that an enveloping, darker staining layer occurs on the margins of the gelatinous layers. Buckling of the gelatinous layer often occurs at pit loci which feature disruption of micellar direction (cf. Figure 16). There is often the suggestion of depressed vessel size in annual rings containing a substantial proportion of gelatinous fibers, but this may be concomitant variation with increased radial growth.

### Analyzing triplets

Individual regressions for ring width and for cell number were computed for each tree. Since three annual rings were analyzed per tree, a series of triplets arose. For ring width there were only 3 significant F-statistics from 93 triplets (see Table 8). Since 5% significant F's or t's would be expected by chance alone, no obvious relationship between ring width and proportion of gelatinous fibers was revealed by standard regression methods. The situation was similar for cell number. As shown in Table 9 there were only 4 significant F's out of 90 triplets. However, despite the low magnitude of the F- and t-statistics, the signs of the regression coefficients for both ring width and cell number are decidedly positive. Specifically, there are 64 positive and 29 negative regression coefficients for ring width, and 66 positive and 24 negative regression coefficients for cell number. These splits of the distributions are both significant beyond the 1% level (Ostle, 1954, p.453; Wallis and Roberts, 1956, p.598).

The development of a series of "t" values (which are individually sign sensitive) permits the observation of the cumulative distribution functions (CDF) for "t" and comparison of this empirical distribution with the null distribution of "t" via the Kolmogoroff-Smirnoff test. These observations are found in Tables 10-12 and Figures 18 and 19. The following formula gives the approximate critical values of the maximum vertical deviation of the empirical from the null distributions at the specified level:

$$\tilde{\epsilon} = \sqrt{\frac{1}{2n} \log \alpha}$$

where  $\alpha$  is the level of the test  
and  $n$  is the sample size.

The above formula and the tabulation of Kolmogoroff's statistic have been published by Birnbaum (1952) and Birnbaum and Tingey (1951). For ring width the maximum discrepancy is 0.21 and this can be compared to the 0.1% level of 0.193 for Kolmogoroff's statistic. For cell number the observed discrepancy is 0.23 as compared to a 0.1% level of 0.195. The discrepancy is somewhat greater with respect to cell number. These results indicate that high proportion of gelatinous fibers is associated with larger annual increments and smaller cell size (in transection).

These results do not materialize in the standard tests of hypotheses (except the sign test) because traditional methods examine only the tails of the empirical t-distributions. Here the shift in the distribution occurred in the central portion of the distribution. In fact, the empirical



Table 8. Regression coefficients, t, and F values for ring width.

Plot - tree - core	Regression coefficient	F values	t
1 - 3 - 2	-0.008948	4.176	-2.0435
1 - 4 - 2	-0.000041	0.004	-0.0632
1 - 5 - 2	0.000861	3.180	1.7832
1 - 6 - 2	0	--	--
1 - 7 - 2	0.000705	1.187	1.0895
1 - 8 - 2	-0.0003961	0.2759	-0.5253
1 - 11 - 2	0.000334	0.362	0.6017
1 - 12 - 2	0.000565	0.036	0.1897
1 - 13 - 2	0.000494	0.0018	0.0424
2 - 55 - 1	0.000836	0.7274	0.8529
2 - 55 - 2	0.005418	9.320	3.0529
2 - 55 - 3	0.003456	2.6582	1.9126
2 - 56 - 1	0.000974	0.2256	0.4750
2 - 56 - 2	-0.007360	0.369	-0.6075
2 - 56 - 3	0.000574	17.8674	4.2770
2 - 57 - 1	0.000382		
2 - 57 - 2	0.002157	0.652	0.8075
2 - 57 - 3	-0.001766	1.9296	-1.3891
2 - 57 - 1	0.001176	0.7872	0.8873
2 - 58 - 2	0.000757	0.700	0.8367
2 - 58 - 3	0.002928	0.3617	0.6014
2 - 59 - 1	0.000181	0.0997	0.3158
2 - 59 - 2	0.000025	0.032	0.1789
2 - 59 - 3	0.000099	1.5349	1.2389
2 - 60 - 1	-0.000072	0	-0
2 - 60 - 2	-0.001941	0.500	-0.7071
2 - 60 - 3	-0.000198	5.8000	-2.4083
2 - 61 - 1	-0.000108	4.4909	-2.1190
2 - 61 - 2	0.000270	0.1287	0.3687
2 - 61 - 3	-0.000765	9.5541	-3.0910
3 - 22 - 2	0.001466	1.935	0.4399
3 - 23 - 2	0.001616	0.2645	0.5143
3 - 24 - 2	0.017301	0.813	0.9017
3 - 25 - 2	0.000901	0.931	0.9649
3 - 26 - 2	-0.000995	2.961	-1.7208
3 - 27 - 2	0.001658	0.649	0.8056
3 - 28 - 2	0.000848	0.502	0.7085
5 - 29 - 2	0.002654	20.753	4.5555
5 - 30 - 2	--	--	--
5 - 31 - 2	--	--	--
5 - 32 - 2	-0.0002650	0.323	-0.5683
5 - 33 - 2	0.003573	11.603	3.4063
5 - 34 - 2	0.002142	2.025	1.4230



Table 8. (continued)

Plot - tree - core	Regression coefficient	F values	t
9 - 50 - 2	--	--	--
9 - 51 - 2	0.000288	35.5581	5.9650
9 - 52 - 2	-0.000289	0.6364	-0.7977
9 - 53 - 2	-0.001921	45.0569	-6.7124
9 - 54 - 2	-0.000001	0	-0
10 - 105 - 2	0.000436	3.8534	1.9630
10 - 106 - 2	0.003899	8.0504	2.8373
10 - 107 - 2	0.000597	0.0253	0.1591
10 - 108 - 2	--	--	--
12 - 109 - 2	-0.003310	2.3007	-1.5168
12 - 110 - 2	0.001440	62.533	7.907
12 - 111 - 2	0.005118	40.8262	6.3895
12 - 112 - 2	0.002085	1.3360	1.1559
12 - 113 - 2	0.003307	0.7660	0.8752
13 - 62 - 2	0.000805	0.072	0.2683
13 - 63 - 2	0.003044	0.754	0.8683
13 - 64 - 2	-0.000142	0.0545	-0.2334
13 - 66 - 2	-0.000547	0.107	-0.3271
13 - 68 - 2	-0.000456	0.666	-0.8161
13 - 69 - 2	-0.000062	0.372	-0.6099
13 - 67 - 2	0.002747	7.477	2.7344
14 - 75 - 2	0.000062	1.589	1.2606
14 - 76 - 2	0.002442	241.833*	15.5510*
14 - 77 - 2	-0.000048	0.320	-0.5657
14 - 78 - 2	0.000055	0.0920	0.3033
14 - 79 - 2	0.001717	12.505	3.5362
14 - 80 - 2	0.003866	9.744	3.1215
16 - 93 - 2	0.003030	19.558	4.4224
16 - 94 - 2	-0.008087	32.392	-5.6914
16 - 95 - 2	0.004122	0.064	0.25308
16 - 96 - 2	-0.020888	1.043	-1.0213
16 - 97 - 2	-0.000005	0.100	-0.3162
16 - 98 - 2	0.001525	4.737	2.1765
18 - 81 - 2	0.005179	69.693	8.3482
18 - 82 - 2	0.001383	0.225	0.4743
18 - 83 - 2	0.000023	3.645	1.9092
18 - 84 - 2	0.001140	0.110	0.3317
18 - 85 - 2	0.002960	0.831	0.9116
18 - 86 - 2	-0.001386	0.061	-0.2470

Table 8. (continued)

Plot - tree - core	Regression coefficient	F values	t
20 - 87 - 2	0.000147	4.026	2.006
20 - 88 - 2	0.002116	114.460	10.6986
20 - 89 - 2	0.004022	14.669	3.8300
20 - 90 - 2	0.002638	314.706*	17.7400*
20 - 91 - 2	-0.000059	0.052	-0.2280
20 - 92 - 2	0.002217	11.294	3.3607
22 - 99 - 2	0.003263	52.183	7.2238
22 - 100 - 2	0.000686	0.990	0.9950
22 - 101 - 2	0.008182	21.448	4.6312
22 - 102 - 2	0.002822	3.407	1.8458
22 - 103 - 2	-0.005910	0.958	-0.9788
22 - 104 - 2	-0.007606	0.464	-0.6812
23 - 70 - 2	0.000281	18.9333	4.3512
23 - 72 - 2	0.000083	16.3000	4.0373
23 - 73 - 2	0.007994	104.3256	10.2140
23 - 74 - 2	-0.000014	0.0230	-0.15166

Table 9. Regression coefficients, t, and F values for cell number.

Plot - tree - core	Regression coefficient	F values	t
1 - 3 - 2	0.003039	0.444	0.6663
1 - 4 - 2	0.000118	0.009	0.094868
1 - 5 - 2	-0.004829	0.232	-0.4816638
1 - 6 - 2	-0.000275	0.1743	-0.4175
1 - 7 - 2	0.000930	6800.00 **	82.46211*
1 - 8 - 2	0.000446	0.1013	0.317645
1 - 11 - 2	0.000212	0.103	0.3209
1 - 12 - 2	0.002496	58.844	7.7051
1 - 13 - 2	0.016353	64.14	8.00865
2 - 55 - 1	0.006049	16.0878	4.0094
2 - 55 - 2	0.006080	23.993	4.8983
2 - 55 - 3	0.000259	0.0107	0.1034
2 - 56 - 1	0.003810	0.22	0.4690
2 - 56 - 2	-0.028678	0.554	-0.7443
2 - 56 - 3	-0.000699	91.12	-9.5457
2 - 57 - 1	-0.041601	0.14	-0.3742
2 - 57 - 2	0.002204	0.365	0.6042
2 - 57 - 3	-0.003872	0.71	-0.8426

Table 9. (continued)

Plot - tree - core	Regression coefficient	F values	t values
2 - 58 - 1	0.002013	0.52	0.7211
2 - 58 - 2	0.003125	61.982	7.8729
2 - 58 - 3	0.004235	14.74	3.8393
2 - 59 - 1	0.003198	0.30	5.4772
2 - 59 - 2	0.00027944	0.419	0.6473
2 - 59 - 3	-0.00269	1.52	-1.2329
2 - 60 - 1	0.000969	0.54	0.7348
2 - 60 - 2	-0.00169106	53.941	-7.3445
2 - 60 - 3	-0.000121	0.15	-0.3873
2 - 61 - 1	0.000145	8.44	2.9052
2 - 61 - 2	0.000596	0.84	0.9165
2 - 61 - 3	-0.002305	3.12	-1.7664
3 - 22 - 2	0.0039663	45.123	6.7174
3 - 23 - 2	0.01000615	2.559	1.5997
3 - 24 - 2	0.0095537	1.740	1.3191
3 - 25 - 2	0.00040841	1.251	1.1185
3 - 26 - 2	-0.00114449	0.885	-0.9407
3 - 27 - 2	0.0009229	2.173	1.4741
3 - 28 - 2	0.00028618	0.007	0.08367
5 - 29 - 2	0.001888	945.25*	30.7449*
5 - 30 - 2	--	--	--
5 - 31 - 2	--	--	--
5 - 32 - 2	-0.00007820	0.0143	-0.1196
5 - 33 - 2	0.00351462	9.6544	3.1072
5 - 34 - 2	0.0018316	0.965	0.9823
9 - 50 - 2	--	--	--
9 - 51 - 2	0.000422	6.98	2.6430
9 - 52 - 2	-0.000424	4.62	-2.1494
9 - 53 - 2	-0.000224	0.002	-0.04472
9 - 54 - 2	0.000133	0.563	0.7503
10 - 105 - 2	0.000639	1.92	1.3856
10 - 106 - 2	0.002276	0.103	0.3209
10 - 107 - 2	0.006339	51.738	7.1930
10 - 108 - 2	--	--	--
12 - 109 - 2	0.002485	0.16	0.4000
12 - 110 - 2	0.002212	9.44	3.0724
12 - 111 - 2	0.013801	17.75	4.2131
12 - 112 - 2	0.008821	456.98*	21.3775*
12 - 113 - 2	0.013022	3.94	1.9849

Table 9. (continued)

Plot - tree - core	Regression coefficient	F values	t values
13 - 62 - 2	-0.003987	0.489	-0.6992
13 - 63 - 2	-0.048018	4.624	-2.1503
13 - 64 - 2	-0.0002557	4.17	-2.0420
13 - 66 - 2	0.0011815	68.292	8.2639
13 - 67 - 2	0.0029061	1.302	1.1410
13 - 68 - 2	0.00050078	0.289	0.5376
13 - 69 - 2	0.00033704	13.750	3.7081
14 - 75 - 2	0.00010181	35.825	5.9904
14 - 76 - 2	0.0044186	1.059	1.0291
14 - 77 - 2	-0.00004024	0.488	-0.6986
14 - 78 - 2	0.00041748	2.320	1.5231
14 - 79 - 2	0.0025512	9.057	3.0095
14 - 80 - 2	0.0066757	68.547	8.2793
16 - 93 - 2	0.003776	8.390	2.8966
16 - 94 - 2	0.0008196	0.250	0.5000
16 - 95 - 2	0.003532	0.029	0.1703
16 - 96 - 2	0.005994	4.482	2.1171
16 - 97 - 2	-0.0003158	4.500	-2.1213
16 - 98 - 2	0.002837	2.440	1.5621
18 - 81 - 2	0.004534	3.499	1.8706
18 - 82 - 2	-0.0025797	0.385	-0.6205
18 - 83 - 2	0.00004333	0.300	0.5477
18 - 84 - 2	0.00307010	0.157	0.3962
18 - 85 - 2	0.00241199	169.921*	13.0354*
18 - 86 - 2	0.00400271	3.545	1.8828
20 - 87 - 2	0.00013621	0.471	0.6863
20 - 88 - 2	0.00126927	0.030	0.1732
20 - 89 - 2	0.00539335	3.509	1.8732
20 - 90 - 2	0.00485051	50.222	7.0867
20 - 91 - 2	-0.000065	0.012	-0.1095
20 - 92 - 2	0.00011941	0.023	0.1516
22 - 99 - 2	0.00829010	11.712	3.4223
22 - 100 - 2	-0.00025851	0.082	-0.2864
22 - 101 - 2	0.01274355	24.568	4.9566
22 - 102 - 2	0.00460761	1.434	1.1975
22 - 103 - 2	-0.0028318	0.678	-0.8234
22 - 104 - 2	-0.0013459	0.099	-0.3146

Table 10. Values for the null distribution of  $t$  for one degree of freedom.<sup>1</sup>

$t$	$P(t \mid V=1)$	$(1-P)$	$t$	$P(t \mid V=1)$	$(1-P)$
0.0	0.5000		3.1	0.90067	
0.1	0.53173		3.2	0.90359	
0.2	0.56283		3.3	0.90634	
0.3	0.59277		3.4	0.90895	
0.4	0.62112		3.5	0.91141	
0.5	0.64758	0.35242	3.6	0.91376	
0.6	0.67202		3.7	0.91598	
0.7	0.69440		3.8	0.91809	
0.8	0.71478		3.9	0.92010	
0.9	0.73326		4.0	0.92202	0.07798
1.0	0.7500	0.2500	4.2	0.92560	
1.1	0.765p5		4.4	0.92887	
1.2	0.77886		4.6	0.93186	
1.3	0.79129		4.8	0.93462	
1.4	0.80257		5.0	0.93717	0.06283
1.5	0.81283	0.18717	5.2	0.93952	
1.6	0.82219		5.4	0.94171	
1.7	0.83075		5.6	0.94375	
1.8	0.83859		5.8	0.94565	
1.9	0.84579		6.0	0.94753	0.05247
2.0	0.85242	0.14758	6.2	0.94910	
2.1	0.85854		6.4	0.95066	
2.2	0.86420		6.6	0.95214	
2.3	0.86934		6.8	0.95352	
2.4	0.87433		7.0	0.95483	0.04517
2.5	0.87888		7.2	0.95607	
2.6	0.88313		7.4	0.95724	
2.7	0.88709		7.6	0.95836	
2.8	0.89081		7.8	0.95941	
2.9	0.89430		8.0	0.96042	0.03958
3.0	0.89758	0.10242	12.706	0.97500	
			25.452	0.98750	
			63.657	0.99500	
				1.00000	

<sup>1</sup> From Pearson and Hartley (1954, p.132).

Table 11. Cumulative distribution of t values for cell number.

Index	t value	CDF	Index	t value	CDF
1	-9.5457	0.01111	46	0.7503	0.51111
2	-7.3445	0.02222	47	0.9165	0.52222
3	-2.1503	0.03333	48	0.9823	0.53333
4	-2.1494	0.04444	49	1.0291	0.54444
5	-2.1213	0.05555	50	1.1185	0.55555
6	-2.0420	0.06667	51	1.1410	0.56667
7	-1.7664	0.07778	52	1.1975	0.57778
8	-1.2329	0.08889	53	1.3191	0.58889
9	-0.9407	0.10000	54	1.3856	0.60000
10	-0.8426	0.11111	55	1.4741	0.61111
11	-0.8234	0.12222	56	1.5231	0.62222
12	-0.7443	0.13333	57	1.5621	0.63333
13	-0.6992	0.14444	58	1.5997	0.64444
14	-0.6986	0.15555	59	1.8706	0.65555
15	-0.6205	0.16667	60	1.8732	0.66667
16	-0.48166	0.17778	61	1.8828	0.67778
17	-0.4175	0.18889	62	1.9849	0.68889
18	-0.3873	0.20000	63	2.1171	0.70000
19	-0.3742	0.21111	64	2.6420	0.71111
20	-0.3146	0.22222	65	2.8966	0.72222
21	-0.2864	0.23333	66	2.9052	0.73333
22	-0.1196	0.24444	67	3.0095	0.74444
23	-0.1095	0.25555	68	3.0724	0.75555
24	-0.04472	0.26667	69	3.1072	0.76667
25	0.08367	0.27778	70	3.4223	0.77778
26	0.094868	0.28889	71	3.7081	0.78889
27	0.1034	0.30000	72	3.8393	0.80000
28	0.1516	0.31111	73	4.0094	0.81111
29	0.1703	0.32222	74	4.2131	0.82222
30	0.1732	0.33333	75	4.8983	0.83333
31	0.317645	0.34444	76	4.9566	0.84444
32	0.3209	0.35555	77	5.4772	0.85555
33	0.3209	0.36667	78	5.9904	0.86667
34	0.3962	0.37778	79	6.7174	0.87778
35	0.40000	0.38889	80	7.0867	0.88889
36	0.4690	0.40000	81	7.1930	0.90000
37	0.50000	0.41111	82	7.7051	0.91111
38	0.5376	0.42222	83	7.8729	0.92222
39	0.5477	0.43333	84	8.00865	0.93333
40	0.6042	0.44444	85	8.2639	0.94444
41	0.6473	0.45555	86	8.2793	0.95555
42	0.6663	0.46667	87	13.0354	0.96667
43	0.6863	0.47778	88	21.3775	0.97778
44	0.7211	0.48889	89	30.7449	0.98889
45	0.7348	0.50000	90	82.46211	1.00000



Table 12. Cumulative distribution of t values for ring width.

Index	t value	CDF	Index	t value	CDF
1	-6.7124	0.01075	47	0.8056	0.50537
2	-5.6914	0.02150	48	0.8075	0.51612
3	-3.0910	0.03225	49	0.8367	0.52688
4	-2.4083	0.04301	50	0.8529	0.53763
5	-2.1190	0.05376	51	0.8683	0.54838
6	-2.0435	0.06451	52	0.8752	0.55913
7	-1.7208	0.07526	53	0.8873	0.56989
8	-1.5168	0.08602	54	0.9017	0.58064
9	-1.3891	0.09677	55	0.9116	0.59139
10	-1.0213	0.10752	56	0.9649	0.60215
11	-0.9788	0.11827	57	0.9950	0.61290
12	-0.8161	0.12903	58	1.0895	0.62365
13	-0.7977	0.13978	59	1.1559	0.63440
14	-0.7071	0.15053	60	1.2389	0.64516
15	-0.6812	0.16129	61	1.2606	0.65591
16	-0.6099	0.17204	62	1.4230	0.66667
17	-0.6073	0.18279	63	1.7832	0.67741
18	-0.5683	0.19354	64	1.8458	0.68817
19	-0.5657	0.20430	65	1.9092	0.69892
20	-0.5253	0.21505	66	1.9126	0.70967
21	-0.3271	0.22580	67	1.9630	0.72043
22	-0.3162	0.23655	68	2.0060	0.73118
23	-0.2470	0.24731	69	2.1765	0.74193
24	-0.2334	0.25806	70	2.7344	0.75268
25	-0.2280	0.26881	71	2.8373	0.76344
26	-0.15166	0.27956	72	3.0529	0.77419
27	-0.0632	0.29032	73	3.1215	0.78494
28	0	0.30107	74	3.3607	0.79569
29	0	0.31182	75	3.4063	0.80645
30	0.0424	0.32258	76	3.5362	0.81720
31	0.1591	0.33333	77	3.8300	0.82795
32	0.1789	0.34408	78	4.0375	0.85870
33	0.1897	0.35483	79	4.2770	0.84946
34	0.2530	0.36559	80	4.3512	0.86021
35	0.2683	0.37634	81	4.4224	0.87096
36	0.3033	0.38709	82	4.5555	0.88172
37	0.3158	0.39784	83	4.6312	0.89247
38	0.3317	0.40860	84	5.9650	0.90322
39	0.3587	0.41935	85	6.3895	0.91397
40	0.4399	0.43010	86	7.2238	0.92473
41	0.4743	0.44086	87	7.9070	0.93548
42	0.4750	0.45161	88	8.3482	0.94623
43	0.5143	0.46236	89	10.2140	0.95658
44	0.6014	0.47311	90	10.6986	0.96774
45	0.6017	0.48387	91	15.5510	0.97849
46	0.7085	0.49462	92	17.7400	0.98924
			03		1.00000

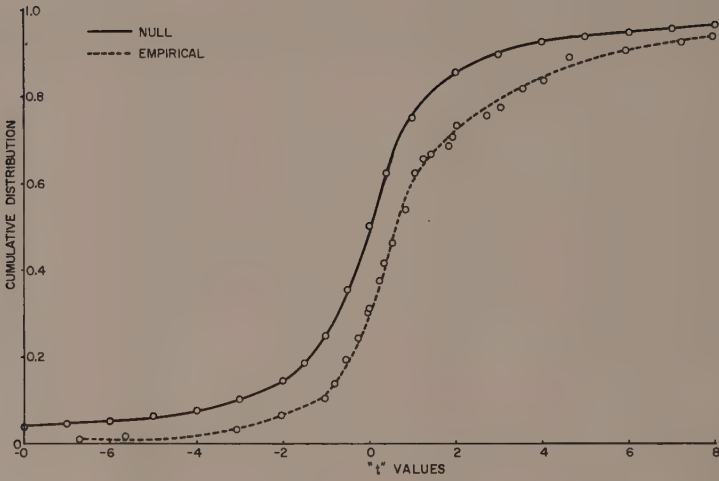


Figure 18. Empirical and null t-distributions for ring width.

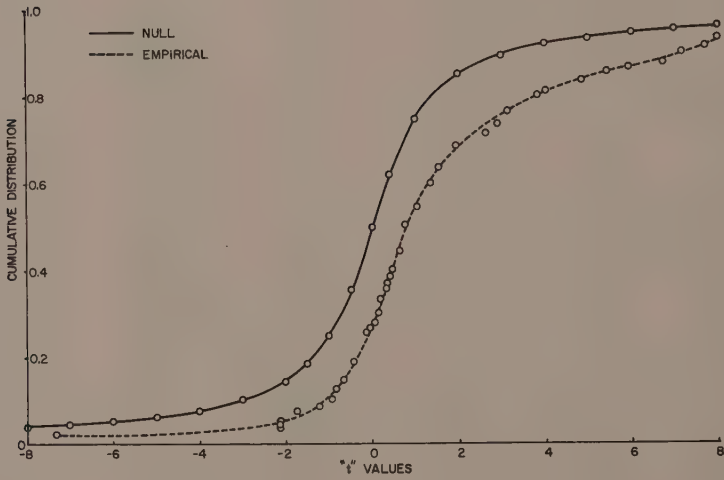


Figure 19. Empirical and null t-distributions for cell number.

and null distributions actually cross (if fully plotted) in the tails of the curves. The Kolmogoroff-Smirnoff technique revealed these effects because it scrutinizes all the percentiles of the distributions, i.e. it is a multiple comparison procedure for all percentiles. Thus "ring-width" and "cell-number" are shown to be positively associated with proportion of gelatinous fibers.

A further elucidation of the nature of the ring-width reaction tissue association can be obtained via Youden's D/d outlier criterion (Youden, 1953). The special case for triplets is relevant. With the statistic, D/d, almost no alternative to homogeneity is immune from detection. This statistic consists of the larger sequential difference between size-ordered triplets (D) divided by the smallest sequential difference between size-ordered triplets (d). The D/d's were computed for ring width and the corresponding analogous statistic, G/g, was computed for the proportion of gelatinous fibers. The G/g data were then divided into two approximately equal groups on the basis of the magnitude of the ring width criterion (D/d). One group consisted of G/g's from triplets where  $D/d \geq 3$ , and was termed "outlier." The other group was established on the basis of  $D/d < 3$ , and was termed symmetric. Both of these groups were tested against an expected distribution which was obtained as follows:

$$P_r (G/g \geq k) = 6/\pi \left( \arccos \frac{k + 1/2}{\sqrt{1 + k + k^2}} \right)$$

(David and Berlyn, 1960)

An accumulative Chi-square test was employed; the results are presented in Table 13. For the outlier group the null hypothesis of homogeneity was rejected at the 2.5% level. The symmetric group had a nonsignificant Chi-square. It appears that strong fluctuation in the factors which determine diameter growth is associated with equally strong fluctuation in the factors that induce the cellular stimulation. Not only is it true that the magnitudes of ring width and proportion of gelatinous fibers are positively associated, but also substantial variations in their causative factors are translated.

Table 13. Cumulative Chi-squares for ring width triplets D/d.<sup>1</sup>

	Groupings				Sums
	A	B	C	D	
Outlier observed	22	9	2	9	42
Expected	26.75	8.65	3.02	3.57	
Chi-square	0.843	0.014	8.258	8.258	9.46*
Symmetric observed	34	9	5	4	52
Expected	33.12	10.71	3.74	4.42	
Chi-square	0.023	0.273	0.425	0.041	0.762 <sup>ns</sup>

<sup>1</sup> The groupings in this table are the original groups of Youden (1953) except that an additional class, E, was grouped with Class D.

## Regression Analysis

Standard multiple linear regression methods were employed to assess the relationships among the numerous variables tabulated in this study. Average "proportion of gelatinous fibers" per tree was designated as the dependent variable for most of these analyses. The multiple linear regressions were of two types: composite regressions over 14 plots, and individual plot regressions.

Mensurational considerations

The independent variables consist of both individual tree factors and soil factors. The soils data were compiled by Brendemuhl (cf. Table 1). There are six soil factors (including site index) contained in this study. There are 11 individual tree factors, which were directly tabulated for the study. The tree variables are further dichotomized into external and internal morphological characters. The 17 factor array with the notation used throughout the study is as follows:

- X<sub>1</sub> Linear lean - degrees
- X<sub>2</sub> Stem basal area - square feet
- X<sub>3</sub> Total height - feet
- X<sub>4</sub> Crown per cent
- X<sub>5</sub> Crown volume - cubic feet
- X<sub>6</sub> Crown surface area - square feet
- X<sub>7</sub> Stem volume - total cubic feet
- X<sub>8</sub> Proportion gelatinous fibers
- X<sub>9</sub> Orthogonal quadratic lean (orthogonal to linear lean)
- X<sub>10</sub> Site index
- X<sub>11</sub> Average silt plus clay content - per cent
- X<sub>12</sub> Available water - per cent
- X<sub>13</sub> Foliar nitrogen - per cent
- X<sub>14</sub> Nitrifiable nitrogen - pounds per acre - 0.48"
- X<sub>15</sub> Available phosphorus - pounds per acre - 0.48"
- X<sub>16</sub> Ring width - millimeters
- X<sub>17</sub> Cell number

All but three of the factors were compiled by standard methods. Stem volume, crown volume, and crown surface area contain some specialized aspects.

Total cubic foot volume was obtained as follows:

$$V = \frac{B.A. \times h}{2.37}$$

where            B.A. = basal area at breast height  
                      h = total height  
                      2.37 = a form factor

This equation was taken from a regional volume table for cottonwood (Gevorkiantz and Olsen, 1955). The total volume calculated in this manner agreed within 1% with the regional table. This method has the advantage that extra sensitivity is derived from using total height to the

nearest foot and diameter to the nearest tenth of an inch, whereas the regional table contained heights to the nearest 10 feet and diameters to the nearest inch. There was little fluctuation in the form factor in the regional table itself.

Crown volume was computed by that paraboloid formula:

$$C.V. = \frac{B.A. \times L}{2}$$

where B.A. = basal area of crown  
L = crown length

Crown surface area was computed from the following equation for the surface of a paraboloid:<sup>5</sup>

$$CSA = \frac{\pi R^4}{6Z^2} \left[ -1 + \left( 1 + \frac{4Z^2}{R^2} \right)^{3/2} \right]$$

where Z = crown length  
R = geometric mean radius of the base of the crown

This attribute approximates the potential photosynthetic area of the tree. Again the form assumption was empirical. These crown measurements are associated with several growth variables as evidenced in Tables 14 and 15.

#### Composite multiple linear regressions

The composite regressions were computed over the 14 plots. Only the total 17 factor analysis will be presented here. Several procedures were developed to exclude variables and some shorter analyses were run (cf. Berlyn, 1960). Table 14 contains all the simple correlation coefficients and Table 15 contains all simple correlation coefficients greater than 0.500. Table 16 is the summary table for the regression.

With only 14 plots the number of soil factors included was limited to six in order to obviate unrealistic inflation of R, the multiple correlation coefficient, or the unrealistic deflation of the error estimate (cf. Snedecor, 1956, p.445). The following illustrates this consideration.

$$R^2 = \frac{SSR}{\Sigma'y^2}$$

where  $R^2$  = multiple linear correlation coefficient  
SSR = sum of squares due to regression  
 $\Sigma'y^2$  = total sum of squares

$$\Sigma'y^2 = \frac{SSR}{R^2}$$

$$\Sigma'y^2 - SSR = \frac{SSR}{R^2} - SSR$$

<sup>5</sup> Courtesy Dr. J. A. Greenwood, Iowa State University Statistical Laboratory, Ames, Iowa, private communication. 1958.

Table 14. Simple correlation coefficients for all variables in the study.

Variables	Correlation coefficients															
	X <sub>1</sub>	X <sub>2</sub>	X <sub>3</sub>	X <sub>4</sub>	X <sub>5</sub>	X <sub>6</sub>	X <sub>7</sub>	X <sub>8</sub>	X <sub>9</sub>	X <sub>10</sub>	X <sub>11</sub>	X <sub>12</sub>	X <sub>13</sub>	X <sub>14</sub>	X <sub>15</sub>	X <sub>17</sub>
X <sub>1</sub>	1.000															
X <sub>2</sub>	0.134	1.000														
X <sub>3</sub>	-0.134	0.488	1.000													
X <sub>4</sub>	0.194	0.198	0.109	1.000												
X <sub>5</sub>	0.307	0.774	0.298	0.407	1.000											
X <sub>6</sub>	0.400	0.285	0.051	0.268	0.695	1.000										
X <sub>7</sub>	0.071	0.972	0.642	0.206	0.720	0.232	1.000									
X <sub>8</sub>	0.564	-0.240	-0.193	0.129	0.053	0.193	-0.271	1.000								
X <sub>9</sub>	0.000	0.163	0.017	0.119	0.405	0.674	0.133	-0.104	1.000							
X <sub>10</sub>	0.014	0.268	0.742	0.087	0.196	0.024	0.397	-0.094	-0.029	1.000						
X <sub>11</sub>	0.097	0.134	0.414	-0.160	-0.088	-0.131	0.240	-0.105	-0.152	0.522	1.000					
X <sub>12</sub>	0.057	0.038	0.334	-0.180	-0.144	-0.169	0.132	-0.079	-0.200	0.419	0.891	1.000				
X <sub>13</sub>	-0.033	-0.026	0.442	0.002	-0.110	-0.161	0.109	-0.112	-0.114	0.659	0.656	0.592	1.000			
X <sub>14</sub>	-0.041	-0.083	0.282	-0.012	-0.006	-0.055	-0.011	-0.108	-0.003	0.592	0.214	0.143	0.575	1.000		
X <sub>15</sub>	0.163	0.066	0.200	0.017	-0.114	-0.112	0.129	0.150	-0.132	0.156	0.648	0.543	0.402	-0.260	1.000	
X <sub>16</sub>	0.098	0.192	0.008	0.174	0.400	0.351	0.117	0.194	0.221	-0.013	-0.241	-0.132	-0.137	0.082	-0.260	1.000
X <sub>17</sub>	0.139	0.033	0.134	0.139	0.189	0.280	0.055	0.187	0.293	0.213	-0.088	-0.058	0.179	0.199	0.180	0.510



Table 15. Simple correlation coefficients greater than 0.500.

Variables	Correlated Factors	r
X <sub>1</sub> , X <sub>8</sub>	lean, proportion gelatinous fibers	0.564
X <sub>2</sub> , X <sub>7</sub>	stem basal area, stem volume	0.972
X <sub>2</sub> , X <sub>5</sub>	stem basal area, crown volume	0.774
X <sub>3</sub> , X <sub>7</sub>	stem height, stem volume	0.642
X <sub>5</sub> , X <sub>6</sub>	crown volume, crown area	0.695
X <sub>5</sub> , X <sub>7</sub>	crown volume, stem volume	0.721
X <sub>6</sub> , X <sub>9</sub>	crown surface area, quadratic lean	0.674
X <sub>16</sub> , X <sub>17</sub>	ring width, cell number	0.510
X <sub>10</sub> , X <sub>3</sub>	site index, stem height	0.742
X <sub>10</sub> , X <sub>11</sub>	site index, average silt plus clay	0.522
X <sub>10</sub> , X <sub>13</sub>	site index, foliar nitrogen	0.659
X <sub>10</sub> , X <sub>14</sub>	site index, nitrifiable nitrogen	0.593
X <sub>11</sub> , X <sub>12</sub>	average silt plus clay, available water	0.891
X <sub>11</sub> , X <sub>13</sub>	average silt plus clay, foliar nitrogen	0.657
X <sub>11</sub> , X <sub>15</sub>	average silt plus clay, available P	0.648
X <sub>12</sub> , X <sub>13</sub>	available water, foliar N	0.594
X <sub>12</sub> , X <sub>15</sub>	available water, available P	0.543
X <sub>13</sub> , X <sub>14</sub>	foliar N, nitrifiable N	0.575

$$\frac{\Sigma' y^2 - SSR}{\Sigma' y^2} = (1 - R^2)$$

$$\text{The estimate of error} = \frac{\Sigma' y^2 - SSR}{(n - k - 1)}$$

where  $n$  = number of units (trees)  
 $k$  = total number of factors  
 $1$  = reduction for the constant

Hence,

$$\left[ \frac{n - k - 1}{y^2} \right] [\text{error estimate}] = (1 - R^2).$$

Anything that makes  $R^2$  unrealistically high makes the error estimate unrealistically low. Furthermore a six factor analysis ( $X_1$ ,  $X_3$ ,  $X_5$ ,  $X_{10}$ , and  $X_{15}$  on  $X_8$ ) had an  $R^2$  of 0.345. The  $R^2$  for 17 factors was 0.615. With the addition of 11 factors there was a 27.0% increase in the explanation of the variation as measured by the sums of squares. It is obvious that information was actually lost by excluding variables. It may be of interest to compare these percentages with the expected percentage increase in  $R^2$  due to the addition of random factors, assuming, say, that lean is the only systematic factor in the regression.

Table 16. Summary of composite 17-factor regression analysis.

Variables	Means	Partial regression coefficients	"t"
X <sub>1</sub>	7.929	0.03525	4.92**
X <sub>2</sub>	1.590	-0.35713	1.36
X <sub>3</sub>	91.964	0.004637	0.92
X <sub>4</sub>	53.741	-0.002919	1.15
X <sub>5</sub>	14414.516	0.00001595	2.94**
X <sub>6</sub>	3411.387	-0.00000795	1.28
X <sub>7</sub>	63.712	-0.0002796	0.05
X <sub>9</sub>	0.000488	-0.001446	1.31
X <sub>10</sub>	100.464	0.001363	0.29
X <sub>11</sub>	12.5048	-0.01599	0.71
X <sub>12</sub>	80.696	-0.0007894	0.24
X <sub>13</sub>	1.904	-0.27540	1.54
X <sub>14</sub>	42.842	0.0001313	0.09
X <sub>15</sub>	12.958	0.008825	2.84**
X <sub>16</sub>	5.764	0.013103	1.10
X <sub>17</sub>	949.964	0.0003036	1.34

$$R^2 = 0.614793$$

$$R = 0.784087**$$

Table 17. Analysis of variance for the 17-factor composite regression analysis.

Source of variation	Degrees of freedom	Sums of squares	Mean squares
Due to regrssion	16	5.4686	0.34179
Deviations about regression	67	3.4264	0.05114
Total	83	8.8950	

$$F = 6.683**$$

$$F_{.01} = 2.29$$

Consider:

$$\begin{aligned}
 R^2 &= \frac{SSR}{\Sigma' y^2} \sim \frac{L^2 + k\sigma^2}{L^2 + (n-1)\sigma^2} \\
 &= \frac{\frac{L^2 + \sigma^2}{\sigma^2} + (k-1)}{\frac{L^2 + \sigma^2}{\sigma^2} + (n-2)} \\
 &= \frac{t^2 L + k-1}{t^2 L + n-2} \\
 &= \frac{t^2 L - 1}{t^2 L + n-2} + \frac{k}{t^2 L + n-2}
 \end{aligned}$$

where

$n$  = total number of units (trees) in the analysis

$k$  = total number of factors in the analysis

$L^2 = (\beta_L^2) (\Sigma' x_1^2)$  = systematic contribution of lean to the numerator of  $R^2$

$t_L^2$  = value of the square of the t-statistic for lean.

It is seen that the expected percentage increase per additional random factor is approximated by

$$\left( \frac{1}{t^2 L + n - 2} \right) 100$$

which equals about 1% in the present study.

As measured by the magnitude of the t-statistic, lean, crown volume, and available phosphorus are highly significantly associated with the proportion of gelatinous fibers. Lean is clearly the factor most strongly related to the proportion of gelatinous fibers. Graphically the relationship is presented in Figures 20, 21, and 22. Figure 20 is a functional plot of all the data. It should be noted that each point is an average of three rings. In cottonwood there are few, if any, gelatinous fibers in vertical boles, hence the regression lines are terminated at the last data points ( $2^\circ$  lean). There are two least squares lines on Figure 20, one being the regression line for lean alone, and the other line having the partial slope (all other factors being evaluated at their respective means). Figure 21 is a grouping of the least linear plots, and Figure 32 is a similar grouping of the most linear plots (i.e. all plots for which the relationship between lean and proportion of gelatinous fibers is significant beyond the 5% level). Quadratic lean (orthogonal to linear lean) was not related to the proportion of gelatinous fibers in these analyses. However, the linear functionality of proportion gelatinous fibers with lean is not applicable over the entire range of lean values, and it is not applicable in every case.

Crown volume has a highly significant "t" value in the large analysis, but its linear correlation coefficient is only 0.053. Furthermore, the sign of the regression coefficient shifts from positive to negative with

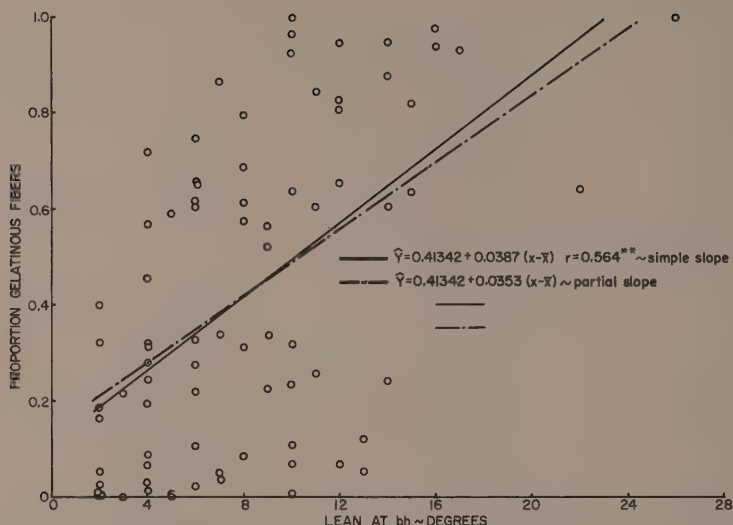


Figure 20. Relation of the proportion of gelatinous fibers to lean for all 14 plots.

the exclusion of variables and the sign also fluctuates from plot to plot. The reason for the former is probably exclusion of intercorrelated negatively related variables and the fact that the magnitude of the coefficient is initially low. The individual plot variation may be ascribed to the fact that crown volume is positively correlated in some cases with good growth conditions and in other cases with senescence and decrease in diameter growth. Table 18 shows the age and sign distribution for all the plots. Although age variation is relatively slight, the two youngest plots show positive relationships between crown volume and the proportion of gelatinous fibers, while the two oldest plots show negative relationships. Note that average proportion of gelatinous fibers per degree lean is fairly constant (0.0523). The only really divergent figure is derived from plot 3, which is almost twice the age of the other plots (74 years approaches senescence for *Populus deltoides*). The regression coefficient is also negative on this plot. The rate and capacity for reaction and depressed with the onset of maturity and the levelling off of diameter growth.

The t-statistic for available phosphorus was also highly significant and the regression coefficient was positive in all analyses. The pH range of these soils was 7-8 and this is the range in which phosphorus is most available to plants. This observation is striking in view of the fact that Brendemuhl's study did not show phosphorus to be severely limiting on these soils. Since tension wood is associated with increased cellulose synthesis this result raises some interesting possibilities which will be dealt with in the discussion.

Table 18. Associated means and plot variables.

Plot No.	Site index	Age	$X_8/X_1$	Average crown vol. cubic feet	lbs/acre available phosphorus 0-48"	$r_{x_8, x_1}$	$b_{x_8, x_1}$
9	87	41	0.0579	8,444	2.0	0.376	0.058
12	88	34	0.0579	19,386	1.5	0.712	0.032
10	89	38	0.0832	16,155	2.0	0.997	0.1235
2	89	44	0.0439	6,499	14.0	0.039	0.0034
20	93	56	0.0459	12,893	1.5	0.227	0.0162
1	95	46	0.0720	63,338	48.0	0.864	0.0500
5	97	53	0.0415	17,736	1.5	0.961	0.082
22	100	38	0.0392	6,404	4.5	0.763	0.0234
18	101	46	0.0647	28,615	3.5	0.810	0.0258
13	103	34	0.0524	13,255	6.5	0.399	0.0316
14	112	37	0.0466	12,097	13.5	0.966	0.0671
3	113	74*	0.0188	22,186	34.5	-0.781	-0.0280
16	120	35	0.0756	21,612	10.5	0.801	0.0622
23	120	46	0.0341	15,066	9.0	0.787	0.0898
$\bar{X}$	100.5	44.5	0.0523				

A number of site and tree growth variables were negatively (variously) correlated with proportion of gelatinous fibers (see Table 16). These relationships are contingent upon the size and life cycle stage of the individual tree. Timber in varying stages of maturity was used in this study. Average ring width is also negatively correlated with many of these same variables. Again radial growth is influenced by the same factors influencing tension wood. It appears that for the species and general age group investigated there is a single standard partial regression coefficient for proportion of gelatinous fibers and lean, except when some critical magnitude of environmental or life cyclic fluctuation is exceeded.

#### Individual plot analyses

Individual 4-factor multiple regressions were computed for each plot and in addition various graphical techniques were employed. Data from this section are voluminous (Berlyn, 1960), and only a representative portion will be presented here. Graphs of the proportion of gelatinous fibers-lean relationships are presented in Figures 23-32. On the individual plot graphs only the least square line for lean alone has been plotted. The partial slopes have excessive fluctuation, which arises because there are only 1 or 2 degrees of freedom for error in the individual plot multiple linear regressions. The confidence interval is extremely large. Note that except for plots 1 and 5 each plotted point is an average of three years' response.



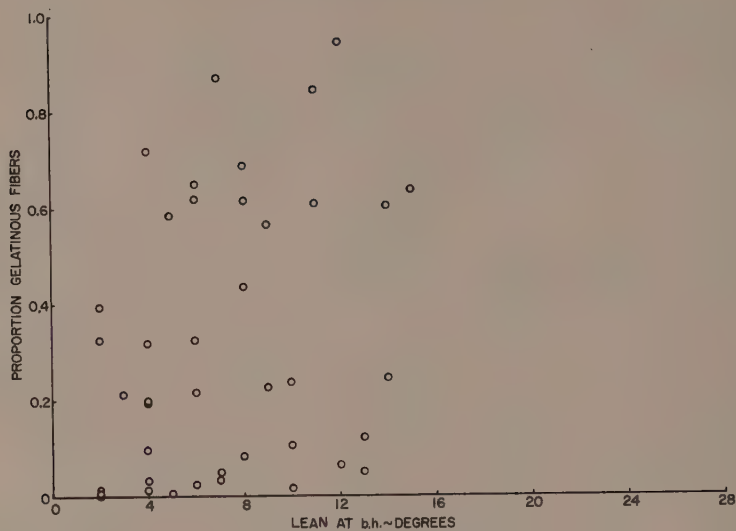


Figure 21. Relation of the proportion of gelatinous fibers to lean for plots 2, 3, 9, 12, 13, 20, 23.

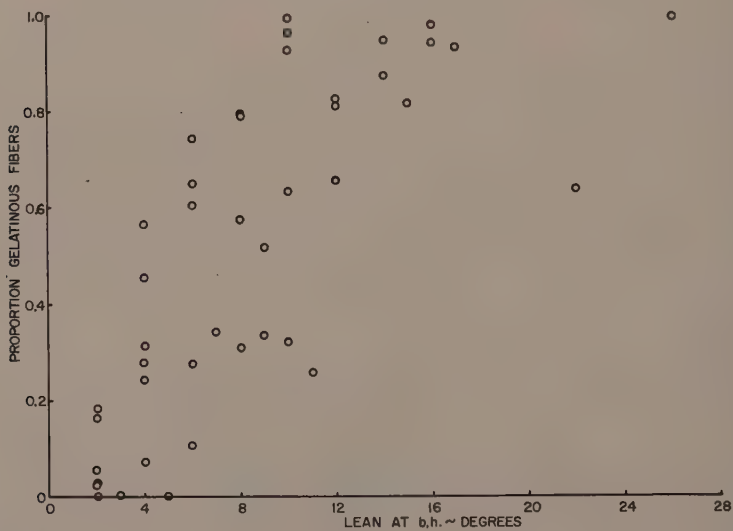


Figure 22. Relation of the proportion of gelatinous fibers to lean for plots 1, 5, 10, 14, 16, 18 and 22.

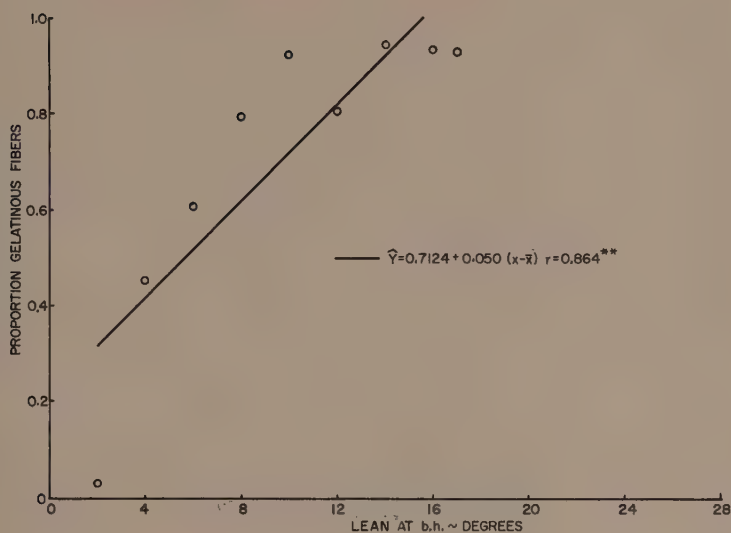


Figure 23. Relation of the proportion of gelatinous fibers to lean for plot 1 and site index 95.

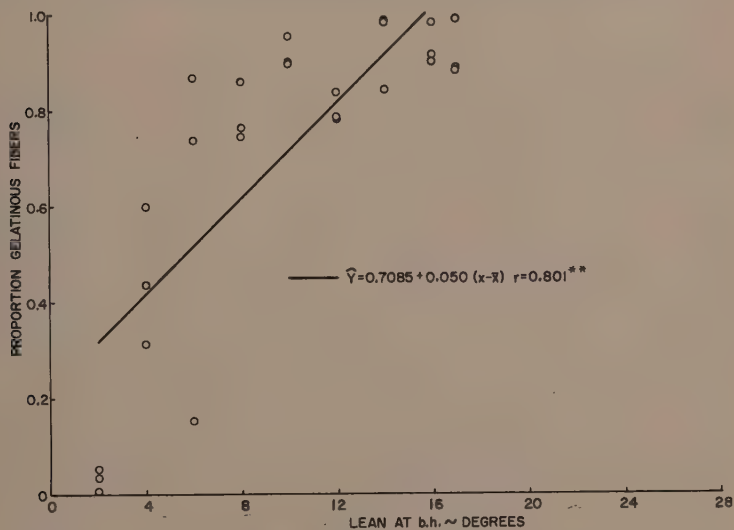


Figure 24. Relation of the proportion of gelatinous fibers to lean for plot 1 and site index 95, showing proportions from all three annual increments sampled per tree.

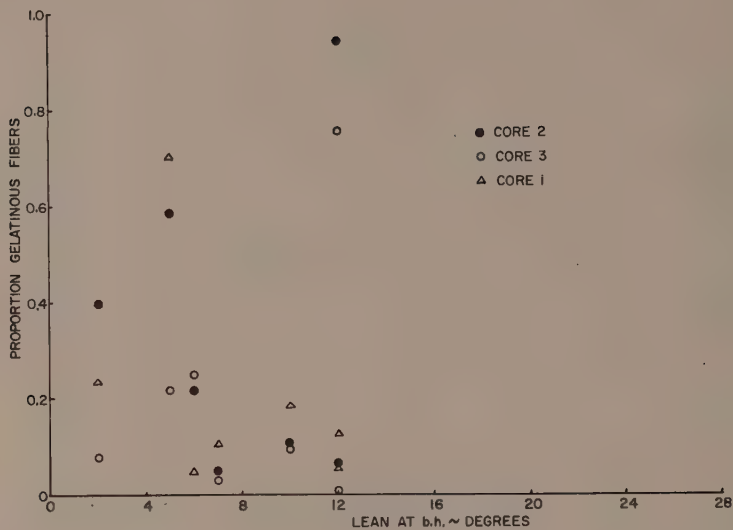


Figure 25. Relation of the proportion of gelatinous fibers to lean for plot 2 and site index 89.

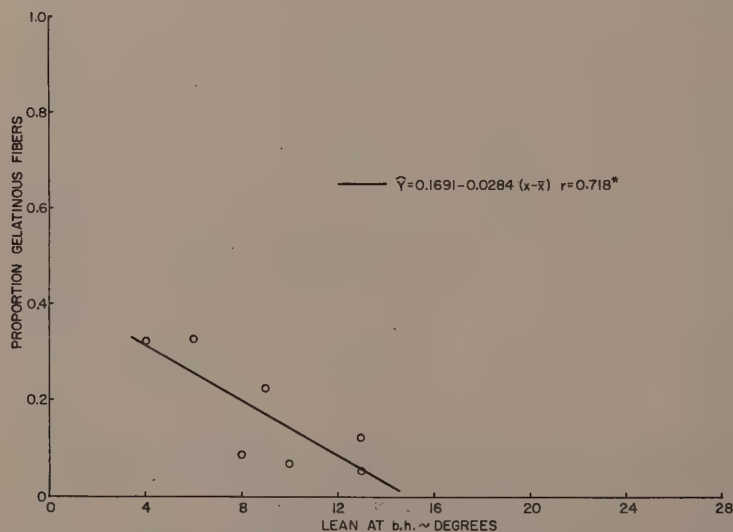


Figure 26. Relation of the proportion of gelatinous fibers to lean for plot 3 and site index 113.

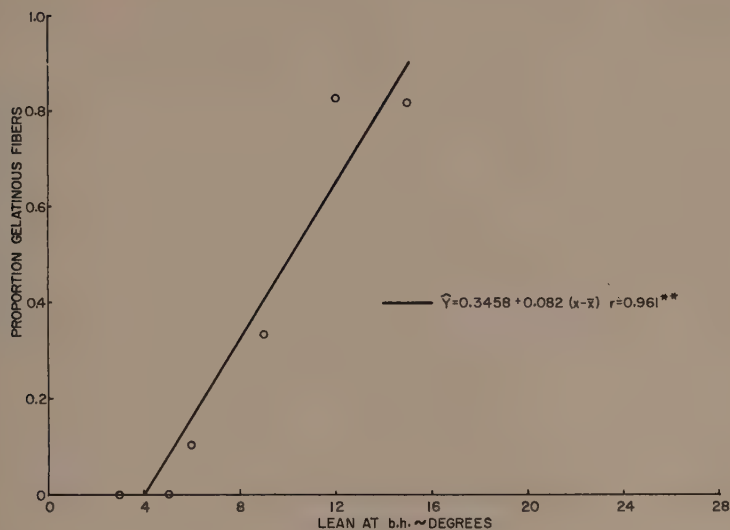


Figure 27. Relation of the proportion of gelatinous fibers to lean for plot 5 and site index 97.

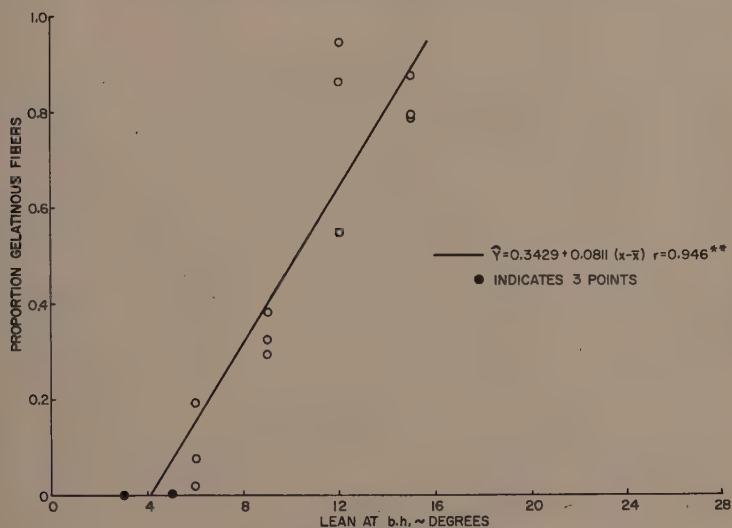


Figure 28. Relation of the proportion of gelatinous fibers to lean for plot 5 and site index 97 showing proportions from all three annual increments sampled per tree.

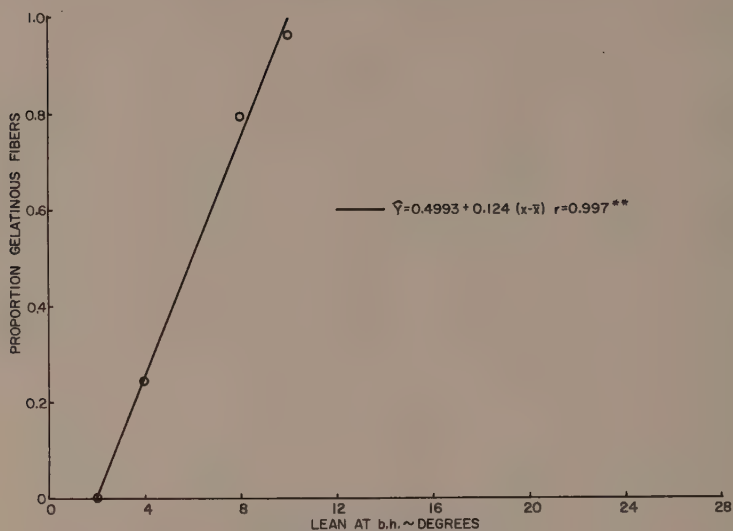


Figure 29. Relation of the proportion of gelatinous fibers to lean for plot 10 and site index 89.

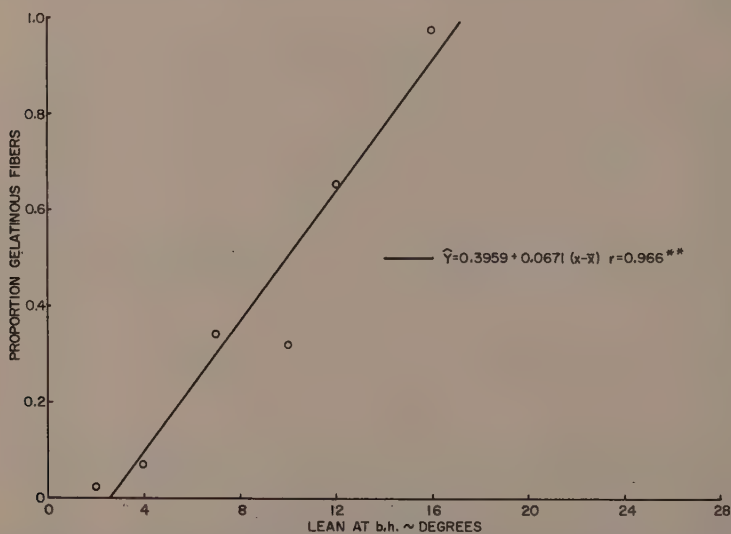


Figure 30. Relation of the proportion of gelatinous fibers to lean for plot 14 and site index 112.



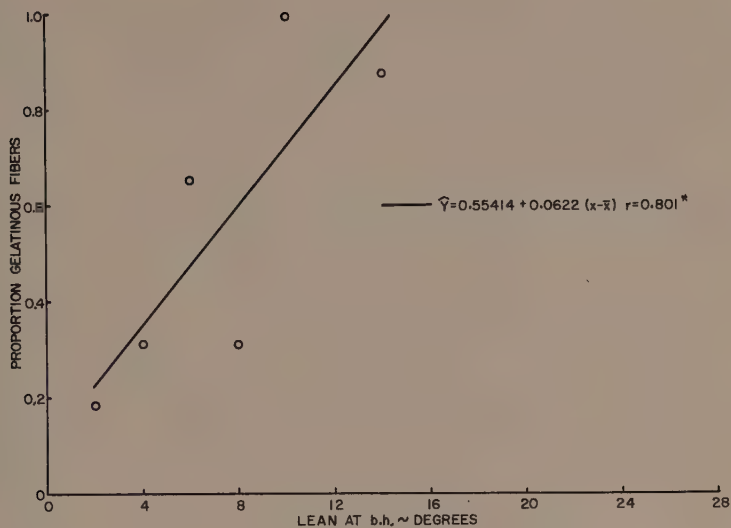


Figure 31. Relation of the proportion of gelatinous fibers to lean for plot 16 and site index 120.

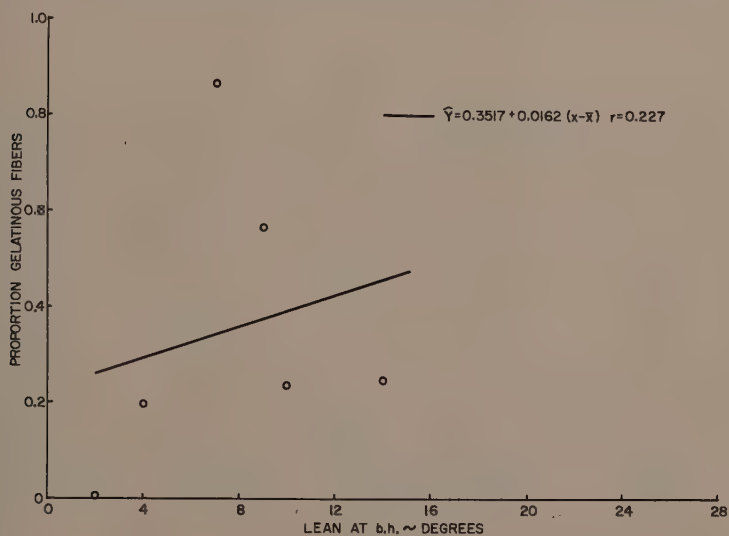


Figure 32. Relation of the proportion of gelatinous fibers to lean for plot 20 and site index 93.

Again the lines of best fit were not drawn past the data points. While the data points appear restricted to a linear range, the over-all curve form could well be curvilinear. The curvilinearity must arise at some point, if only because the limits of the ordinate are 0 and 1. In some cases the curve may approach 1 asymptotically and in other cases the curve achieves the maximum directly and then maintains it throughout the subsequent x-range.

No regression line was drawn for plot 2; instead, a scatter diagram is plotted for all three cores. The lack of functionality with lean was apparently translated circumferentially. Plot 3 is the only plot with a negative slope. As previously mentioned this stand was senescent (74 years). Duration of lean has a negative relation with reaction, and on plot 3 the heavily leaning trees may have been locked in position for a long time while the smaller leans are of more recent origin (derived from additional canopy space due to mortality of adjacent trees). Plot 20 had been cut over just prior to sampling, and some change of orientation had probably occurred. On plot 20 the "t" for lean is not significant, but the "t's" for crown volume and total height are highly significant. The residual trees had formerly been suppressed and this may, in part, explain the strong negative relationship between crown size and tension wood on this plot. The trees with the smallest crowns were the physiologically youngest and responded most. Lean was under fluctuation because of the low density of the residual stand.

Only the lean stands out as a constant factor in the individual plot analyses, although it is not operative on some plots. It is obvious that, for a given lean, the anatomical expression of this morphogenetic phenomenon is modified by environmental factors.

## DISCUSSION

The chemical and physical properties of xylem are determined by the expression of the lignin-cellulose ratio in the cell walls. The walls of stimulated cells become swollen and stained purple by chloriodide of zinc, indicating the presence of long-chain cellulose molecules, whereas the walls of unstimulated cells in situ are not appreciably swollen or stained. However, extracted cellulose from unstimulated tissues is iodine stainable after swelling by zinc chloride (Schorger, 1926, p. 214; Bonner, 1950, p. 362). The blue complex apparently cannot form when lignin bonding or structural interpenetration is present. The lack of structural rigidity and lamellar unification, occurrence of intermicellar movement, and greater amount of hydrophilic material are possible sources of the dimensional instability of tension wood.

The "gelatinous" layer (highly crystalline cellulose) has greater density than lignified cell wall substance. According to Frey-Wyssling there is no "mass deficit" between tension wood and normal wood. Therefore the question arises whether the space vacancy created by the absence of lignin is actually occupied by more cellulose micelles of usual size fluctuation, larger micelles, smaller micelles, or some combination. Apparently there is a distribution of micelle size and degree of crystallinity associated with cellulose biosynthesis. Frey-Wyssling (1957)

states that the presence of noncellulosic constituents limits and causes defective cellulose crystallization, but this is not a factor in substances like polyethylene glycol which also have micellar structure. The role of phosphorus in cellulose synthesis may be important in answering these questions. It is now believed that cellulose synthesis (at least in some organisms) proceeds through uridine triphosphate (UTP) carrier molecules (Whelan, 1959). Glucose and UTP combine to form uridine diphosphate glucose units (UDPG) which add to primer chains. The acceleration of cellulose synthesis in tension wood may account for the increased phosphorus demand revealed in this study. This should be examined at more critical levels of phosphorus.

Studies involving antimetabolites may provide important information about tension wood. The shifting levels of metabolites are probably related to negative feedback mechanisms similar to those currently being found fundamental in other regulatory functions. The absolute nature of the cytological response and the distributional nature of the histological responses are evidence of cyclical phenomena. This implies that the metabolic pathway only proceeds when required levels of certain metabolites (components of the system) are present. The distributional form of the histological response arises from: (1) the cambial production of small groups of stimulated cells, and (2) the abrupt cambial fluctuation resulting from interruptions, possibly at various points in the metabolic cycle. Regardless of the source of the inducing complex, the induction comes very early in the ontogeny of the cell.

Reaction tissue tends to develop where it opposes a deforming force and where it, in effect, maintains or restores a specific morphogenetic pattern. In angiosperms the locus of reaction tissue is so disposed that the concomitant contractive force will tend to restore the morphogenetic pattern, which presumably has selective value. Despite earlier viewpoints (cf. Hartman, 1942; Sinnott, 1951, 1952) the phylogenetic development is a direct product of the evolutionary process. Mechanical tissue in general has regulatory functions. This can be observed in climbing vines, petioles, and suitably stimulated herbaceous stems, as well as in the stems and branches of woody plants. The reaction tissues are "normal" physiological and morphological phenomena. They are not abnormal, in the sense that plant vigor is not depressed. The very interesting problem that remains to be answered is why, in the two great groups of higher plants, the morphological and physiological processes involved assumed such diverse character to accomplish the same effect. The vertical crown position must have high adaptive value.

The most immediate measures of environmental conditions in this study were "ring-width" (radial growth) and "cell number" (cambial division). Both of these quantities were significantly and positively correlated with the proportion of gelatinous fibers. Furthermore, the same factors that cause fluctuation in reaction tissue cause equally strong fluctuation in radial growth. The cytohistological observations also indicate that below a certain metabolic threshold (as revealed by radial growth) no reaction tissue is produced irrespective of the amount of

stimulation. There is also a maximum expression of a given amount of stimulation, and beyond this point no additional increase in metabolism, as revealed by radial growth, will cause an increase in reaction. Thus, for a given amount of stimulation the reaction is limited to certain metabolic intervals as expressed by radial growth.

However, the results presented in this report are only one randomization of a general age class. In addition to the general environmental framework the capacity to "react" is a function of age and lifecycle stage, as well as magnitude and duration of stimulus. For example, with younger plant material relationships may be more linear, and more positive relationship with the gross growth factors may exist.

### SUMMARY

1. A biometric technique was developed for the study of reaction tissue in Populus deltoides. Images of cross sections, including the cambium and 3 annual increments taken from the upper side of leaning cottonwood stems, were projected on paper grid systems. Counts of stimulated and nonstimulated cells in randomly selected grids were recorded.
  - a. Significant but small positive correlation exists between adjacent grid squares, and significant but small negative correlation exists between distant squares.
  - b. A gain in efficiency of 129% was obtained by using the weighted means of samples of eight grid squares instead of the unweighted means of individual squares. Variance was significantly greater than binomial variance. Transformations were not beneficial.
2. The induction of the gelatinous layer occurs early in cellular ontogeny. The cambium produces stimulated cells in small groups, but abrupt variations occur, possibly from blockage at various points in the metabolic pathway.
3. Higher proportions of gelatinous fibers are associated with larger ring width and with smaller cells.
4. Strong fluctuation in the factors which determine radial growth is associated with equally strong fluctuation in the factors that induce reaction tissue. The association of reaction tissue and the factors controlling radial growth occur in certain metabolic intervals.
5. Lean was the strongest correlate with the proportion of gelatinous fibers. Tension wood increased with increasing lean and for the age group and ecological situations of the trees examined in this study, there appears to be one over-all regression coefficient for proportion of gelatinous fibers regressed on lean.
6. The rate and capacity for reaction tissue production in woody plants



are depressed with the onset of senescence, the duration of stimulus, and the levelling off of diameter growth.

7. Available phosphorus was related to the proportion of gelatinous fibers. The relationship was highly significant and positive. This result may be related to the increased cellulose biosynthesis associated with tension wood.
8. Crown volume was correlated with the proportion of gelatinous fibers, but its effect varies depending on the age and condition of the tree. Crown volume was highly correlated with many of the other soil and tree variables.
9. Rapidly grown material had comparatively larger amounts of tension wood than equivalently leaning, slow-grown timber. Uniformity of growth conditions is also important in producing uniform properties (in this respect).
10. Openings in the canopy are a source of lean and therefore of tension wood. Hence, proper stockings and perhaps association with the more tolerant silver maple (*Acer saccharinum* L.) should be considered as possible means of preventing quality loss. Another large loss in merchantability of cottonwood occurs in the margins of stands because of phototropic responses. This loss might also be minimized by border rows of some geotropic species.

#### LITERATURE CITED

- Bailey, I. W. and Thomas Kerr. 1935. The visible structure of the secondary wall and its significance in physical and chemical investigations of tracheary cells and fibers. *Jour. Arnold Arboretum* 16: 273-300.
- Berlyn, Graeme P. 1959. A biometric technique for reaction tissue research. *Proc. Iowa Acad. Sci.* 66:98-102.
- \_\_\_\_\_. 1960. Factors affecting the incidence of reaction tissue in *Populus deltoides* Bartr. Unpubl. Ph.D. Thesis. Iowa State University Library, Ames, Iowa. 88 pp.
- Birnbaum, Z. W. 1952. Numerical tabulation of the distribution of Kolmogoroff's statistic for finite sample size. *Jour. Amer. Stat. Assn.* 47:425-441.
- \_\_\_\_\_. and F. H. Tingey. 1951. One-side confidence contours for probability distribution functions. *Annals Math. Stat.* 22:592-596.
- Bonner, James. 1950. *Plant biochemistry*. Academic Press, Inc., New York, N. Y.
- \_\_\_\_\_. and Arthur W. Galston. 1952. *Principles of Plant Physiology*. W. H. Freeman and Co., San Francisco. Calif.
- Brendemuehl, R. H. 1957. Growth, yield, and site requirements of eastern cottonwood. Unpubl. Ph.D. Thesis. Iowa State University Library, Ames, Iowa.

- Burns, George P. 1920. Eccentric growth and the formation of redwood in the main stem of conifers. Vermont Agric. Exp. Sta. Bull. 219.
- Busgen, M. and E. Munch. 1929. The Structure and Life of Forest Trees. John Wiley and Sons, Inc., New York, N.Y.
- Chow, K.Y. 1946. A comparative study of the structure and chemical composition of tension wood and normal wood in beech (*Fagus sylvatica* L.). Forestry 20:62-77.
- Dadswell, H.E. 1945. Timbers of the New Guinea region. Tropical Woods 83:1-14.
- \_\_\_\_\_ and A.B. Wardrop. 1949. What is reaction wood? Australian Forestry 13:22-33.
- \_\_\_\_\_ and \_\_\_\_\_. 1955. The structure and properties of tension wood. Holzforschung 9(4):97-104.
- David, H. T. and G. P. Berlyn. 1960. Analyzing triplets. (dittoed) Iowa State University Statistical Laboratory, Ames, Iowa
- Ewart, A. J. and A. J. Mason-Jones. 1906. The formation of redwood in conifers. Annals of Botany 20:201-204.
- Fraser, Donald A. 1952. Initiation of cambial activity in some forest trees in Ontario. Ecology 33:259-273.
- Gevorkiantz, S. R. and L. P. Olsen. 1955. Composite volume tables for timber and their application in the Lake States. U.S. Dept. Agric. Forest Service Tech. Bull. No. 1104.
- Haberlandt, G. 1914. Physiological Plant Anatomy. 4th ed. Macmillan and Company, Ltd., St. Martin's Street, London.
- Hartig, Robert. 1901. Holzuntersuchungen Altes und Neues. Verlag von Julius Springer, Berlin.
- Hartmann, Franz. 1932. Untersuchungen über Ursachen und Gesetzmässigkeit exzentrischem Dickenwachstums bei Nadel- und Laubbaumen. Forstwissenschaftliches Centralblatt 54:497-517, 541-566, 581-590, 622-634.
- \_\_\_\_\_. 1942. Das statische Wuchsgesetz bei Nadel- und Laubbäumen neue Erkenntnis über Ursache, Gesetzmässigkeit und Sinn des Reaktionholzes. Springer - Verlag, Wien.
- Jaccard, P. 1938. Exzentrisches Dickenwachstum und anatomisch-histologische. Differenzierung des Holzes. Berichte der Schweizerischen botanischen Gesellschaft 48:491-502.
- \_\_\_\_\_. 1940. Tropisme et bois de reaction provoques par la force centrifuge ches des feuillus. Berichte der Schweizerischen botanischen Gesselschaft 50:279-284.
- Jacobs, M. R. 1945. The growth stresses of woody stems. Australia Commonwealth Forestry Bur. Bull. No. 28.
- Jayme, G. 1951. Über die Bedeutung des Zugholzanteils in Pappelhölzern. Holz Roh-u Werkstoff 9:173-175.
- Kaiser, Margaret. 1955. Frequency and distribution of gelatinous fibers in eastern cottonwood. Amer. Jour. Bot. 42:331-334.
- \_\_\_\_\_ and M. Y. Pillow. 1955. Tension wood in eastern cottonwood. Central States For. Exp. Sta. Tech. Paper No. 149.
- \_\_\_\_\_ and K. D. Stewart. 1955. Fiber size in *Populus deltoides* Marsh. in relation to lean of trunk and position in trunk. Bull. Torrey Bot. Club 82:57-61.



- Lassen, L.E. 1958. Effect of tension wood on density, toughness, and endwise compression of cottonwood. Unpubl. M.S. Thesis, Iowa State University Library, Ames, Iowa.
- Marra, Alan A. 1942. Characteristics of tension wood in hard maple, Acer saccharum Marsh. Unpubl. M.S. These, New York State College of Forestry Library, Syracuse, N.Y.
- Messeri, A. 1954. Caratteristiche dimensionali e strutturali della fibre di tensione di un campione di pioppo. Cellulosa e Carta, Roma 5:8-10. (Original not available, abstracted in Forestry Abstracts 16:2154.)
- Newcombe, Frederick C. 1895. The regulatory formation of mechanical tissue. Botanical Gazette 20:441-448.
- Onaka, F. 1949. Studies on compression and tension wood. Wood Res., Kyoto No. 1 (In Japanese, English translation).
- Ostle, Bernard. 1954. Statistics in Research. Iowa State College Press, Ames, Iowa.
- Priestly, J.H. and Dorothy Tong. 1927. The effects of gravity upon cambial activity in trees. Proc. Leed Phil. Soc. 1:199-208.
- Schorger, A.W. 1926. The Chemistry of Cellulose and Wood. McGraw-Hill Book Co., Inc., New York, N.Y.
- Scott, D.R.M. and S.B. Preston. 1955. Development of compression wood in eastern white pine through the use of centrifugal force. For. Sci. 1:178-182.
- Sinnott, E.W. 1951. The morphogenetic significance of reaction wood. Science 114(2967):487-488.
- \_\_\_\_\_. 1952. Reaction wood and regulation of tree form. Amer. Jour. Bot. 39:69-78.
- Snedecor, George W. 1956. Statistical Methods. 5th ed. The Iowa State College Press, Ames, Iowa.
- Spurr, Stephen H. and Matti J. Hyvarinen. 1954a. Compression wood in conifers as a morphogenetic phenomenon. Bot. Rev. 20:551-560.
- \_\_\_\_\_. 1954b. Wood fiber length as related to position in tree and growth. Bot. Rev. 20:561-575.
- Thomson, George W. 1956. Growth of plantation black walnut in south-eastern Iowa as related to certain soil properties. Unpubl. Ph.D. Thesis, Iowa State University Library, Ames, Iowa.
- Volk, William. 1958. Applied Statistics for Engineers. McGraw-Hill Book Co., Inc., New York, N.Y.
- Wahlgren, H.E. 1956. Effect of tension wood on the longitudinal shrinkage and specific gravity of eastern cottonwood. Unpubl. M.S. Thesis, Iowa State University Library, Ames, Iowa.
- \_\_\_\_\_. 1957. Tension wood in overcup oak. U.S. For. Prod. Lab. Rept. No. 2089.
- Wallis, W.A. and H.V. Roberts. 1956. Statistics. The Free Press, Glencoe, Illinois.
- Wardlaw, C.W. 1952. Phylogeny and Morphogenesis. Macmillan and Company, Ltd. St. Martin's Street, London.
- Wardrop, A.B. 1956. The nature of reaction wood. V. The distribution and formation of tension wood in some species of Eucalyptus. Australian Jour. Bot. 4:152-156.

- \_\_\_\_\_ and H.E. Dadswell. 1948. The nature of reaction wood. I. The structure and properties of tension wood fibers. Australian Jour. Scient. Res., Series B, Biological Sciences 1:3-16.
- \_\_\_\_\_ and \_\_\_\_\_. 1955. The nature of reaction wood IV. Variation in cell wall organization of tension wood fibers. Australian Jour. Bot. 3(2):177-189.
- \_\_\_\_\_ and E. Scaife. 1956. Occurrence of peroxidase in tension wood of angiosperms. Nature (London) 178:867.
- Wershing, Henry F. and I.W. Bailey. 1942. Seedlings as experimental material in the study of "Redwood" in conifers. Jour. For. 30:411-414.
- Westing, A.H. 1959. Studies on the physiology of compression wood formation. Unpubl. Ph.D. Thesis. Yale University School of Forestry Library, New Haven, Conn.
- Whelan, W.J. 1959. The enzymic synthesis and degradation of cellulose and starch. In: Honeyman, J., ed. Recent Advances in the Chemistry of Cellulose and Starch. pp. 307-336. Interscience Publishers, Inc., New York, N.Y.
- White, J. 1908. The formation of redwood in conifers. Proc. Roy. Soc. Victoria 20:107-124.
- Youden, W.J. 1953. Sets of three measurements. Scientific Monthly 77:143-147.